

# Introduction to Motor Drive Systems

12

## 12.0 Introduction

A motor drive is a system that provides to a mechanical load with continuous range process speed and torque control (as compared to discrete speed control as in gear boxes or multispeed motors). A motor drive system is capable of adjusting both speed and torque of a dc or an ac motor. Motor drive systems are one of the most important and most interesting fields in electrical and power electronics engineering. The above description is clear if one considers the crucial role played by the motor drive systems in all our daily lives but also the multitiered social benefits they entail. Since the invention of the electric motor, which converts electric energy into mechanical energy, it has been used in all kinds of applications the range of which continues to expand. The range of applications of motor drive systems includes the following:

- Transportation: electric vehicles, electric ships, and electric aircrafts.
- Industrial production lines: robots, cranes, and lifts.
- Appliance: machine tools.

The advantage of the electric motor drive systems are the following:

- Flexible control characteristics.
- Starting and braking is easy and simple.
- Provides a wide range of torques over a wide range of speeds (both ac and dc motor).
- Availability of wide range of electric power.
- Works to almost any type of environmental conditions.
- No exhaust gases emitted.
- Capable of operating in all four quadrants of torque—speed plane.
- Can be started and accelerated at very short time.

Power requirements covered by these systems are a fraction of a watt up to thousands or millions of watts.

The vision of motor drive systems thrust is to develop the necessary technology so that motor drive capabilities can be economically embedded inside future electric motors with minimal impact on their size, weight, and environmental robustness. Moreover, it is very important that these motor drive systems must be manufacturable with a minimal cost premium, while demonstrating environmental robustness and reliability characteristics that match those of conventional motors today. Consistent with these minimal impact objectives, the input power quality and EMI characteristics of future motor drive systems must approach those of the motors excited directly from the utility grid.

As the cost of electrical power and fuel inevitably increase during coming years, the lifetime cost savings generated by the introduction of electric motor drive systems will make them increasingly attractive for new applications.

Therefore, as is immediately apparent from the above, the object of study of electric motor drive systems has numerous practical applications, which involve very considerable substantiality economic and social benefits. Some of these include the improvement of means of transporting people and goods, to improve both quantity and quality of industrial production, reducing environmental pollution, and the general rise of living standards and technological human societies.

The advent of microprocessors, new high power semiconductor devices, and new motors has made it possible to design motor drive systems that exhibit excellent controllability, high efficiency, high power density, and high reliability. Therefore, the interest in motor drive systems is rising, and ever-growing complexity requires the student insight of almost all the spectrum of science in electrical and electronic engineering.

With the advent of power electronics technology, a great opportunity has been given to build advanced control techniques and develop them with the appropriate hardware and software algorithms. Especially with power converters, which are capable of supplying motors with voltages varying in amplitude and frequency, allowing complete speed and torque control.

The construction of a high-performance motor drive system requires a detailed understanding of machine characteristics and associated interactions with power electronic drives.

The choice of an electrical drive depends on a number of factors. Some important factors are as follows:

- Steady-state operation requirements (nature of speed—torque characteristics, speed regulation, speed range, efficiency, duty cycle, quadrants of operation, speed fluctuations, rating, etc.).
- Transient operation requirement (values of acceleration and deceleration, starting, braking, speed reversing).
- Requirement of sources (types of source, its capacity, magnitude of voltage, power factor, harmonics, etc.).
- Capital and running cost, maintenance needs, life periods.
- Space and weight restrictions.
- Environment and location.
- Reliability.

## 12.1 Electric Motor Drive Systems

The general form of an electric motor drive system or the so-called variable speed drive (VSD), which is shown in [Fig. 12.1](#), consists of the following main parts:

- Electrical power supply
- Power electronics converter
- Electric motor
- Mechanical load
- Control unit
- Control observer and measuring unit

The functions of the motor drive system stages shown in [Fig. 12.1](#) are discussed in the following sections.

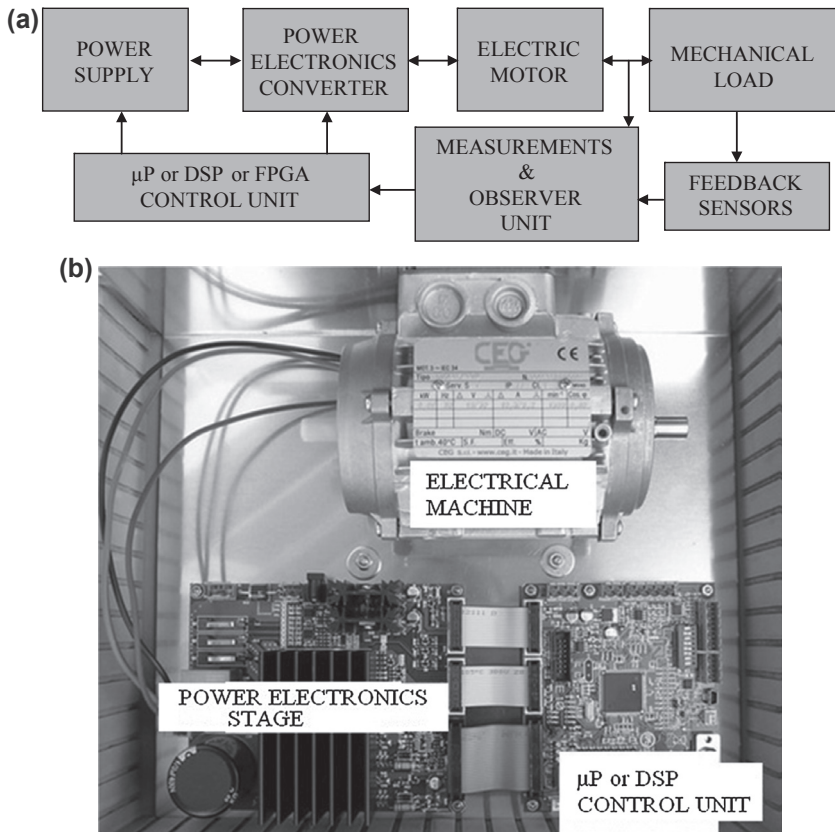


**Figure 12.1** Electric motor drive system. (a) Block diagram of an electric motor drive system; (b) overview of an electric motor drive system.

### 12.1.1 The Electrical Power Supply

The electrical power source provides electrical power under dc or ac voltage. As a power source, in most cases, we provide a symmetrical three-phase ac voltage from the grid produced by the more modern generators in large thermal power stations and minor, especially in recent years, from renewable sources such as wind, solar energy, etc. On the other hand, may provide the voltage to the power source is constant and comes from either rectification of the alternating voltage from the utility grid or from batteries or photovoltaic arrays, or ultimately even fuel cells.

Depending on the type of electric motor and power source, we should have to choose the right converter to feed our motor with the voltage required to operate correctly. In many cases, where the available power source is not suitable for powering the electric motor (i.e., ac power to dc motor and vice versa) converter that follows, except the control, and has designed the conversion of power in a form that can utilize the camera and in that sense it is necessary for its operation.

### 12.1.2 Power Electronics Converter

As can be seen from Fig. 12.1(a) the power electronics converter is applied between the electrical power supply and the electric motor. Its purpose is simply to control the speed, the torque, the current, or any other parameter of the motor. This is achieved by controlling the output voltage and current of the power converter. The type of converter to be used depends on the application. Depending on the generated output voltage of the power converter and the power absorbed by the load current of the inverter, it is able to either transfer power from the input source to the electric motor or from the motor to the input source. Fig. 12.2 presents the possible four quadrants of operation of a power electronics converter which depend on the direction of the output current and the polarity of the output voltage of the converter. For example, when an electric vehicle is running uphill, the electric motor is drawing power from the battery through the converter and since during this mode of operation the output voltage and current of the converter are positive, the converter operates in the first quadrant. However, when the electric vehicle is running downhill, the electric motor operates as a generator feeding power to the battery through the converter and since during this mode of operation the output voltage is positive and the output current is negative, the converter operates in the second quadrant.

### 12.1.3 Control Unit

The control unit includes the hardware and control software algorithm necessary to monitor and control the required electric motor drive system. The main aim of the control unit is to create at any instant the required gating signals of the power converter semiconductor switches through a software algorithm. The software algorithm decides the type of gating signals to be applied to the semiconductor switches created upon its input data about the status of the motor drive system. The control unit could be implemented using a microprocessor ( $\mu\text{P}$ ) or a digital signal processor (DSP) unit. As can be

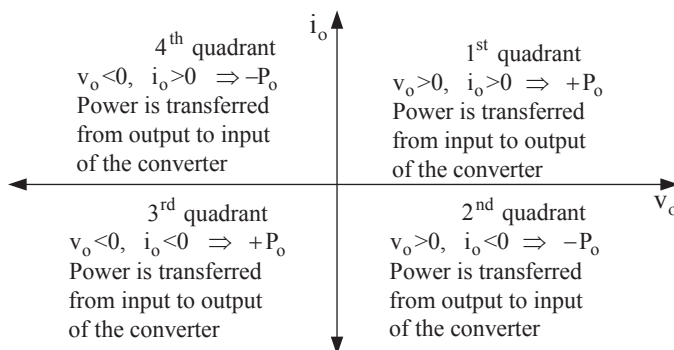


**Figure 12.2** Possible four quadrants of operation of a power electronics converter.

seen from Fig. 12.1(a) the microprocessor receives all necessary information of the motor drive system through the measurements and observer unit. This information consists of voltages, currents, rotational speed, magnetic flux of the motor, or any other information which is needed by control technique power electronics, amplitude and frequency of the input voltage of the electric motor, so that the electric motor drive system has the desired response. Each of these units is required to operate with maximum performance and best possible cooperation with other units so that the overall system to function optimally.

### 12.1.4 Electric Motor

The electric motor is defined as any electromechanical device that converts electrical energy into mechanical and vice versa. The electric motor is the heart of an electric motor drive system. The power converters and the control applied to them have a single purpose: to achieve the desired operation of the electric motor to obtain the desired result of the mechanical load. Depending on the type of load, the power source, the existence or noninverter, and various other techno-economical criteria relating to each application choose the type of motor used in this electric motor drive system. The machines found in electric motor drive systems are distinguished by loading it into two major categories: dc motors and ac motors. Each of these categories encompasses several subcategories but with significant differences in characteristics and function. Fig. 12.3 presents the main categories of electric motors used in VSD systems.

### 12.1.5 Mechanical Load

The mechanical load is connected to the motor shaft of a motor drive system providing interchange mechanical power with the motor. The mechanical load is a key factor in the

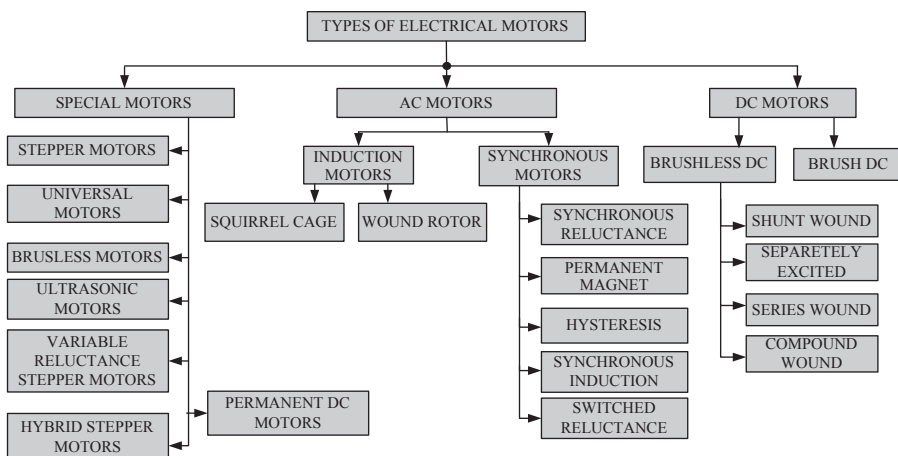


Figure 12.3 Major types of electric motors.

design of an electric motor drive system. The purpose of each electric motor drive system is to give the appropriate action in an appropriate way to load, so that to obtain the desired operating behavior. Therefore, the design of a motor drive system begins with an examination of the type of the load that is applied to the motor. For this reason, before proceeding to any other step in the design, it will be necessary to know the characteristic torque—speed and power—load speed. Here are some typical examples of loads encountered in industrial applications along with their respective characteristics:

- Constant power load: The load torque  $T_L(\omega_L)$  is inversely proportional to the speed  $\omega_L$ . The mechanical strength of the load  $P_L(\omega_L)$  remains constant for any speed  $\omega_L$ . Typical characteristics of these loads are shown in Fig. 12.4(a). Most of these loads are electric motor tools.
- Fixed load torque: The torque load  $T_L(\omega_L)$  is constant, while the mechanical power  $P_L(\omega_L)$  is a linear function of the load speed  $\omega_L$ . Typical characteristics of these loads are shown in Fig. 12.4(b). Most of these loads are conveyors.
- Linear load torque: The torque load  $T_L(\omega_L)$  is linear, while the mechanical power  $P_L(\omega_L)$  is a parabolic function with the load speed  $\omega_L$ . Typical characteristics of these loads are shown in Fig. 12.4(c). These types of loads include fans and centrifugal pumps depending on the type of the impeller.

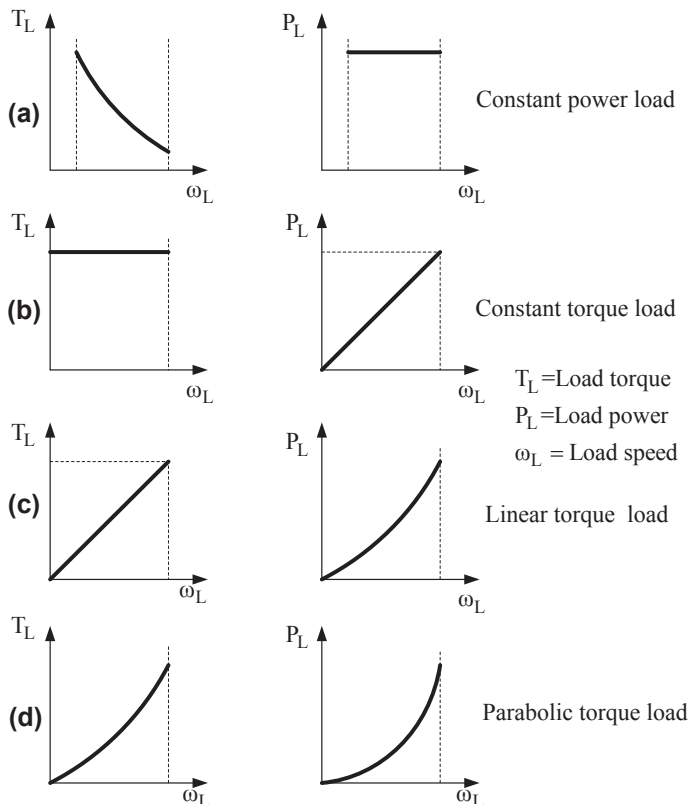


Figure 12.4 Characteristics of different types of mechanical loads.

- Parabolic load torque: The torque load  $T_L(\omega_L)$  is parabolic, while the mechanical power  $P_L(\omega_L)$  is a third degree depending on the load speed  $\omega_L$ . Typical characteristics of these loads are shown in Fig. 12.4(d). These types of loads include fans and centrifugal pumps depending on the type of the impeller.

When the type of the mechanical load is known then the design of the electric motor drive system can be started. With this procedure, unpredicted phenomena such as overloading the motor, system instability, slow response, overheating and excessive power consumption can be avoided. These phenomena are created by the miscalculation of the type of mechanical load.

## 12.2 DC Motor Drive Systems

The dc motor historically precedes the ac motor. Because of its ability to provide easy speed and torque control, was for decades the only choice for electric drive systems requiring variable speed operation. The ease of control is that generally in a dc motor rotation speed is proportional to the applied voltage to the armature and the developing torque is proportional to the armature current (this is clearly only for separately excited dc motors). Therefore, as is already evident, it is quite simple to control such a motor (e.g., through a dc—dc converter). The dc motors have been used for many years in electric drive systems and was considered indispensable for variable speed. Only the last 20 years been able to replace them by the asynchronous ac motors (induction motors) driven by advanced control techniques.

The operation of a conventional electric dc motor is based on the interaction of the stator and rotor fields. The stator field is generated by permanent magnets (PMs) (excitation) that are usually firmly fixed to the stator of the motor. The rotor field is generated in the rotor of the motor by rotating winding armature, and this constitutes an electromagnet. Key role in the operation of the motor plays the dc commutator. The role of the commutator is to keep the torque of a dc motor from reversing every time the coil moves through the plane perpendicular to the magnetic field. The commutator is a split-ring device that operates like a mechanical rectifier. This is necessary because the armature winding is rotating and without the commutator the motor will stop immediately the first time two opposite poles will lie across each other.

There is also the possibility that the dc motor does not have PMs in the stator, but electromagnet coil (as excitation), which is the most common practice. The motor is called a dc motor field winding. Therefore, by varying the current flowing through the electromagnet (called the field or alternatively winding excitation coil) may change the typical speed—torque motor. Depending on how the field winding of a dc motor is excited (powered) there are four types of dc motors as follows:

- a) Separately excited dc motors (Fig. 12.5(a))
- b) Shunt excited dc motors (Fig. 12.5(b))
- c) Series excited dc motors (Fig. 12.5(c))
- d) Compound excited dc motors (Fig. 12.5(d))

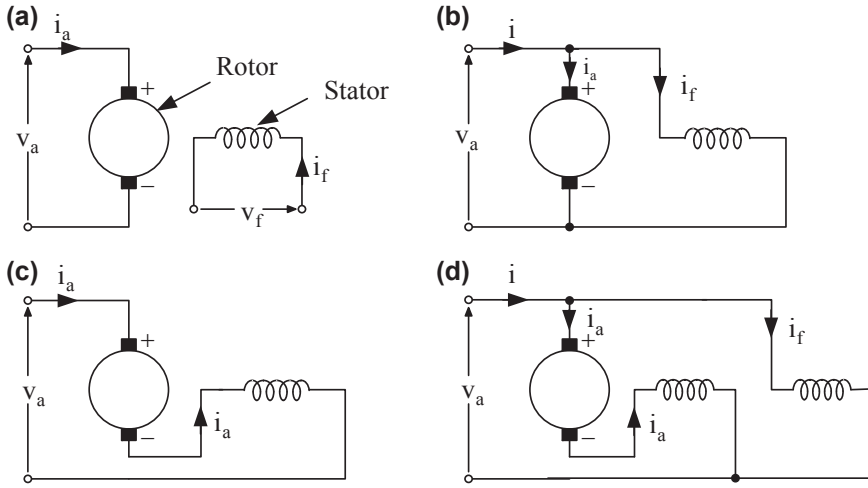


**Figure 12.5** Types of dc motors. (a) Separately excited dc motors; (b) shunt excited dc motors; (c) series excited dc; (d) compound excited dc motors.

Fig. 12.6 shows the cross section of a dc motor with windings or PMs on the rotor. Also, Fig. 12.6(c) shows the interaction between the stator and rotor field that creates the rotor forces and, consequently, the rotation of the electric motor.

Fig. 12.7 shows the equivalent circuit of a separate excited dc motor.

The equations that describe a separate excited dc motor can be found from Fig. 12.7 and are the following:

$$v_f = \text{rotor field voltage} = R_f i_f + L_f \frac{di_f}{dt} \quad (12.1)$$

$$v_a = \text{armature voltage} = R_a i_a + L_a \frac{di_a}{dt} + e_g \quad (12.2)$$

$$e_g = \text{electromotive force or back emf} = K_v \omega_m i_f \quad (12.3)$$

$$T_e = \text{developed electromagnetic torque} = K_t i_f i_a \quad (12.4)$$

$$T_e = J \frac{d\omega_m}{dt} + B \omega_m + T_L \quad (12.5)$$

where

$i_a$  = armature current, A

$i_f$  = rotor current, A

$R_a$  = armature internal resistance,  $\Omega$

$R_f$  = rotor internal resistance,  $\Omega$



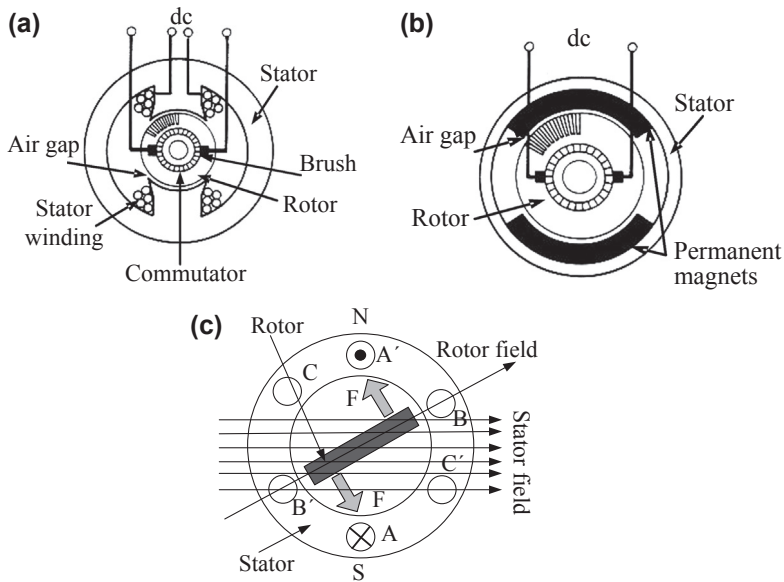


**Figure 12.6** Cross section of a dc motor. (a) With windings on the rotor; (b) with permanent magnets on the rotor; (c) interaction between the stator field and the rotor field that creates the rotation of the electric motor.

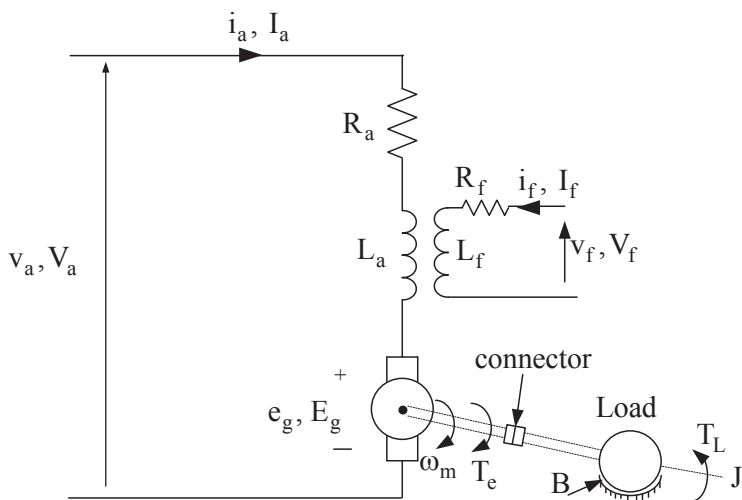


**Figure 12.7** Equivalent circuit of a separate excited dc motor (capital character variables are used for the steady-state analysis).

$\omega_m$  = motor mechanical speed, rad/s (1 rad/s = 9.55 RPM)

$T_L$  = load torque, Nm

$K_v$  = back-EMF constant, volt·s/rad

$K_f$  = field constant, volt·s/rad

$K_t$  = torque constant, Nm/W

$B$  = frictions constant, Nm/rad/s

$J$  = rotor moment of inertia, kg m<sup>2</sup>.

Assuming that the armature voltage  $v_a$  has a constant value  $V_a$ , the armature current  $i_a$  has a constant value  $I_a$  and the respective field values are also constant, then using Eq. 12.7 and the previous equations, the following equations are found for the steady-state operation of a dc motor:

$$\begin{aligned} T_e &= \text{developed electromagnetic torque of the motor} \\ &= K_a \Phi_f I_a = \frac{E_g I_a}{\omega_m} \quad \text{Nm} \end{aligned} \quad (12.6)$$

where

$K_a$  = design constant of the armature

$$\omega_m = \text{motor mechanical speed} = \frac{V_a - I_a R_a}{K_v \Phi_f} \quad \text{rad/s} \quad (12.7)$$

$$E_g I_a = T_e \omega_m \quad (\text{electrical energy conversion to mechanical}) \quad (12.8)$$

$$\Phi_f = \text{magnetic flux of the rotor} = K_f I_f \quad \text{Wb} \quad (12.9)$$

$$V_a = \text{armature voltage} = E_g + R_a I_a \quad \text{V} \quad (12.10)$$

$$E_g = \text{back emf} = K_v \Phi_f \omega_m \quad \text{V} \quad (12.11)$$

$$P_i = \text{Input active power of the motor} = I_a V_a + I_f V_f \quad \text{W} \quad (12.12)$$

$$P_{s \text{ cu}} = \text{rotor copper losses} = I_f^2 R_f \quad \text{W} \quad (12.13)$$

$$P_{r \text{ cu}} = \text{armature copper losses} = I_a^2 R_a \quad \text{W} \quad (12.14)$$

$$P_{\text{rotational}} = \text{mechanical losses (friction + ventilation + ...)} \quad \text{W} \quad (12.15)$$

$$\begin{aligned} P_{sl} &= \text{losses due to ununiform current of the windings} \\ &\approx 1\% \text{ of the output power } W \end{aligned} \quad (12.16)$$

$$P_{\text{magn}} = \text{core losses} = 1\% \text{ to } 5\% \text{ of output power } W \quad (12.17)$$

$$\begin{aligned}
 P_e &= \text{rotor electromagnetic power} \\
 &= I_a E_g = T_e \omega_m = P_i - P_{scu} - P_{rcu} - P_{sl} \quad W
 \end{aligned}
 \tag{12.18}$$

$$\begin{aligned}
 P_m &= \text{mechanical power developed on the motor shaft} \\
 &= P_e - P_{\text{rotational}} = I_a E_g - P_{\text{rot}} = T_m \omega_m
 \end{aligned}
 \tag{12.19}$$

$$\begin{aligned}
 T_m &= \text{mechanical torque on the motor shaft} \\
 &= T_e - \frac{P_{\text{rotational}}}{\omega_r} \quad \text{Nm}
 \end{aligned}
 \tag{12.20}$$

$$\eta\% = \text{motor efficiency} = \frac{P_m}{P_i} 100
 \tag{12.21}$$

Eqs. (12.6) and (12.7) indicate that the developed speed and torque of a dc motor can be controlled by the average armature voltage  $V_a$ . This is done by utilizing a power electronic converter between the power source and the motor armature. Fig. 12.8 shows the power flow and losses in a dc motor.

Fig. 12.9 shows the torque and power characteristics of a separate excited dc motor. As can be seen from this figure, the speed of the motor is controlled up to its rated value through the armature voltage and for values above the rated speed is controlled through its field current.

A dc machine is able to operate as a motor or as a generator. According to Eq. (12.18) when the torque has the same sign as that of the rotational speed, then the motor produces positive output mechanical power, which means that the motor absorbs electric power from the source through the converter and operate as a motor. However, when the torque and rotational speed have opposite signs, then the motor produces negative output mechanical power and operates as a generator transferring through the converter electric power to the input source. When the motor operates as a generator, load is that which gives the kinetic energy of the motor axis. This indicates that a dc machine can operate in any of the following four quadrant modes:

**First quadrant mode ( $P_e = (\omega_m)(T_e) = \text{positive}$ , motoring with clockwise rotation):** In this operating mode the dc machine operates as a motor developing positive torque and

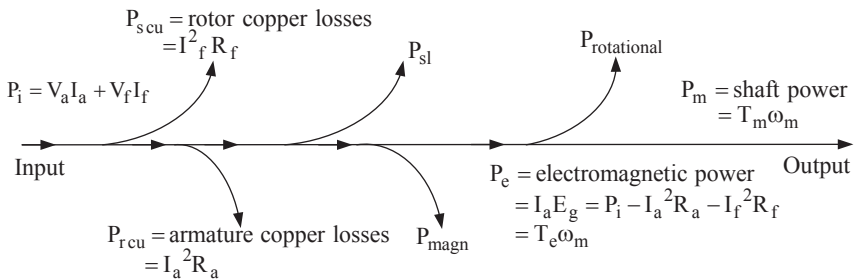
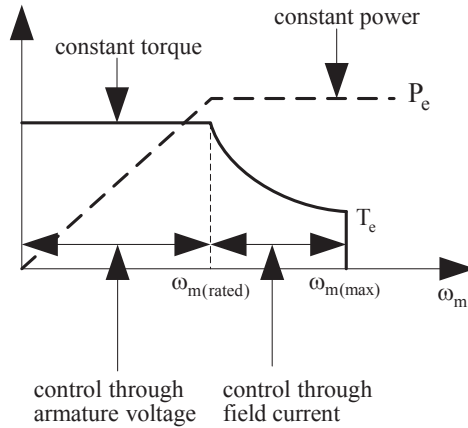


Figure 12.8 Power flow within a separate excited dc motor.



**Figure 12.9** Torque and power characteristics of a separately excited dc motor.

rotates with positive speed (i.e., clockwise rotation). The quadrant of this operating mode is the first and is presented in Fig. 12.10. An example of this mode is when an electric vehicle runs uphill and electrical energy is taken from the batteries through a converter, which is applied to an electric motor, and the motor converting the electrical energy to mechanical moves the electric vehicle.

**Second quadrant mode ( $P_e = (+\omega_m)(-T_e) = -ve$ , generating with clockwise rotation):** In this operating mode, negative torque with positive speed is applied to the shaft of dc machine converting the motoring mode to generating mode. This means that the

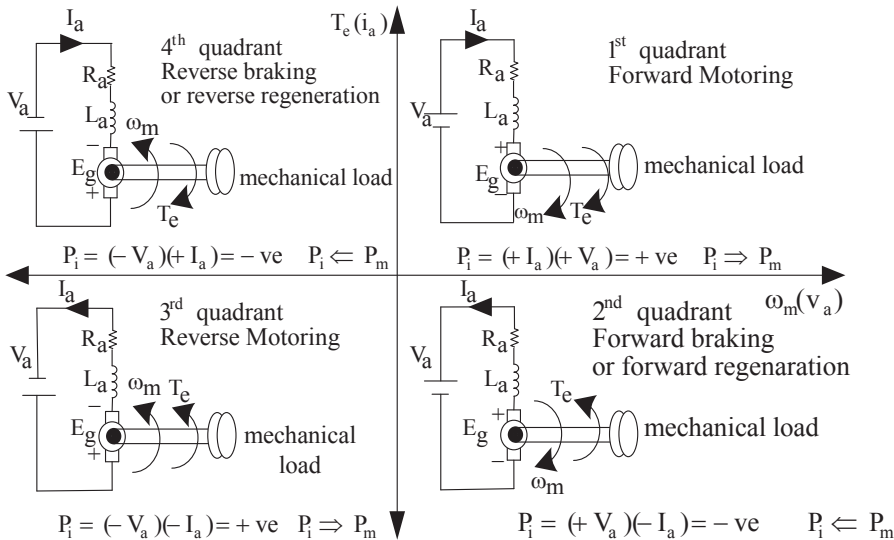


**Figure 12.10** The four possible quadrant modes of operation of a separately excited dc machine.

mechanical load is providing kinetic energy to the shaft of the electric machine converting the motor to a generator that produces electrical energy which is fed to the input source through the armature and the power electronics converter. The quadrant of this operating mode is the second and is presented in Fig. 12.10. An example of this mode is when an electric vehicle travels downhill and the electric machine operates as a generator producing electrical power. During this mode the braking of the electric machine is achieved and since energy is saved during this mode this type of braking is called regenerative braking.

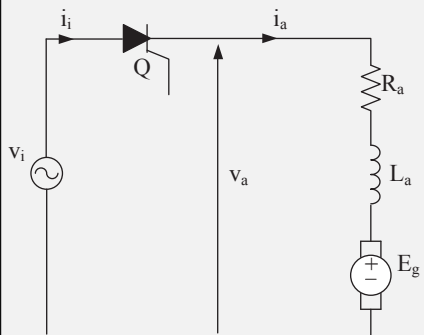
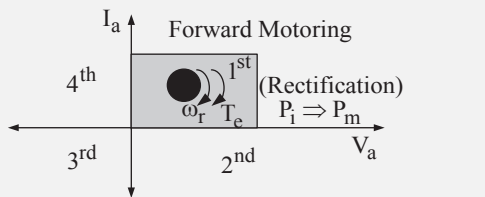
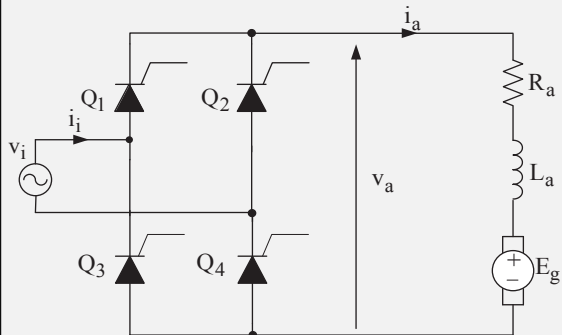
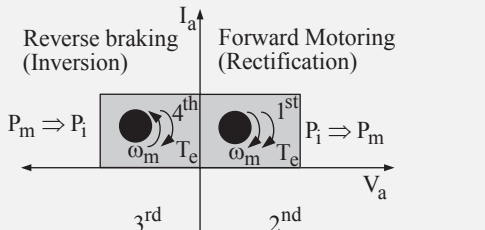
**Third quadrant mode ( $P_e = (-\omega_m)(-T_e) = \text{positive, motoring with counterclockwise rotation}$ ):** In this operating mode the dc machine operates as a motor developing negative torque and rotating with negative speed (i.e., counterclockwise rotation). The quadrant of this operating mode is the third and is presented in Fig. 12.10. An example of this mode is an electric vehicle when is running in backwards.

**Fourth quadrant mode ( $P_e = (-\omega_m)(+T_e) = -\text{ve, generating with counterclockwise rotation}$ ):** In this operating mode the dc machine produces a positive torque and rotates with negative speed, which means that the mechanical load torque fed to the shaft of the electric motor causes the machine to become a generator and feeds electricity to the input source through the armature. The operating area of this mode is the fourth quadrant of Fig. 12.10. An example of this mode is when an electric vehicle travels downhill and the electric machine through the transmission systems gets kinetic energy, then the electric machine operates as a generator producing electrical energy that transfers to the input source through the power electronics converter. During this mode the braking of the machine is achieved, and since energy is saved during this mode this type of braking is called regenerative braking.

Depending on the motor used and the type of the input power supply the dc motor drive systems can employ one of the following power electronics topology:

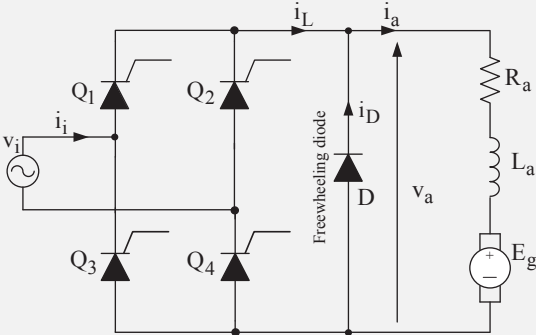
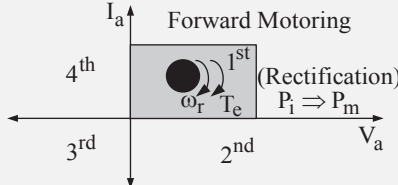
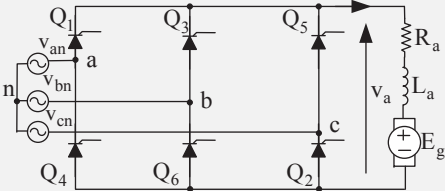
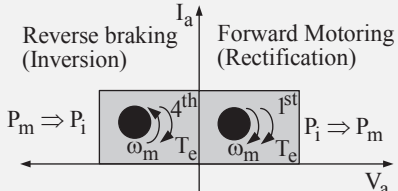
- i) **Thyristor rectifiers.** Table 12.1 presents different types of rectifiers and their respective possible quadrants of operation. The thyristor rectifiers, which are used in high-power motor drives applications, exhibit the following disadvantages:
  - 1) Due to their input current poor quality (low order current harmonic components) they need a large input filter.
  - 2) Poor input power factor.
  - 3) When a single rectifier is used they cannot handle bidirectional power flow and, consequently, four-quadrant operation is not possible.
  - 4) Since the thyristor devices are unidirectional switches, they do not have the capability for transferring energy from the output to the input. That means regenerative braking is not possible and, consequently, the efficiency of the motor drive is considerably reduced. In this case the so-called dynamic braking is used which is shown in Fig. 12.11. When dynamic braking is needed the input voltage  $v_i$  is disconnected through thyristor Q, and at the same time the switch S is turned on so that the kinetic energy, which is stored in the rotor, can be consumed by the braking resistance  $R_b$ . At this point it should be mentioned, that there is also the plugging braking which is achieved by reversing the armature current flow. This current reversal is created from the reversal of the electromotive force and, consequently, the equations  $V_a = -E_g - I_a R_a$  and  $I_a = -(V_a + E_g)/R_a$  hold. This means that a large negative torque (i.e., braking torque) is produced.
- ii) **Regenerative or pulse width modulation (PWM) rectifiers.** These rectifier topologies, which are presented in Table 12.2, do not present the abovementioned disadvantages of

Table 12.1 DC motor drive systems employing thyristor rectifiers—cont'd

Thyristor rectifier topology	Quadrant(s) operation
 <p><b>a) Half-wave rectifier</b> (Power capability up to 1 hp)</p>	
 <p><b>b) Single-phase full-bridge rectifier</b> (Power capability up to 20 hp)</p>	

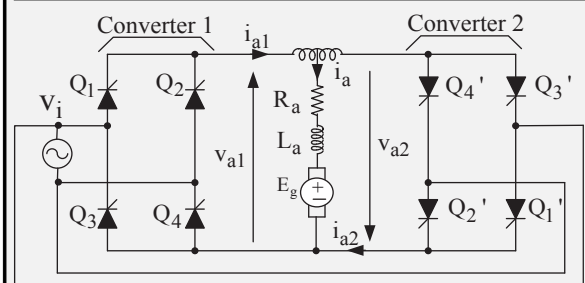
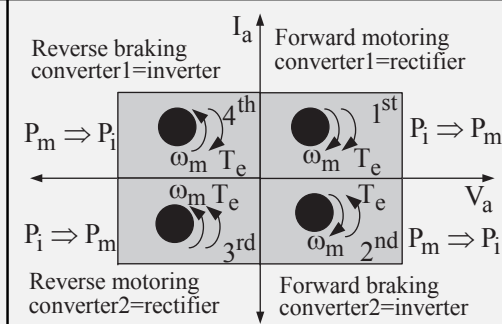
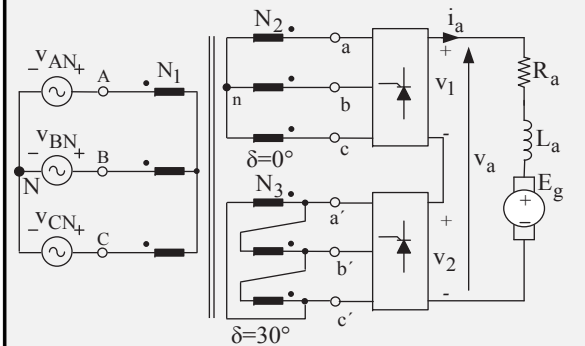
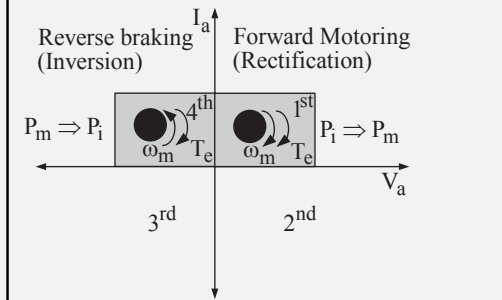
Continued

Table 12.1 DC motor drive systems employing thyristor rectifiers—cont'd

Thyristor rectifier topology	Quadrant(s) operation
 <p><b>c) Single-phase-bridge rectifier with freewheeling diode</b> (to avoid negative armature voltage) (Up to 20 hp)</p>	 <p>Forward Motoring Reverse braking (Inversion) Rectification <math>P_i \Rightarrow P_m</math></p>
 <p><b>d) Three-phase or six-pulse rectifier</b> (Up to 150 hp)</p>	 <p>Forward Motoring Reverse braking (Inversion) Rectification <math>P_m \Rightarrow P_i</math> <math>P_i \Rightarrow P_m</math></p>

Continued

Table 12.1 DC motor drive systems employing thyristor rectifiers

Thyristor rectifier topology	Quadrant(s) operation
<div></div> <p><b>e) Two parallel connected converters</b> (Up to 20 hp)</p>	<div></div>
<div></div> <p><b>f) 12-Pulse rectifier</b> (up to 300 hp)</p>	<div></div>



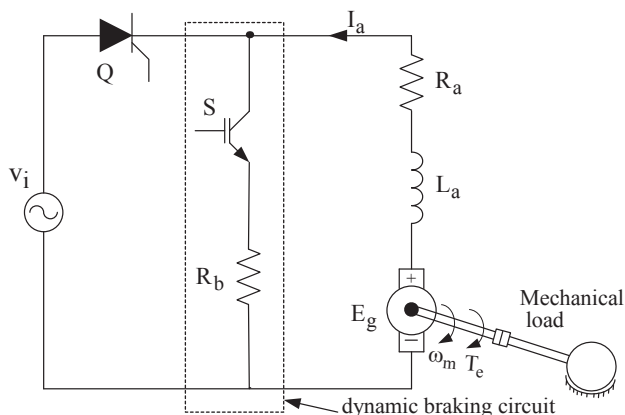


**Figure 12.11** DC motor drive system with dynamic braking.

thyristor rectifiers. The power semiconductor switches that are used for their implementation can be MOSFETs, IGBTs, GTOs, or MCTs depending on the output power requirements. In these motor drive systems when the electric machine operates as a motor then the power electronics topology operates as a rectifier rectifying the input ac source to dc and, consequently, transferring electrical power from the input ac source to the armature winding of the motor. When the electric machine operates as a generator then the power electronics topology operates as an inverter converting the dc voltage to ac and, consequently, transferring electrical power from the armature to the input ac source. The switching rectifiers were analyzed in Chapter 9.

- iii) **dc–dc converters or dc–dc choppers.** The basic characteristic of these motor drive systems, which are presented in Table 12.3, is that their input source voltage is dc. These motor drive systems are used from small to medium electrical power rating requirements.

Fig. 12.12 shows the operating modes of the step-down or first quadrant chopper presented in Table 12.3. Moreover, Fig. 12.13 shows the operating modes of the step-up or second quadrant chopper presented in Table 12.3. Finally, Fig. 12.14 shows the operating modes of the two-quadrant chopper presented in Table 12.3.

Fig. 12.15 shows the operating modes of the full-bridge or four-quadrant chopper presented in Table 12.3.

Fig. 12.16 shows a dc motor drive system that utilizes a three-phase PWM rectifier. The semiconductor switches depending on the power requirements of the electric machine and the mechanical load can be MOSFETs, IGBTs, GTOs, or MCTs. As shown in Fig. 12.16 the control system utilizes two control loops, one for controlling the speed of the motor and an inner loop for controlling the armature current. At this point it should be mentioned, that the implementation of the control circuit of a motor drive system utilizes a  $\mu\text{P}$  or a DSP so that to be able to program the control of any variable of the electric motor drive system. Finally, to achieve a fast and stable response of the control system a proportional-integral-derivative controller is applied to both feedback loops.

**Table 12.2 DC motor drive systems employing regenerative pulse width modulation (PWM) (or so-called switching) rectifier topologies**

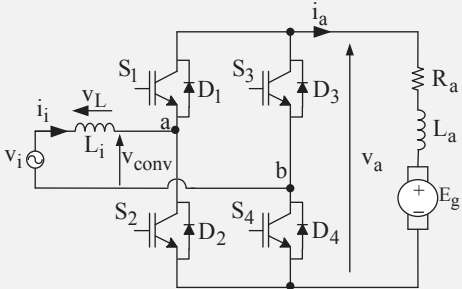
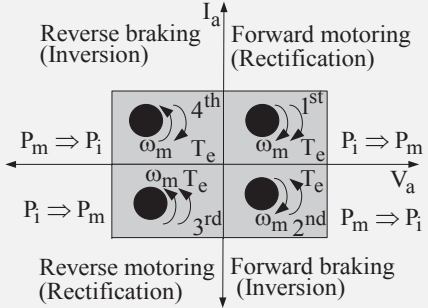
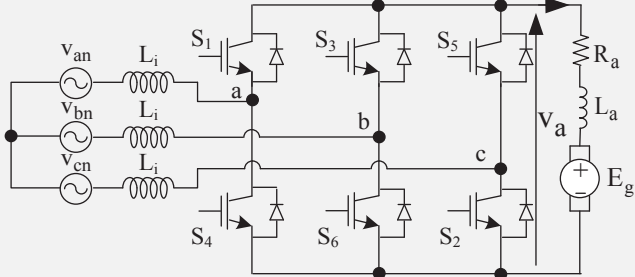
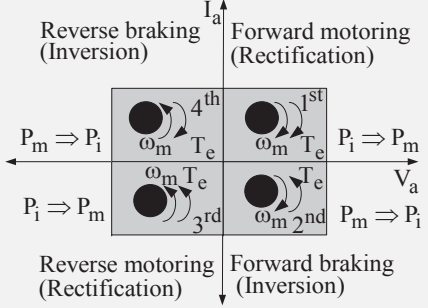
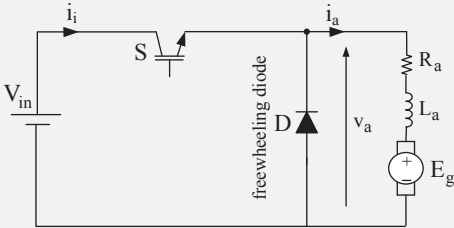
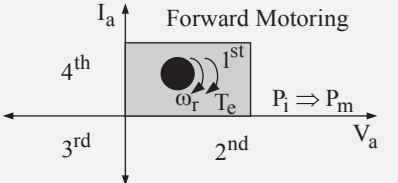
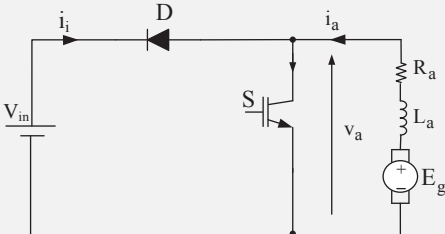
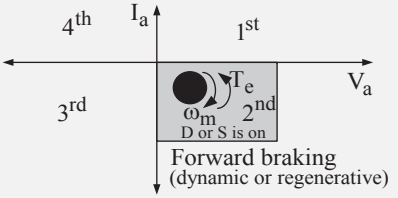
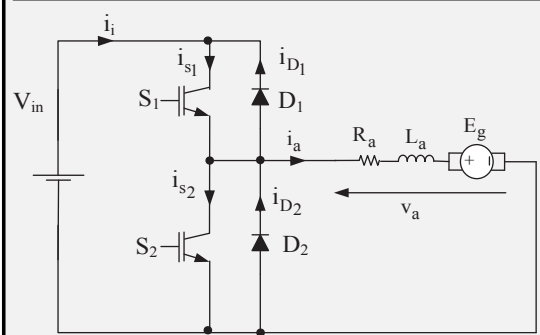
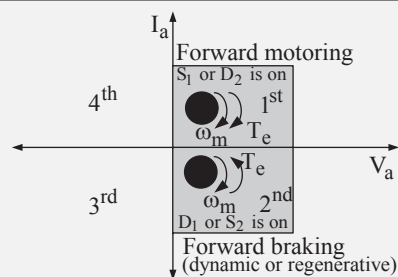
Switching rectifier topology	Quadrant(s) operation
 <p><b>a) Single-phase regenerative PWM rectifier</b></p>	
 <p><b>b) Three-phase regenerative PWM rectifier</b></p>	

Table 12.3 DC motor drive systems employing dc–dc converters—cont'd

dc–dc converter topology	Quadrant(s) of operation
 <p><b>a) Step-down chopper or first quadrant chopper</b></p> <ul style="list-style-type: none"> <li>When S is on and D is off: forward motoring.</li> <li>When S is off and D conducts: motor current decreases through freewheeling diode and the motor still in forward rotation.</li> </ul>	
 <p><b>b) Step-up chopper or second quadrant chopper</b></p> <ul style="list-style-type: none"> <li>When S is on and D is off: electrical energy is stored in <math>L_a</math>. During this mode forward dynamic braking is achieved.</li> <li>When S is off and D conducts: electrical power is transferred to the dc source and the motor operates in the forward braking regeneration mode.</li> </ul>	

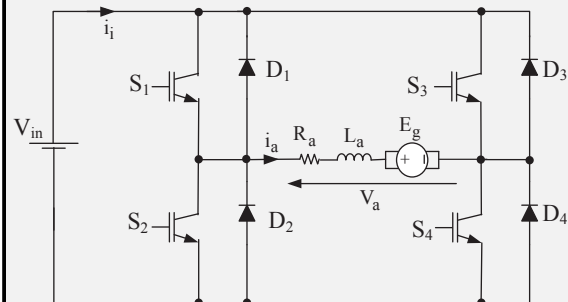
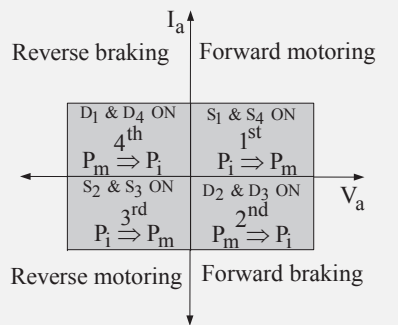
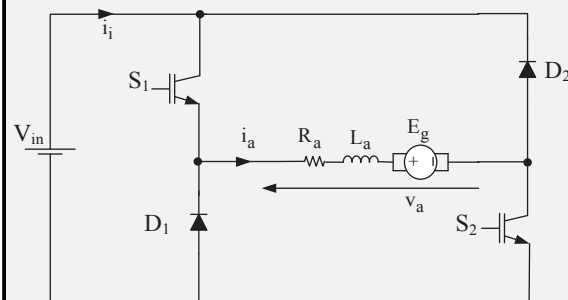
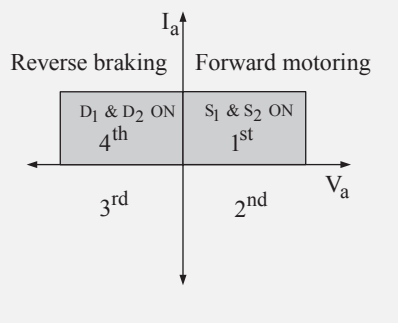
Continued

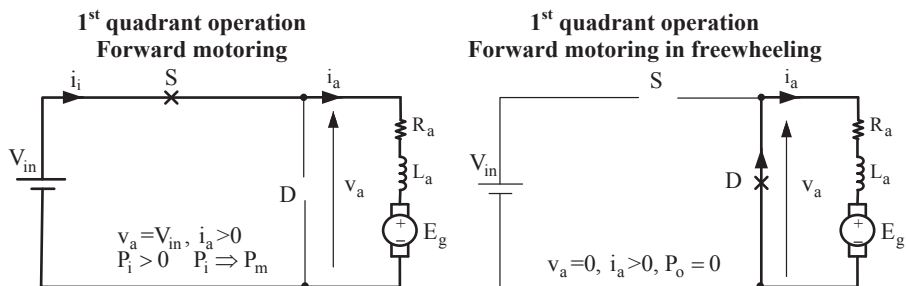
Table 12.3 DC motor drive systems employing dc–dc converters—cont’d

dc–dc converter topology	Quadrant(s) of operation
<div></div> <p><b>c) Two-quadrant chopper</b></p> <ul style="list-style-type: none"><li>• When <math>S_1</math> is on: forward motoring</li><li>• When <math>D_1</math> is on: forward regenerative braking</li><li>• When <math>S_2</math> is on: forward dynamic braking</li><li>• When <math>D_2</math> is on: motor current decreases through freewheeling diode and the motor still in forward rotation.</li></ul>	<div></div>

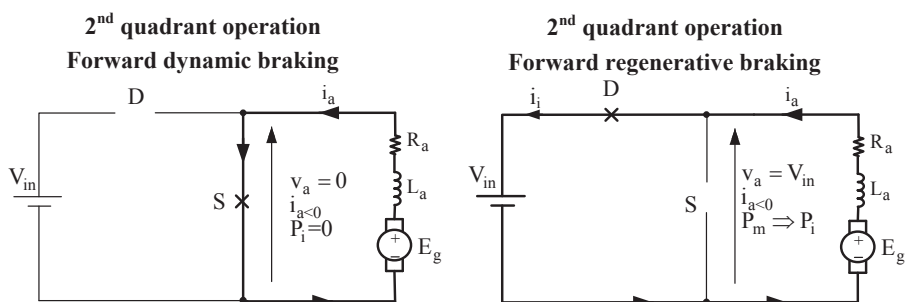
Continued

Table 12.3 DC motor drive systems employing dc–dc converters

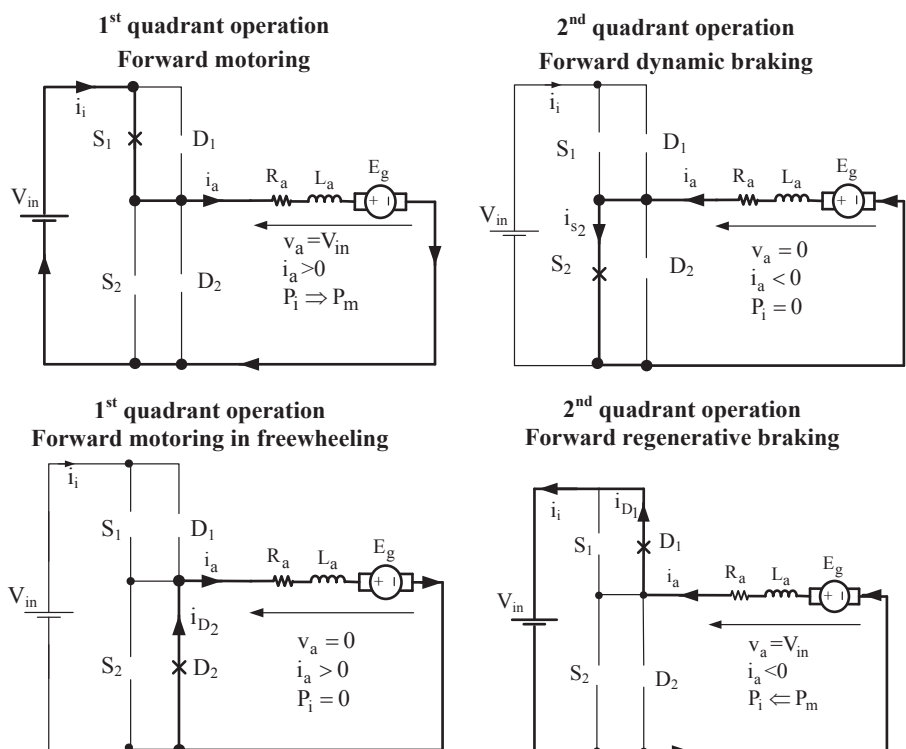
dc–dc converter topology	Quadrant(s) of operation
 <p><b>d) Four-quadrant full-bridge chopper</b></p>	
 <p><b>e) Two-quadrant or half-bridge chopper</b></p>	



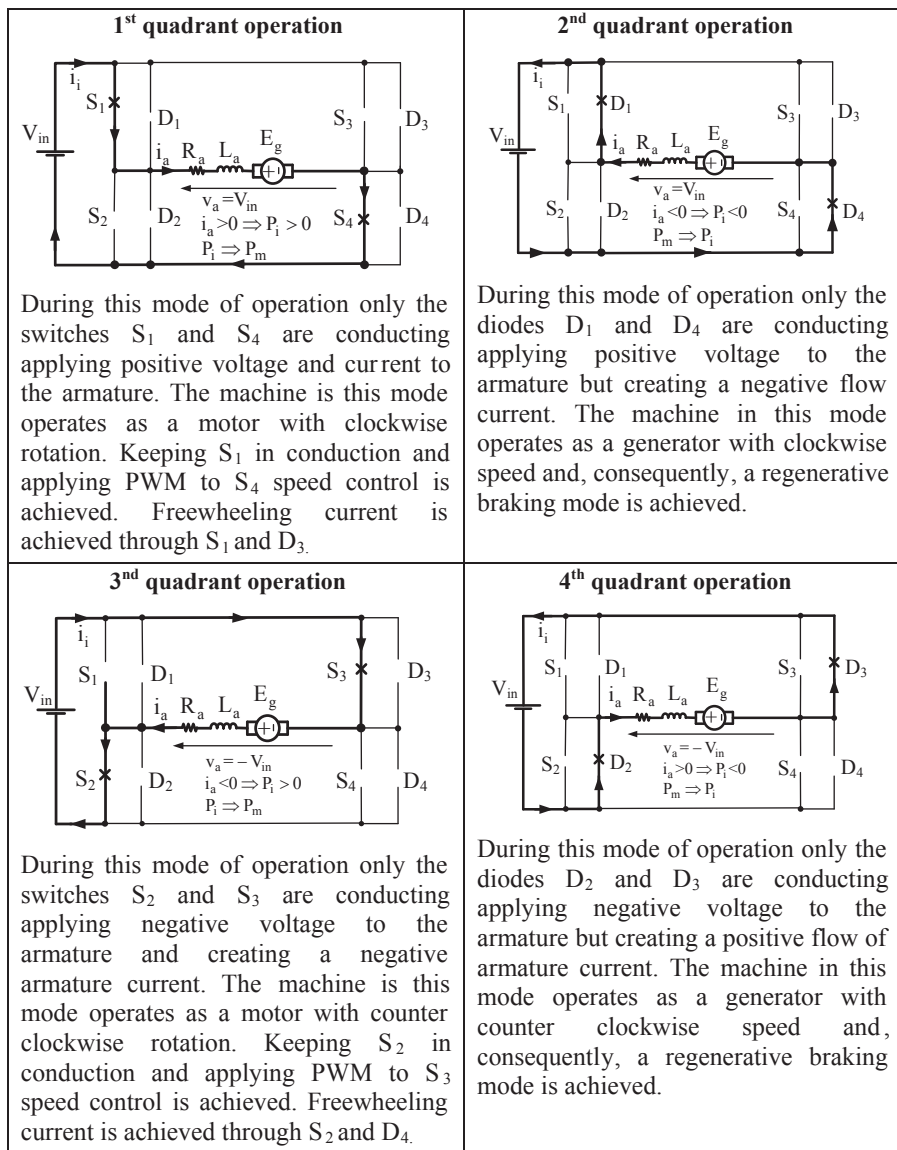
**Figure 12.12** Operating modes of the step-down or first quadrant chopper presented in [Table 12.3](#).



**Figure 12.13** Operating modes of the step-up or second quadrant chopper presented in [Table 12.3](#).



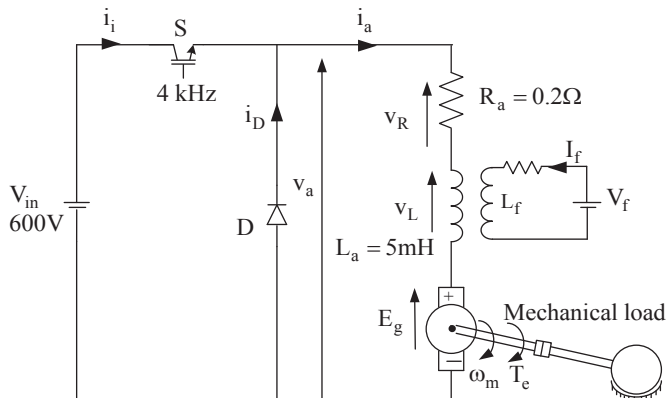
**Figure 12.14** Operating modes of the two-quadrant converter presented in [Table 12.3](#).



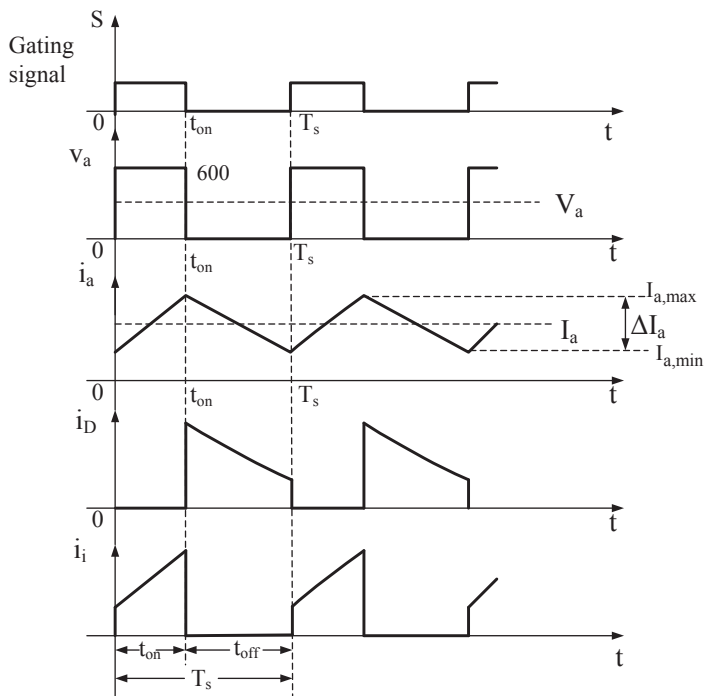
**Figure 12.15** Operating modes of the full-bridge four-quadrant converter presented in Table 12.3.





**Example 12.1—cont'd****Solution**

a) The waveforms of the dc motor drive system are shown below.



**Key waveforms of example 12.1**

Using the output voltage waveform the average output voltage is:

$$\begin{aligned} V_a &= \text{armature average voltage} = \frac{1}{T_s} \int_0^{T_s} v_a(t) dt \\ &= \frac{1}{T_s} \left[ \int_0^{t_{on}} V_{in} dt + \int_0^{T_s} 0 \cdot dt \right] = V_{in} \frac{t_{on}}{T_s} = V_{in} t_{on} f_s = V_{in} D \end{aligned} \quad (1)$$

where

$$D = \text{duty cycle} = \frac{t_{on}}{T_s}.$$

From the above circuit, the following equation exists:

$$v_a = \text{armature voltage} = R_a i_a + L_a \frac{di_a}{dt} + e_g \quad (2)$$

Moreover, at steady state the armature voltage and current and back electromagnetic force (EMF) have constant values and, consequently, then Eq. (2) becomes:

$$V_a = R_a I_a + E_g \quad \text{since} \quad \frac{dI_a}{dt} = 0 \quad (3)$$

The speed of the dc motor is given by:

$$\omega_m = \text{motor mechanical speed} = \frac{E_g}{K_v I_f} = \frac{V_a - R_a I_a}{K_v I_f} \quad (4)$$

Eq. (4) indicates that the speed of the motor can be varied by varying the armature voltage  $V_a$ . Therefore, if the rated speed of the motor is to be reduced by 50%, then the armature voltage must be reduced to half (i.e., to 300 V) and, consequently, the duty cycle will be:

$$D = \frac{V_a}{V_{in}} = \frac{300}{600} = 0.5 \quad (5)$$

The developed torque is  $T_d = K_t I_f I_a$ , and the field current is assumed to be always constant. Therefore, when the rated torque is reduced to 20% of its rated value the armature current will be reduced to 20% of its rated value which is  $(200)(0.2) = 40$  A.

The mechanical speed of the motor is  $\omega_m = \frac{E_g}{K_v I_f}$ , and the field current according to the specifications of the motor is always constant. Therefore, according to this equation when  $\omega_m$  drops to half the back-EMF will drop to half of its rated value.

$$E_{g(\text{rated})} = V_{a(\text{rated})} - R_a I_{a(\text{rated})} = 600 - (0.2)(200) = 560V$$

$$E_{g(\text{speed}50\%)} = \frac{E_{g(\text{rated})}}{2} = 280V$$

When the switch is on then the voltage across the inductor is given by:

$$v_L = L \frac{di_a}{dt} = V_{in} - R_a I_a - E_g \quad (6)$$

Therefore, using the above equation the range of change of the motor armature current is

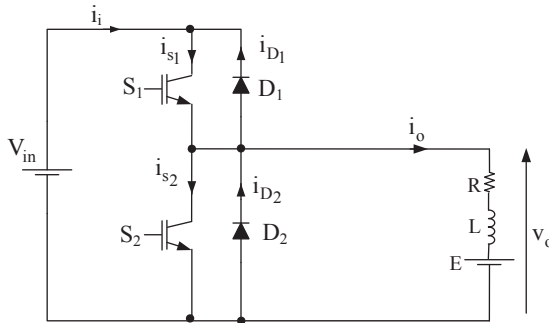
$$\frac{di_a}{dt} = \frac{V_{in} - R_a I_a - E_g}{L} \quad \text{or} \quad \frac{\Delta I_a}{t_{on}} = \frac{V_{in} - R_a I_a - E_g}{L} \quad (7)$$

Therefore, the armature peak to peak current ripple is given by:

$$\begin{aligned} \Delta I_{a(on)} &= \frac{V_{in} - R_a I_a - E_g}{L} t_{on} = \frac{V_{in} - R_a I_a - E_g}{L} D T_s \\ &= \frac{V_{in} - R_a I_a - E_g}{L f_s} D = \frac{600 - (40)(0.2) - 280}{(5 \times 10^{-3})(4000)} (0.5) = 7.8 \text{ A} \end{aligned}$$

### Example 12.2

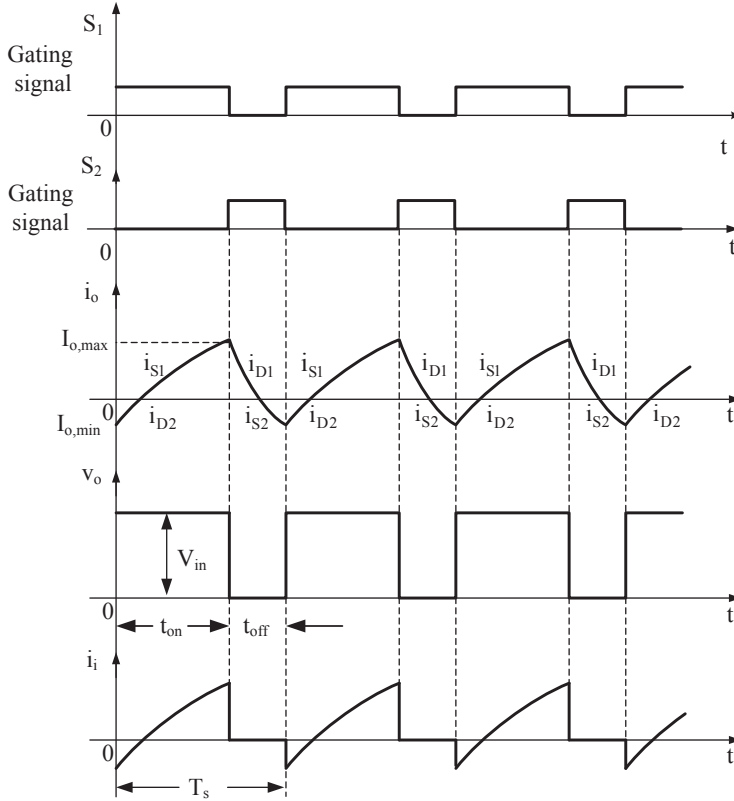
Perform the analysis of the following two-quadrant chopper under continuous output current operation.



### Solution

As it was shown from the equivalent circuits of Fig. 12.14, the main characteristic of this converter is that although the output voltage is always positive, the output current can take positive and negative values, contrary to the first quadrant converters, that allow only positive current values at their output. For this reason, the two-quadrant chopper has the advantage to transfer power from the load to the input source and vice versa. As can be seen from the above converter, the semiconductor devices  $S_1$  and  $D_2$  comprise a buck converter that operates during forward motoring mode (i.e.,

in the first quadrant) and the semiconductor devices  $S_2$  and  $D_1$  comprise a boost converter that operates during forward regenerative mode (i.e., in the second quadrant). The two figures below present the key waveforms of the converter when operating in the first and second quadrants, respectively.



**(a): First quadrant operation waveforms with continuous output current**

For the given converter, the following equations hold:

$$i_o = \frac{V_{in} - E}{R} \left(1 - e^{-t/\tau}\right) + I_{min} e^{-t/T_s} \quad \text{for } 0 \leq t \leq t_{on}$$

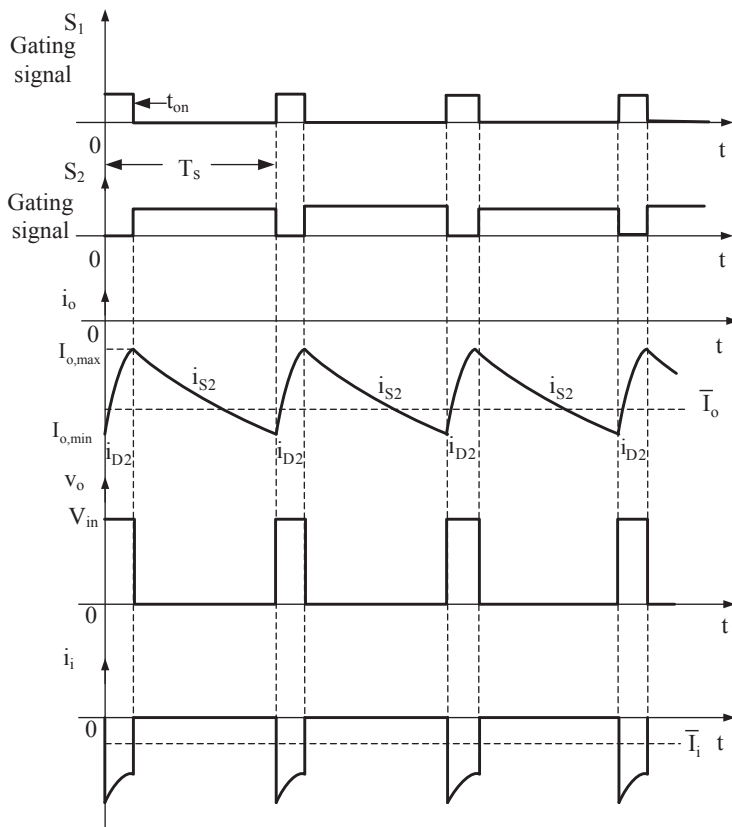
and

$$i_o = -\frac{E}{R} \left(1 - e^{-t'/\tau}\right) + I_{max} e^{-t'/\tau} \quad \text{for } t_{on} \leq t \leq T_s$$

where

$$I_{o,max} = \frac{V_{in}}{R} \frac{(1 - e^{-t_{on}/\tau})}{(1 - e^{-T_s/\tau})} - \frac{E}{R} \quad I_{o,min} = \frac{V_{in}}{R} \frac{(e^{t_{on}/\tau} - 1)}{(e^{T_s/\tau} - 1)} - \frac{E}{R}$$

$$\tau = \frac{L}{R} \quad t' = t - t_{on}$$



**(b): Second quadrant operation waveforms with continuous output current**

If  $I_{o,min} > 0$ , the converter operates only in the first quadrant and, consequently, the semiconductor devices  $S_2$  and  $D_2$  are not conducting. If  $I_{o,max} < 0$ , the converter operates only in the second quadrant, and, consequently, the semiconductor devices  $S_1$  and  $D_1$  are not conducting. If  $I_{o,max} > 0$  and  $I_{o,min} < 0$  the converter operates partly in the first and partly in the second quadrant and, consequently, all semiconductor devices are participating in the operation of the converter.

The average output voltage for continuous output current when the converter operates in the first quadrant (i.e., as buck converter) is given by:

$$\bar{V}_o = V_{in}D$$



Moreover:

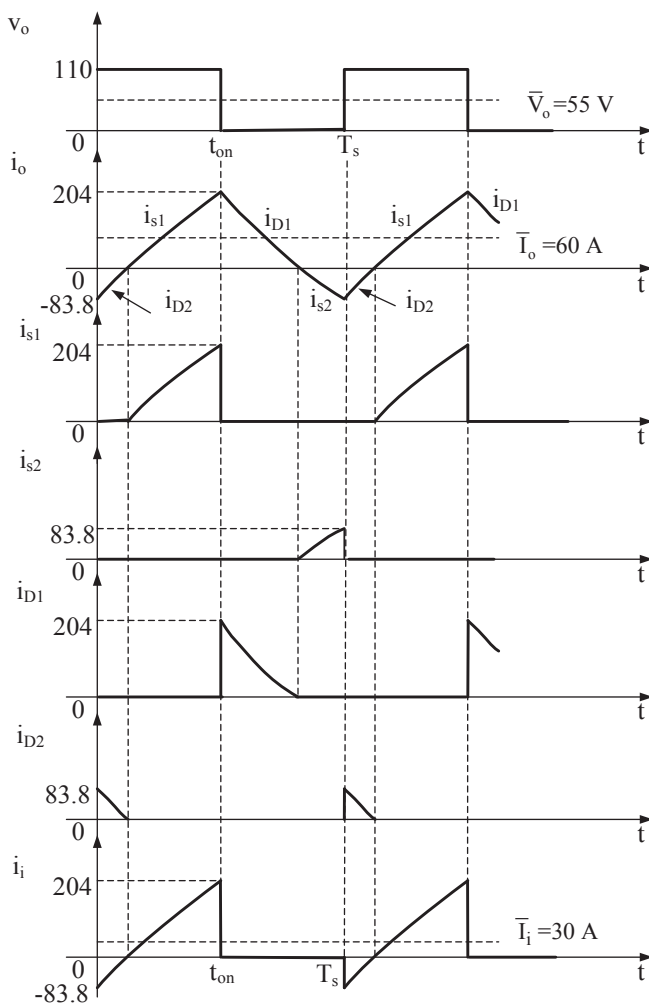
$$\frac{t_{on}}{\tau} = \frac{1250}{800} = 1.562 \quad \frac{T_s}{\tau} = \frac{2500}{800} = 3.125$$

Therefore, the following results are found:

$$I_{o,max} = \frac{110(1 - e^{-1.562})}{0.25(1 - e^{-3.125})} - \frac{40}{0.25} = 204 \text{ A}$$

$$I_{o,min} = \frac{110(e^{1.562} - 1)}{0.25(e^{3.125} - 1)} - \frac{40}{0.25} = -83.8 \text{ A}$$

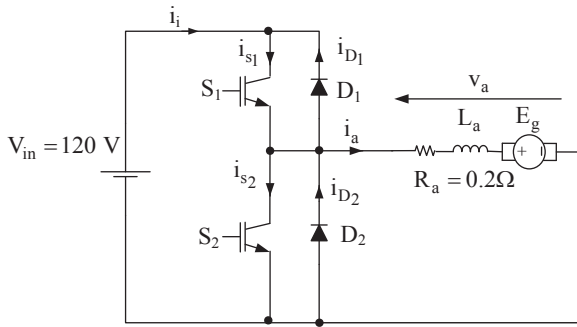
c) The waveforms of the corresponding variables are shown below.



Key waveforms of example 12.3

### Example 12.4

A small electric vehicle is powered from a 120 V battery bank and uses a series wound dc motor. The dc motor during motoring and regenerative modes is controlled by the converter which is shown below. The armature resistance is  $0.2 \Omega$  and the armature voltage constant is  $12 \text{ mV s/rad}$ . During a downhill regeneration mode the motor speed is 900 rpm and the armature current is pure dc of 100 A. Calculate the required duty cycle and the available braking power.



### Solution

As can be seen from the above converter, the semiconductor devices  $S_1$  and  $D_2$  comprise a step-down converter that operates during forward motoring mode and the semiconductor devices  $S_2$  and  $D_1$  comprise a step-up converter that operates during forward regenerative mode. The above converter is a two-quadrant converter that operates in the first and fourth quadrants. Due to the diode  $D_2$  the motor armature voltage is always positive and only the armature current takes positive and negative values. According to the above figure, the following equations hold:

$$E_g = \text{electromotive force} = \omega_m K_a I_a = \left( 900 \times \frac{2\pi}{60} \right) \times 12 \times 10^{-3} \times 100$$

$$= 113 \text{ V}$$

$$V_a = E_g - I_a R_a = 113 - 100 \times 0.2 = 63 \text{ V}$$

Therefore, during forward regenerative mode, where the boost converter operates, the following transfer function holds:

$$\frac{V_a}{V_{\text{battery}}} = \frac{1}{1 - D}$$



and consequently the duty cycle is given by :  $D = 1 - \frac{V_a}{V_{\text{battery}}} = 1 - \frac{63}{100} = 0.37$ .

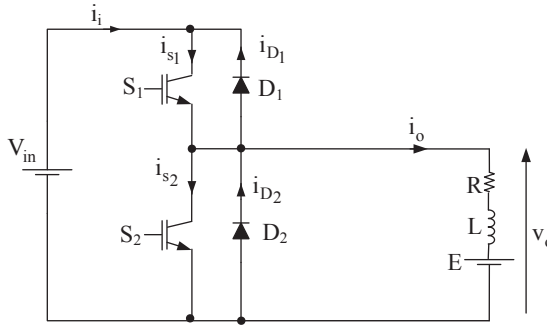
Also, the power delivered to the battery is given by

$$P_{\text{delivered}} = V_a I_a = 63 \times 100 = 6.3 \text{ kW}.$$

### Example 12.5

The converter shown below has the following parameters:  $V_{\text{in}} = 110 \text{ V}$ ,  $R = 0.15 \Omega$ ,  $E = 50 \text{ V}$ ,  $T_s = 4000 \mu\text{s}$ , and  $L$  has very large value so that the output current can be considered to be pure dc. Perform the following:

- Find the time  $t_{\text{on}}$  if  $i_o = \bar{I}_o = 100 \text{ A}$ . Also, draw the waveforms of variables  $v_o$  and  $i_i$ .
- Show that the input power is equal to the output power when the converter is considered to be ideal.
- Repeat (a) and (b) when  $i_o = \bar{I}_o = -100 \text{ A}$ .



### Solution

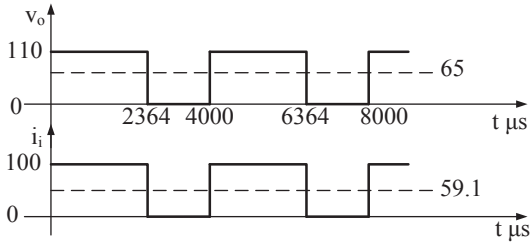
- a) The average output voltage is:

$$\bar{V}_o = E + R\bar{I}_o = 50 + 0.15 \times 100 = 65 \text{ V}$$

Using the equation  $\bar{V}_o = V_{\text{in}}D$  the value of the turn-on time is given by:

$$t_{\text{on}} = \frac{\bar{V}_o T_s}{V_{\text{in}}} = \frac{65 \times 4000 \times 10^{-6}}{110} = 2364 \mu\text{s}$$

The waveforms of variables  $v_o$  and  $i_i$  are shown below.



b) The average input current is:

$$\bar{I}_i = \frac{1}{T} \int_0^T i_i dt = \frac{1}{T_s} \int_0^{t_{on}} i_i dt = \frac{1}{4000} \int_0^{2364} 100 dt = \frac{2364}{4000} \times 100 = 59.1 \text{ A}$$

$$P_i = \text{input power} = V_{in} \bar{I}_i = 110 \times 59.1 = 6.50 \text{ kW}$$

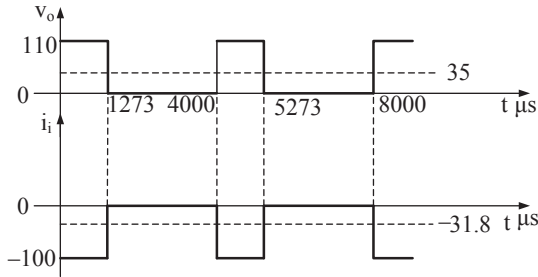
$$P_o = \text{output power} = \bar{V}_o \bar{I}_o = 65 \times 100 = 6.50 \text{ kW}$$

Consequently, input power = output power.

c)  $\bar{V}_o = E + R \bar{I}_o = 50 - 0.15 \times 100 = 35 \text{ V}$

$$t_{on} = \frac{35 \times 4000 \times 10^{-6}}{110} = 1273 \text{ } \mu\text{s}$$

The waveforms of variables  $v_o$  and  $i_i$  are shown below.



$$\begin{aligned} \bar{I}_i &= \frac{1}{T} \int_0^T i_i dt = \frac{1}{T_s} \int_0^{t_{on}} i_i dt = \frac{1}{4000} \int_0^{2364} (-100) dt = \frac{1273}{4000} (-100) \\ &= -31.8 \text{ A} \end{aligned}$$

$$P_i = \text{input power} = V_{in} \bar{I}_i = 110 \times (-31.8) = -3.5 \text{ kW}$$

$$P_o = \text{output power} = \bar{V}_o \bar{I}_o = 35 \times (-100) = -3.5 \text{ kW}$$

Therefore, input power = output power.

## 12.3 AC Motor Drive Systems

The AC electric motors are commonly used in practice covering a wide range of applications. There are many types of AC motors with different features and modes. They are divided into single-phase, two-phase, three-phase, and multiphase, depending on the number of ac supply voltages. Also, they are divided into synchronous and asynchronous motors, depending on the speed of rotation during normal operation. In most practical high power applications the three-phase motors are used which are supplied by three symmetrical ac voltages with  $120^\circ$  phase displacement. The ac motors, when compared to the dc ones are exhibiting the following advantages and disadvantages:

### Advantages

- 1) Higher power density
- 2) Higher reliability due to the absence of commutator and brushes
- 3) They need less maintenance
- 4) Lower implementation cost
- 5) Simple and robust implementation
- 6) Range of power of a few fractions to several thousand horse power motors

### Disadvantages

- 1) More complex control techniques

The disadvantage of the ac motors is overcome by controlling them using state-of-the-art semiconductor devices and digital systems [ $\mu$ Ps, DSPs, and field-programmable gate arrays (FPGAs)]. Using  $\mu$ Ps an ac motor can be controlled as a dc motor. The advantages of ac motors overcome their disadvantages and that is the reason that in most applications the ac motors are used.

There are two main categories of ac motors:

- 1) The ac asynchronous or induction motor
- 2) The ac synchronous motor

**Synchronous motors:** The synchronous motors, as indicated by their name rotate synchronously with the frequency of the input supply. Their operation is based on the interaction of two fields: the field excitation and armature field. The armature field, which is sinusoidally distributed on the stator, usually is created by three-phase windings which are located on the stator. The field excitation is placed on the rotor. It is usually an electromagnet (coil excitation or field winding), which is fed with constant voltage through brush. However, with the great research and the latest advances in technology have occurred resulting materials PMs with high remanence (up to 1.2 T) and high power binding together (up to 1000 kA/m), such as alloys

neodymium–iron–boron placed in the rotor surface. These materials allowed the replacement of the field winding usually require power brushes with a PM that does not need power supply. These motors are called PM synchronous motors and have received great research interest, and already used in practical applications with significant results. It is a more simple and reliable motor and have lower losses (and hence better performance) than the corresponding squirrel-cage rotor synchronous motors. Another type of synchronous motors, which gather attention for motor drive applications, are the reluctance motors (RMs). In the stator there are again three-phase windings of modern motors described above. The rotor, however, that consist of either PMs or electromagnets constructed in such a way as to show a small gap in the straight line (d) and large in the transverse axis (q) (i.e., small and large magnetic resistance, respectively). The existence of proportional spacing and, consequently, variable magnetic induction leads to the development of forces that turn the rotor to the position of minimum magnetic energy.

**Asynchronous motors or induction motors:** The asynchronous induction motors, as their name indicates, generally are rotating at a speed slightly less than the synchronous speed. The stator of the motor is identical to the stator of the synchronous motor and has a stable three-phase winding, creating a rotating and evenly distributed sinusoidal stator magnetic field. This field is directed to the synchronous speed. The operation of three-phase asynchronous motors is based on the phenomenon of creating EMF induced in the windings of the rotor by the rotating magnetic field of the stator windings. That is why these electric motors are called induction motors. There are two types of induction motors: (1) the squirrel-cage rotor and (2) the wound-rotor or slip ring induction motors. The main difference between them is the design of the motor rotor. The rotor in a squirrel-cage motor is made of conducting bars short-circuited by rings at both ends, while the rotor in the wound-rotor motor consists of windings similar to the stator windings. The advantages and disadvantages of these motors are presented in [Tables 12.4 and 12.5](#), respectively. Due to its simple construction, low construction cost, high efficiency, minimum maintenance, and high reliability, the squirrel-cage-rotor induction motor is widely used. The wound-rotor induction motor is rarely used and only about 10% of the industrial applications are using this type of motors.

**Table 12.4 Squirrel-cage induction motor**

Advantages	Disadvantages
<ul style="list-style-type: none"><li>• Lower cost</li><li>• Robust and simple construction</li><li>• High starting torque</li><li>• High running torques</li><li>• Easily reversed</li><li>• No moving contacts</li><li>• Higher efficiency</li><li>• Minimum maintenance</li></ul>	<ul style="list-style-type: none"><li>• Low starting torque</li><li>• Starting current is 7 times the full load current</li><li>• Speed control is not possible</li></ul>

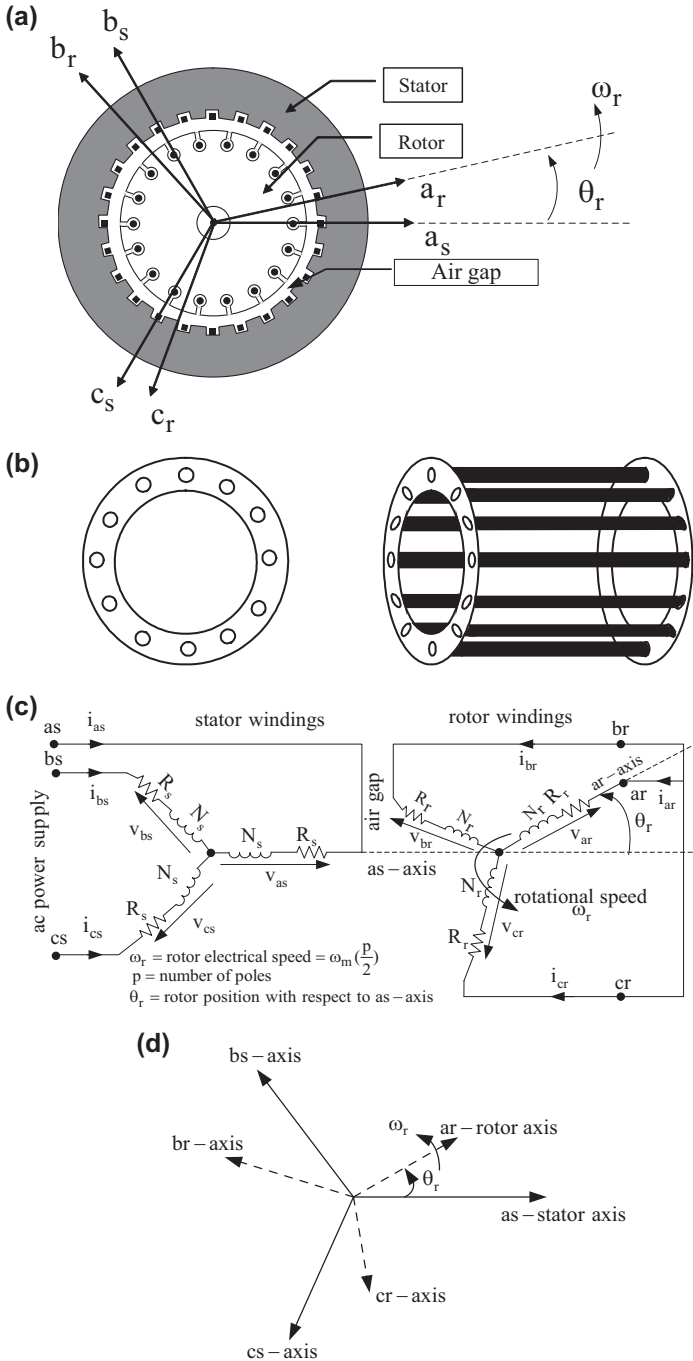
**Table 12.5 Wound-rotor or slip ring induction motor**

Advantages	Disadvantages
<ul style="list-style-type: none"> <li>• Ability to produce high starting torques at low starting currents. Starting current is comparatively less and it is 2–2.5 times the full load current</li> <li>• The motor can be started direct on line without the necessity of soft starters</li> <li>• Speed control by rotor resistance method is possible</li> </ul>	<ul style="list-style-type: none"> <li>• High cost</li> <li>• Lower efficiency</li> <li>• Higher degree of maintenance</li> <li>• Moving contacts and hence lower reliability</li> </ul>

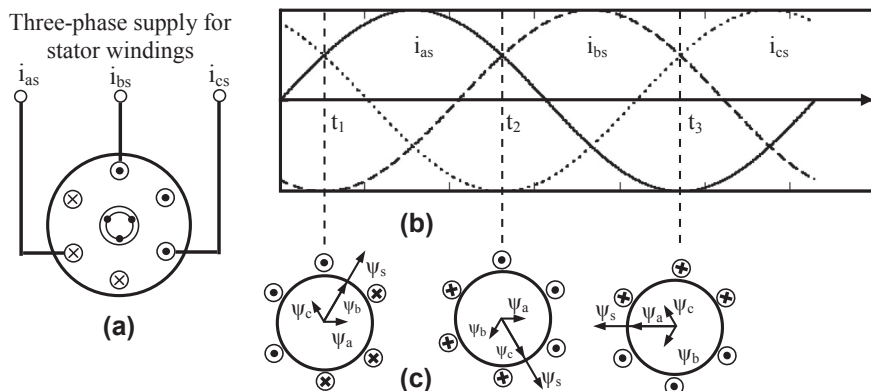
## 12.4 Asynchronous or Induction Motors

Fig. 12.17 shows a typical layout of a three-phase asynchronous motor where we see the poles of the rotor as well as the three-phase stator coordinates  $a_s$ – $b_s$ – $c_s$  which have a phase difference corresponding to the axes  $a_r$ – $b_r$ – $c_r$ . Similar to the stator, the rotor consists of iron core and windings. The core of the rotor is cylindrical made of steel and constructed in such away to create grooves in the axial region where the windings are placed. In this case the electric motor is said to be motor with squirrel-cage rotor. If the electric motor is a rotor cage type, in the core grooves, bars made from copper or aluminium or any other suitable alloy material are placed with their ends short-circuited with rings of the same material. Of the two types of three-phase motors reported the most common electric drive systems are those with cage rotor type because in case of power inverter, it is not required to connect external components to the rotor windings. It should be mentioned that the cage just described is the basis for all asynchronous motors. Certainly, based on the strength of the electric motor, speed, frequency, and voltage, there are manufacturing variations (deep grooves, double cage, etc.) while the construction materials (copper or aluminum) are selected according to the design requirements.

To produce rotational magnetic field, the stator windings must be properly placed (phase difference  $120^\circ$ ) and currents must flow through them which have among them a phase difference of  $120^\circ$ . To make easier the analysis of the induction motor, it has been assumed that the three-phase stator windings are flown by three symmetrical currents  $i_{as}$ ,  $i_{bs}$ , and  $i_{cs}$  with a phase difference of  $120^\circ$  among them as shown in Fig. 12.18.



**Figure 12.17 Schematic presentation of a squirrel-cage asynchronous motor.** (a) Cross section and the three-phase stator and rotor axes; (b) squirrel-cage rotor; (c) stator and rotor windings of a symmetrical asynchronous motor; (d) phasor diagram of stator and rotor three-phase axes ( $a_s$ – $b_s$ – $c_s$  and  $a_r$ – $b_r$ – $c_r$ , respectively).



**Figure 12.18** A three-phase symmetrical power supply provides a rotating magnetic field in an induction motor. (a) Stator windings; (b) stator winding phase currents; (c) stator rotating field.

### 12.4.1 Principles of Operation of Induction Motor

When the stator windings are fed by a symmetrical three-phase ac voltage system, they generate a rotating magnetic in the gap of the motor. The speed of this field depends on the electrical supply frequency,  $f$ , and the number of poles of the stator windings and is given by the following relationship:

$$\begin{aligned} \omega_e &= \text{electrical speed of the synchronously rotating reference frame} \\ &\text{with respect to stationary one} \\ &= \frac{2\omega}{P} \text{ rad/s} \end{aligned} \quad (12.22)$$

where

$f$  = stator or ac supply frequency Hz

$\omega$  = stator or ac supply electrical frequency =  $2\pi f$  rad/s

$P$  = induction machine number of poles.

Knowing that  $1 \text{ rad/s} = 9.55 \text{ rpm}$ , then from Eq. (12.22) the synchronous speed in rpm is given by:

$$\begin{aligned} n_e &= \text{synchronous speed of the rotating field} \\ &= \frac{2\omega}{P} (9.55) = \frac{2\pi f}{P} (9.55) = \frac{60f}{P} \text{ rpm} \end{aligned} \quad (12.23)$$

**i) Motor operation when the rotor is stationary (i.e.,  $n_r = 0$ )**

The behavior of the asynchronous motor, when rotor is stationary (i.e.,  $n_r = 0 \text{ rpm}$ ), is similar to that of a transformer, where in its magnetic circuit an air gap is inserted. In this case the induced voltages and currents (i.e., stationary rotor), have the same frequency as that of the ac supply voltage. The three-phase currents of the rotor create their own rotating field which interacts with the corresponding stator, thus creating

rotation of the rotor and, consequently, torque. Therefore, according to the conditions mentioned above, the induced per-phase voltages of the stator and rotor windings are given by the following equations:

$$v_{as} = \hat{V}_{as} \cos \omega t \quad v_{bs} = \hat{V}_{bs} \cos(\omega t - 120^\circ) \quad v_{cs} = \hat{V}_{cs} \cos(\omega t - 240^\circ) \quad (12.24)$$

$$v_{aro} = \hat{V}_{aro} \cos \omega_r t \quad v_{bro} = \hat{V}_{bro} \cos(\omega_r t - 120^\circ) \quad (12.25)$$

$$v_{cro} = \hat{V}_{cro} \cos(\omega_r t - 240^\circ)$$

$$\omega_r = \omega \quad (12.26)$$

(when rotor is stationary)

where

$\omega_r$  = electrical speed or electrical frequency of the rotor induced voltages in rad/s

$\omega$  = stator or input frequency =  $2\pi f$  rad/s

$$\hat{V}_{as} = \text{amplitude of the stator phase voltage} = 2\pi f K_s N_s \psi_\delta \quad \text{V} \quad (12.27)$$

$$\begin{aligned} \tilde{V}_{as} &= \text{rms value of the stator phase voltage} \\ &= \frac{2\pi f K_s N_s \psi_\delta}{\sqrt{2}} = 4.44 f K_s N_s \psi_\delta \quad \text{V} \end{aligned} \quad (12.28)$$

$$\begin{aligned} \hat{V}_{aro} &= \text{amplitude of rotor phase voltage} \\ &= 2\pi f_r K_r N_r \psi_\delta = 2\pi f K_r N_r \psi_\delta \quad \text{V} \end{aligned} \quad (12.29)$$

(when the rotor is not rotating)

$$\begin{aligned} \tilde{V}_{aro} &= \text{rms value of rotor phase voltage} \\ &= 4.44 f_r K_r N_r \psi_\delta = 4.44 f K_r N_r \psi_\delta \quad \text{V} \end{aligned} \quad (12.30)$$

(when the rotor is not rotating)

$K_s, K_r$  = stator and rotor winding construction factors

$N_s, N_r$  = stator and rotor winding number of turns per phase

$\psi_\delta$  = resultant air gap magnetic flux Wb

$f$  = stator frequency Hz

$f_r$  = rotor frequency Hz.

When the motor is stationary, using Eqs. (12.28) and (12.30), the following equation is obtained:

$$\frac{\hat{V}_{as}}{\tilde{V}_{aro}} = \frac{\tilde{V}_{as}}{\tilde{V}_{aro}} = \frac{K_s}{K_r} = \frac{N_s}{N_r} \quad (12.31)$$



Also it should be mentioned, that when the rotor is stationary the two magnetic fields (stator and rotor) are rotating with the same speed which results to a starting torque different than zero.

ii) Motor operation when the rotor is running with speed  $n_r < n_e$

If it is assumed that the motor operates in steady state and rotates with rotor speed  $n_r < n_e$  rpm, then for an observer who is sitting on the rotor, the air-gap magnetic field looks to rotate with a speed of  $n_e - n_r$  rpm. The difference between the motor speed and the synchronous speed is called the slip speed and is given by:

$$n_{sl} = n_e - n_m \text{ rpm} \quad (12.32)$$

where

$n_e$  = synchronous speed and  $n_m$  = mechanical speed of the motor.

The slip speed normalized by the synchronous speed is called simply “slip” and is given by:

$$s = \text{slip} = \frac{n_e - n_m}{n_e} = \frac{\omega_e - \omega_r}{\omega_e} = \frac{\omega_{sl}}{\omega_e} \quad (12.33(a))$$

or

$$s\% = \frac{n_e - n_r}{n_e} \times 100 \quad (12.33(b))$$

where

$\omega_e$  = electrical speed of synchronously rotating magnetic field rad/s.

$$\omega_r = \text{rotor electrical speed} = \omega_m \left( \frac{P}{2} \right) \text{ rad/s} \quad (12.34)$$

Using Eq. (12.32) the speed of the rotor can be found and is given as:

$$n_m = \text{rotor speed} = n_e(1 - s) \text{ rpm} \quad (12.35)$$

When the motor is stationary (i.e.,  $n_m = 0$  rpm), then from Eq. (12.31) it results that the slip  $s = 1$ ; and when the rotor speed is equal to the synchronous speed (i.e.,  $n_m = n_e$ ), then from Eq. (12.31) it results that the slip is  $s = 0$ .

The frequency of the induced voltages and currents of the rotor windings is related to the frequency of the ac supply source with the following equation:

$$f_r = \frac{P}{2} \frac{n_e - n_m}{60} = \frac{P}{2} s \frac{n_e}{60} = sf \text{ Hz} \quad (12.36)$$

**Example 12.6**

A three-phase six pole induction motor has the following specifications:

Rated power = 20 hp, ac supply line-to-line voltage = 208 V, 60 Hz, Y-connected, transfers 15 kW when the slip is 5%.

Calculate the following:

- a) The synchronous speed.
- b) The rotor speed.
- c) The electrical frequency of the rotor.

**Solution**

- a)  $n_e = 120 \frac{f}{P} = 120 \frac{60}{6} = 1200 \text{ rpm.}$
- b)  $n_m = n_e(1 - s) = 1200(1 - 0.05) = 1140 \text{ rpm.}$
- c)  $n_m = n_e(1 - s) = 1200(1 - 0.05) = 1140 \text{ rpm.}$

**Example 12.7**

A three-phase four pole induction motor has the following specifications:

Line-to-line voltage = 460 V, 60 Hz, rated power = 100 hp, transferring rated power when the slip is  $s = 0.05$ .

Calculate the following:

- a) The synchronous speed.
- b) The mechanical speed of the motor.
- c) The frequency of the rotor voltage windings.
- d) The speed of the slip.

**Solution**

- a)  $n_e = 120 \frac{f}{P} = 120 \frac{60}{4} = 1800 \text{ rpm.}$
- b)  $n_m = n_e(1 - s) = 1800(1 - 0.05) = 1710 \text{ rpm.}$
- c)  $f_r = sf = (0.05)(60) = 3 \text{ Hz.}$
- d)  $n_{sl} = n_e - n_r = 1800 - 1710 = 90 \text{ rpm.}$

### 12.4.2 Equivalent Circuits and Steady-State Equations of Induction Motor

In the past, various types of equivalent circuits have been proposed for induction motors, which exhibited a number of advantages and disadvantages. Some of these circuits are suitable for steady-state analysis and some for transient analysis. Specifically when these models are supplied from a voltage source inverter, then

they have additional problems due to the high order harmonic components. In this area, research efforts are presented to create a general or generalized model that can cover the largest possible number of modes of induction motor. In this chapter the classical per-phase equivalent circuit will be presented, exhibiting good behavior in the transient and steady-state modes of operation. It is worth noting that in most papers dealing with control of induction motors the classical equivalent circuit is used. Fig. 12.19 shows the complete classical per-phase equivalent circuit of a three-phase induction motor when it is in steady-state mode of operation.

Using Fig. 12.19 the input voltage vector  $\vec{V}_s$  is given by the following equation:

$$\vec{V}_s = (R_s + jX_s) \vec{I}_s + \vec{V}_m \quad (12.37)$$

where

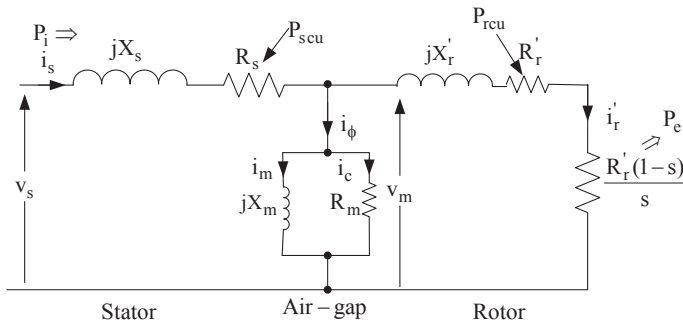
$R_s$  = stator resistance and  $X_s$  = stator reactance =  $2\pi fL_s$ .

The resistance  $R'_r$  represents the per-phase rotor copper losses and the resistance  $\frac{R'_r(1-s)}{s}$  represents the per-phase output power when the slip is  $s$ .

Also, using Fig. 12.19, the following steady-state equations are obtained:

$$P_{scu} = \text{stator copper losses} = 3\tilde{I}_s^2 R_s \text{ W} \quad (12.38)$$

$$P_{rcu} = \text{rotor copper losses} = 3\tilde{I}_r'^2 R'_r \text{ W} \quad (12.39)$$



where

$v_s$  = stator phase voltage;  $i_s$  = stator phase current;

$v_m$  = magnetic circuit voltage;  $i_\phi$  = magnetic circuit current;

$i_m$  = current of the magnetic circuit reactance;  $R_s$  = stator per phase resistance;

$X_s$  = stator per phase reactance;  $i_r'$  = rotor per phase current referred to the stator;

$R'_r$  = rotor per phase resistance referred to the stator;

$X'_r$  = rotor per phase reactance referred to the stator;

$R_m$  = magnetic circuit resistance;  $X_m$  = reactance of the magnetic circuit inductance;

$s$  = slip;

$P_e$  = electromagnetic or developed power;

**Figure 12.19** Steady-state equivalent circuit for one phase of a three-phase induction motor with the rotor parameters referred to the stator. The resistance  $R'_r$  represents the per-phase rotor copper losses and the resistance  $R'_r(1-s)/s$  represents the per-phase output power when the slip is  $s$ .

$$P_c = \text{core losses} = 3 \frac{\tilde{V}_m^2}{R_m} \approx 3 \frac{\tilde{V}_s^2}{R_m} \text{ W} \quad (12.40)$$

$$P_g = \text{power that goes through air gap to the rotor} = 3 \tilde{I}_r'^2 \frac{R'_r}{s} \text{ W} \quad (12.41)$$

$P_e$  = motor electromagnetic or developed power

$$= P_g - P_{\text{rcu}} = 3 \tilde{I}_r'^2 \frac{R'_r}{s} (1 - s) = P_g (1 - s) \text{ W} \quad (12.42)$$

$T_e$  = motor developed electromagnetic torque

$$\begin{aligned} &= \frac{P_e}{\omega_m} = \frac{3}{\omega_m} \tilde{I}_r' \frac{R'_r}{s} (1 - s) \\ &= \frac{P_g (1 - s)}{\omega_e (1 - s)} = \frac{P_g}{\omega_e} \end{aligned} \quad (12.43)$$

$$P_i = \text{Input power drawn by the motor} = 3 \tilde{V}_s \tilde{I}_s \cos \phi = P_c + P_{\text{scu}} + P_g \text{ W} \quad (12.44)$$

$P_m$  = mechanical power developed on the shaft of the motor

$$= P_e - \text{losses (friction + ventilation +)} \quad (12.45)$$

$$= P_e - P_{\text{rotational}} \text{ W}$$

$$T_m = \text{mechanical output torque of the motor} = T_e - \frac{P_{\text{rotational}}}{\omega_m} \text{ Nm} \quad (12.46)$$

$$\eta \% = \text{motor efficiency} = \frac{P_m}{P_i} \times 100 \quad (12.47(a))$$

or

$$\eta \% = \text{motor efficiency} = \frac{P_e - P_{\text{friction}}}{P_c + P_{\text{s cu}} + P_g} \times 100 \quad (12.47(b))$$

where

$\tilde{V}_s$  = rms value of the stator phase voltage

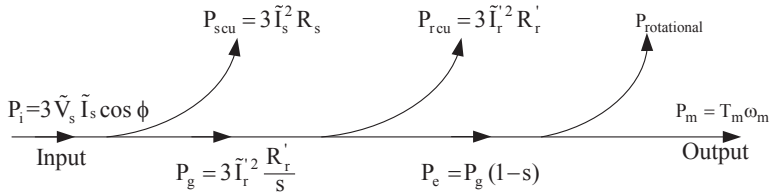
$\tilde{I}_s$  = rms value of the stator phase current

$\phi$  = displacement angle between stator voltage and current or displacement factor angle

$\tilde{V}_m$  = rms value of the magnetic circuit phase voltage

$\omega_m$  = motor mechanical speed

$P_{\text{rotational}}$  = friction and ventilation losses.



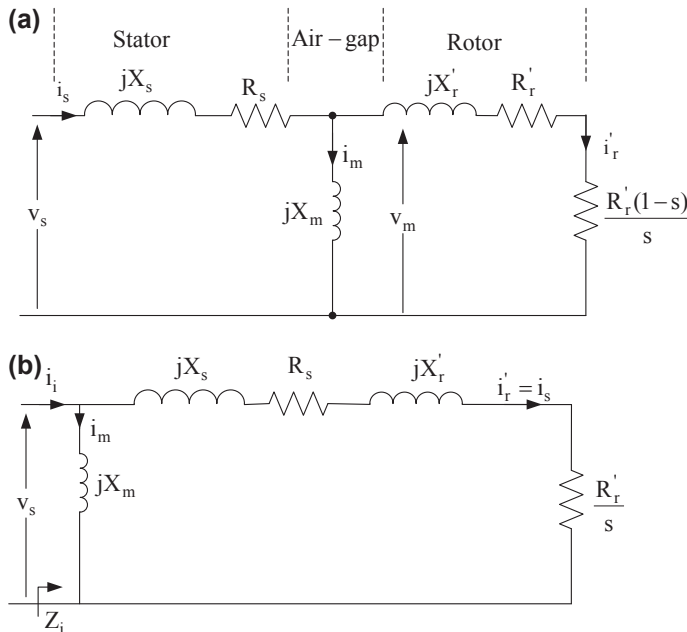
**Figure 12.20** Power flow and losses of an induction motor.

Fig. 12.20 shows the power flow and losses of an induction motor.

An approximate equivalent circuit of an induction motor can be obtained when the parallel resistance  $R_m$  of the magnetic circuit is neglected neglecting at the same time the respective core losses from the torque and output power equations. Therefore, the equivalent circuit of Fig. 12.19 can be approximated as shown in Fig. 12.21(a). Moreover, if  $X_m^2 \gg (R_s^2 + X_s'^2)$ , then  $v_s \approx v_m$  and, consequently, the circuit of Fig. 12.21(a) can be further approximated as shown in Fig. 12.21(b).

Using Fig. 12.21(b) and knowing that  $\bar{Z}_i = Z_i \angle \phi$ , then the following equations are obtained:

$$Z_i = \frac{-X_m(X_s + X_r') + jX_m\left(R_s + \frac{R_r'}{s}\right)}{\left(R_s + \frac{R_r'}{s}\right) + j(X_m + X_s + X_r')} \quad (12.48)$$



**Figure 12.21** (a) Approximate per-phase steady-state equivalent circuit of an induction motor when the resistance  $R_m$  is neglected. (b) Approximate per-phase steady-state equivalent circuit of an induction motor when  $X_m^2 \gg (R_m^2 + X_s'^2)$ .

$\phi$  = displacement factor angle

$$= \pi - \tan^{-1} \left( \frac{R_s + \frac{R_r'}{s}}{X_s + X_r'} \right) + \tan^{-1} \left( \frac{X_s + X_r' + X_m}{R_s + \frac{R_r'}{s}} \right) \quad (12.49)$$

$$\tilde{I}_r' = \frac{\tilde{V}_s}{\left[ \left( R_s + \frac{R_r'}{s} \right)^2 + (X_s + X_r')^2 \right]^{1/2}} \quad (12.50)$$

Substituting Eq. (12.50) into Eq. (12.41) and Eq. (12.41) into Eq. (12.43), the following equation is obtained:

$$T_e = \text{Torque} - \text{speed characteristic} = \frac{3\tilde{V}_s^2 R_r'}{s\omega_e \left[ \left( R_s + \frac{R_r'}{s} \right)^2 + (X_s + X_r')^2 \right]^{1/2}} \quad (12.51)$$

Fig. 12.22 shows a typical torque—speed characteristic of an induction motor which is symmetrical about the synchronous speed (i.e.,  $s = 0$ ). As shown in Fig. 12.21 depending on the slip value the induction machine can operate in any of the following three operation regions: (1) motor region when  $0 \leq s \leq 1$ , (2) positive regeneration region when  $s < 0$ , and (3) negative regeneration region when  $s > 1$ .

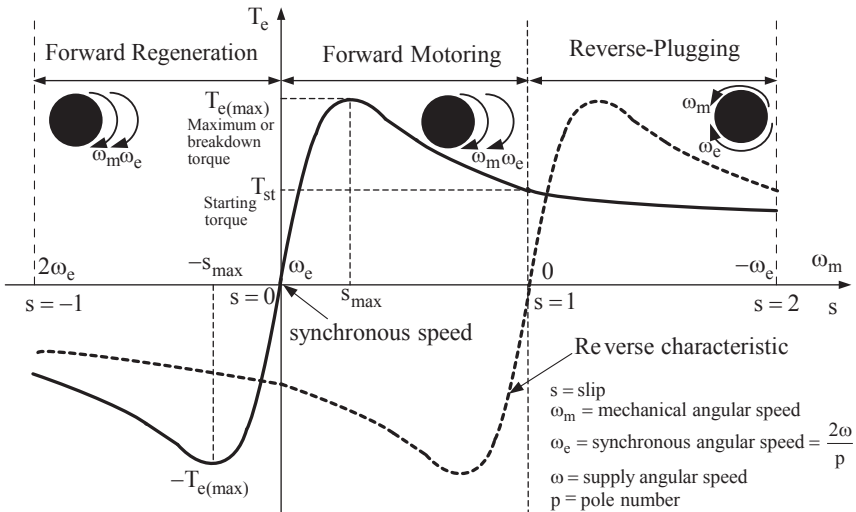


**Figure 12.22** Torque—speed characteristics of an induction machine with constant voltage and frequency.

At starting, the speed of the motor is  $\omega_m = 0$  and the slip  $s = 1$  and, consequently, using Eq. (12.41) the starting torque of the motor is found and is given by the following equation:

$$T_{st} = \text{starting torque} = \frac{3R'_r \tilde{V}_s^2}{\omega_e \left[ \left( R_s + \frac{R'_r}{s} \right)^2 + (X_s + X'_r)^2 \right]} \quad (12.52)$$

Using Eq. (12.51) and setting  $\frac{dT_e}{ds} = 0$ , then the slip for maximum torque can be calculated and is given by the following equation:

$$s_{\max} = \pm \frac{R'_r}{\left[ (R_s)^2 + (X_s + X'_r)^2 \right]^{\frac{1}{2}}} \quad (12.53)$$

Substituting  $s = +s_{\max}$  into Eq. (12.51) the maximum torque during motoring mode is found and is given by:

$$T_{\max(\text{motor})} = \frac{3 \tilde{V}_s^2}{2\omega_e \left[ R_s + \sqrt{R_s^2 + (X_s + X'_r)^2} \right]} \quad (12.54)$$

Substituting  $s = -s_{\max}$  into Eq. (12.51) the maximum torque during regenerative mode is found and is given by:

$$T_{\max(\text{regen})} = \frac{3 \tilde{V}_s^2}{2\omega_e \left[ -R_s + \sqrt{R_s^2 + (X_s + X'_r)^2} \right]} \quad (12.55)$$

### Example 12.8

A three-phase 480 V, 50 Hz induction motor draws 60 A with power factor 0.85. The stator copper losses are 2 kW and the rotor copper losses are 700 W. The core losses are 1800 W and the friction + ventilation losses are 600 W. Calculate the following:

- The air-gap power.
- The converted power.
- The output power.
- The motor efficiency.

### Solution

a)  $P_i = \text{Input power} = \sqrt{3}\tilde{V}_{ab}\tilde{I}_a \cos\phi = \sqrt{3}(480)(60)(0.85) = 42.4 \text{ kW}$

$P_g = P_i - P_{\text{scu}} = 42400 - 2000 = 40.4 \text{ kW}.$

b)  $P_e = P_g - P_{\text{rcu}} = 40400 - 700 = 39.7 \text{ kW}.$

c)  $P_m = \text{mechanical power developed on the motor shaft}$   
 $= P_e - P_{\text{core}} - P_{\text{rotational}} = 39700 - 1800 - 600 = 37.3 \text{ kW}.$

d)  $\eta\% = \frac{P_m}{P_i} = \frac{37.3}{42.4} = 88\%.$

### 12.4.3 Induction Motor General Equations

Using Fig. 12.17 the stator and rotor phase voltages, currents, and magnetic fluxes are given by the following equations:

$$\text{Stator phase voltage equations} \begin{cases} v_{as} = R_{as}i_{as} + \frac{d\psi_{as}}{dt} \\ v_{bs} = R_{bs}i_{bs} + \frac{d\psi_{bs}}{dt} \\ v_{cs} = R_{cs}i_{cs} + \frac{d\psi_{cs}}{dt} \end{cases} \quad (12.56)$$

$$\text{Rotor phase voltage equations} \begin{cases} v_{ar} = R_{ar}i_{ar} + \frac{d\psi_{ar}}{dt} \\ v_{br} = R_{br}i_{br} + \frac{d\psi_{br}}{dt} \\ v_{cr} = R_{cr}i_{cr} + \frac{d\psi_{cr}}{dt} \end{cases} \quad (12.57)$$

or in vector form

$$\vec{v}_{abcs} = \vec{R}_s \vec{i}_{abcs} + \frac{d\vec{\psi}_{abcs}}{dt} \quad (12.58)$$

$$\vec{v}_{abcr} = \vec{R}_r \vec{i}_{abcr} + \frac{d\vec{\psi}_{abcr}}{dt} \quad (12.59)$$

where

$$\vec{v}_{abcs} = \begin{bmatrix} v_{as} \\ v_{bs} \\ v_{cs} \end{bmatrix} \quad \vec{i}_{abcs} = \begin{bmatrix} i_{as} \\ i_{bs} \\ i_{cs} \end{bmatrix} \quad \vec{\psi}_{abcs} = \begin{bmatrix} \psi_{as} \\ \psi_{bs} \\ \psi_{cs} \end{bmatrix}$$



$$\vec{V}_{abcr} = \begin{bmatrix} V_{ar} \\ V_{br} \\ V_{cr} \end{bmatrix} \quad \vec{i}_{abcr} = \begin{bmatrix} i_{ar} \\ i_{br} \\ i_{cr} \end{bmatrix} \quad \vec{\psi}_{abcr} = \begin{bmatrix} \psi_{ar} \\ \psi_{br} \\ \psi_{cr} \end{bmatrix}$$

$$\vec{R}_s = \begin{bmatrix} R_s & 0 & 0 \\ 0 & R_s & 0 \\ 0 & 0 & R_s \end{bmatrix} \quad \vec{R}_r = \begin{bmatrix} R_r & 0 & 0 \\ 0 & R_r & 0 \\ 0 & 0 & R_r \end{bmatrix}$$

$V_{as}, V_{bs}, V_{cs}$  = stator phase voltages

$i_{as}, i_{bs}, i_{cs}$  = stator phase currents

$V_{ar}, V_{br}, V_{cr}$  = rotor phase voltages

$i_{ar}, i_{br}, i_{cr}$  = rotor phase currents

$R_s, R_r$  = stator and rotor per-phase winding resistance, respectively

$\psi_{as}, \psi_{bs}, \psi_{cs}$  = stator winding magnetic flux

$\psi_{ar}, \psi_{br}, \psi_{cr}$  = rotor winding magnetic flux.

For a linear magnetic system the stator and rotor magnetic fluxes can be written as follows:

$$\begin{bmatrix} \vec{\psi}_{abcs} \\ \vec{\psi}_{abcr} \end{bmatrix} = \begin{bmatrix} \vec{L}_s & \vec{L}_{sr} \\ (\vec{L}_{sr})^T & \vec{L}_r \end{bmatrix} \begin{bmatrix} \vec{i}_{abcs} \\ \vec{i}_{abcr} \end{bmatrix} \quad (12.60)$$

where

$$\vec{L}_s = \begin{bmatrix} L_{ms} + L_{ls} & -\frac{L_{ms}}{2} & -\frac{L_{ms}}{2} \\ -\frac{L_{ms}}{2} & L_{ms} + L_{ls} & -\frac{L_{ms}}{2} \\ -\frac{L_{ms}}{2} & -\frac{L_{ms}}{2} & L_{ms} + L_{ls} \end{bmatrix} \quad (12.61)$$

$$\vec{L}_r = \begin{bmatrix} L_{mr} + L_{lr} & -\frac{L_{mr}}{2} & -\frac{L_{mr}}{2} \\ -\frac{L_{mr}}{2} & L_{mr} + L_{lr} & -\frac{L_{mr}}{2} \\ -\frac{L_{mr}}{2} & -\frac{L_{mr}}{2} & L_{mr} + L_{lr} \end{bmatrix} \quad (12.62)$$

$$\vec{L}_{sr} = L_{sr} \begin{bmatrix} \cos\theta_r & \cos(\theta_r + 2\pi/3) & \cos(\theta_r - 2\pi/3) \\ \cos(\theta_r - 2\pi/3) & \cos\theta_r & \cos(\theta_r + 2\pi/3) \\ \cos(\theta_r + 2\pi/3) & \cos(\theta_r - 2\pi/3) & \cos\theta_r \end{bmatrix} \quad (12.63)$$

$L_{ls}, L_{lr}$  = stator and rotor leakage inductance, respectively (H)

$L_{ms}, L_{mr}$  = stator and rotor magnetizing inductance, respectively (H)

$L_{sr}$  = mutual inductance between stator and rotor windings (H)

$\theta_r = \theta_r(0) + \int_0^t \omega_r(t)dt$  = angle between the stator phase axes  $a_s$ – $b_s$ – $c_s$  and the rotor axes  $a_r$ – $b_r$ – $c_r$ .

When the general equations of an induction motor are presented it is more convenient to be referred to the stator winding by using the appropriate turns ratio.

$$\vec{i}'_{abcr} = \text{rotor current referred to the stator winding} = \frac{N_r}{N_s} \vec{i}_{abcr} \quad (12.64)$$

$$\vec{v}'_{abcr} = \text{rotor voltage referred to the stator winding} = \frac{N_s}{N_r} \vec{v}_{abcr} \quad (12.65)$$

$$\vec{\psi}'_{abcr} = \text{rotor magnetic flux referred to the stator winding} = \frac{N_s}{N_r} \vec{\psi}_{abcr} \quad (12.66)$$

where

$N_s$  = stator number of turns and  $N_r$  = rotor number of turns.

The magnetizing and mutual inductance are related with the same direction of the magnetic flux and, consequently, the following equations for  $L_{ms}$ ,  $L_{mr}$ , and  $L_{sr}$  hold:

$$L_{ms} = \frac{N_s}{N_r} L_{sr} \quad (12.67)$$

$$L'_{sr} = \frac{N_s}{N_r} L_{sr}$$

$$= L_{ms} \begin{bmatrix} \cos\theta_r & \cos(\theta_r + 2\pi/3) & \cos(\theta_r - 2\pi/3) \\ \cos(\theta_r - 2\pi/3) & \cos\theta_r & \cos(\theta_r + 2\pi/3) \\ \cos(\theta_r + 2\pi/3) & \cos(\theta_r - 2\pi/3) & \cos\theta_r \end{bmatrix} \quad (12.68)$$

$$L_{mr} = \left( \frac{N_r}{N_s} \right)^2 L_{ms} \quad (12.69)$$

Assigning

$$L_r' = \left( \frac{N_s}{N_r} \right)^2 L_r \quad (12.70)$$

then from Eq. (12.62), the following equation results:

$$\vec{L}_r' = \begin{bmatrix} L_{mr} + L_{lr}' & -\frac{L_{ms}}{2} & -\frac{L_{ms}}{2} \\ -\frac{L_{ms}}{2} & L_{ms} + L_{lr}' & -\frac{L_{mr}}{2} \\ -\frac{L_{ms}}{2} & -\frac{L_{ms}}{2} & L_{ms} + L_{lr}' \end{bmatrix} \quad (12.71)$$

The voltage and currents of the induction motor referred to the stator windings can be written in vector form as follows:

$$\begin{bmatrix} \vec{v}_{abcs} \\ \vec{v}_{abcr}' \end{bmatrix} = \begin{bmatrix} \vec{R}_s + \vec{L}_s \frac{d}{dt} & \vec{L}_{sr}' \frac{d}{dt} \\ (\vec{L}_{sr}')^T \frac{d}{dt} & \vec{R}_r' + \vec{L}_r' \frac{d}{dt} \end{bmatrix} \begin{bmatrix} \vec{i}_{abcs} \\ \vec{i}_{abcr}' \end{bmatrix} \quad (12.72)$$

where

$$\vec{R}_r' = \left( \frac{N_s}{N_r} \right)^2 \vec{R}_r \quad (12.73)$$

The developed electromagnetic torque of an induction motor is also given by the following equation:

$$T_e = J \left( \frac{2}{P} \right) \frac{d\omega_m}{dt} + T_L \quad (12.74)$$

where

$T_e$  = developed electromagnetic torque

$J$  = rotor inertia factor (Nm s<sup>2</sup>)

$T_L$  = load torque

$P$  = number of poles

$\omega_m$  = rotor mechanical angular speed.

The developed torque of an induction motor in vector form can be written as follows:

$$T_e = \frac{3}{2} \left( \frac{P}{2} \right) \vec{\psi}_s \times \vec{i}_s \quad (12.75)$$

where

$\vec{\psi}_s$  = stator magnetic flux vector;  $\vec{i}_s$  = stator current vector.

Knowing that the stator and rotor magnetic flux vectors are given by  $\vec{\psi}_s = L_s \vec{i}_s + L_m \vec{i}_r$  and  $\vec{\psi}_r = L_r \vec{i}_r + L_m \vec{i}_s$ , respectively, then by substituting  $\vec{i}_s$  into Eq. (12.73(a)), the following equation results:

$$T_e = \frac{3}{2} \left( \frac{P}{2} \right) \frac{L_m}{L_r L'_s} |\vec{\psi}_s| |\vec{\psi}_r| \sin \delta_\psi \quad (12.76)$$

where

$$L'_s = L_s L_r - L_m^2$$

$\delta_\psi$  = angle between the magnetic flux vectors  $\vec{\psi}_s$  and  $\vec{\psi}_r$ .

Eq. (12.76) indicates that if the magnitudes of the magnetic fluxes are kept constant, then by controlling the angle  $\delta_\psi$  the developed electromagnetic torque of the induction motor is controlled. Finally, the instant value of the induction motor input active power is given by:

$p_i$  = instantaneous value of the input active power of an induction machine

$$= v_{as} i_{as} + v_{bs} i_{bs} + v_{cs} i_{cs} \quad (12.77)$$

#### 12.4.4 Reference Frame Theory and Dynamic Models of an Induction Motor

The equivalent circuit of Fig. 12.21 is used only for steady-state analysis. In this section the dynamic equivalent circuit will be presented which can be used for the study of the dynamic behavior of an induction motor. The study of the dynamic behavior of the induction motor presents different complications due to coupling effect between the stator and rotor phases where the coupling parameters are changing with respect to the rotor position. Therefore, the parameters of the differential equations, which describe the induction motor, must change with respect to time.

If the three-phase ac supply of an induction motor is symmetrical, which is true since it is supplied through an inverter, then the two rectangular axes or the so-called d-q model is used. Using these rectangular axes models, the time variant parameters are eliminated and the motor parameters are expressed in the decoupled d-q axes. The d-q axes model of a motor can be expressed in a stationary or in a rotating reference frame. In the stationary reference frame the d-q components are

referred to the stator ( $ds^s$  and  $qs^s$ ) and in the rotating reference frame the d–q components are rotating. The rotating reference frame can be constant on the rotor or can be rotating with synchronous speed. The advantage of using a motor model in the synchronous rotating reference frame is that, assuming a symmetrical three-phase input ac supply the motor variables in the steady state are presented as dc components. Consequently, an easier control process is achieved.

### 12.4.5 Different Types of Transformations for Induction Motor Control Applications

As it was mentioned before for the induction motor drive systems there is the necessity to transform one reference frame to another. These transformations are the following:

- 1) Transformation from stationary three-phase reference frame to two-phase orthogonal arbitrary rotating reference frame ( $a_s$ – $b_s$ – $c_s$  axes to  $ds^x$ – $qs^x$  axes)

The transformation from the three-phase  $a_s$ – $b_s$ – $c_s$  axes system to two-phase arbitrary rotating reference plane with  $ds^x$ – $qs^x$  axes (in some bibliography are referred  $\alpha$  and  $\beta$  axes), which is also called Park transformation, is useful for three reasons. The first reason is that it transforms the three-phase system of the motor into two-phase and, consequently, the analysis of the motor is simplified. The second reason is that it simplifies the calculations of the control circuit of the inverter that drives the induction motor. The third reason is that by choosing the appropriate reference axes system the time variable quantities can be transformed to time invariant vectors (i.e., dc quantities). Fig. 12.23 shows the transformation  $a_s$ – $b_s$ – $c_s$  to  $ds^x$ – $qs^x$  axes where s denotes that these components are referred to the stator and the superscript x denotes that these components are arbitrary frame components. The d-axis is called direct axis and the q-axis is called quadrature axis.

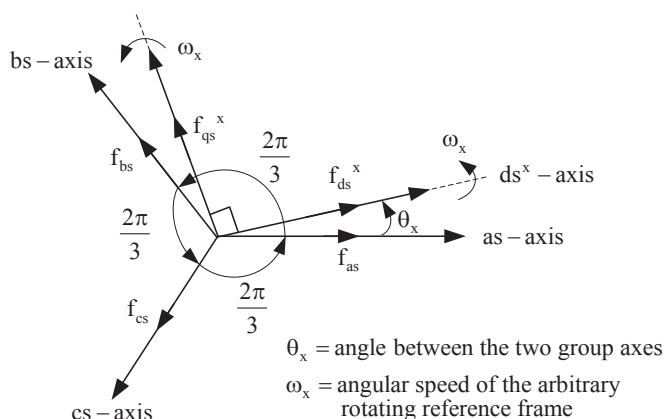


**Figure 12.23** Phasor diagram of the transformation from stationary three-phase reference frame to two-phase orthogonal arbitrary rotating one ( $a_s$ – $b_s$ – $c_s$  axes to  $ds^x$ – $qs^x$  axes).

According to Fig. 12.23 for the variable transformation from  $a_s$ - $b_s$ - $c_s$  to  $ds^x$ - $qs^x$ , the following equation is obtained:

$$\begin{bmatrix} f_{ds^x} \\ f_{qs^x} \\ f_{0s^x} \end{bmatrix} = T_{ds^x-qs^x}^{as-bs-cs} \begin{bmatrix} f_{as} \\ f_{bs} \\ f_{cs} \end{bmatrix} = \frac{2}{3} \begin{bmatrix} \cos\theta_x & \cos\left(\theta_x - \frac{2\pi}{3}\right) & \cos\left(\theta_x - \frac{4\pi}{3}\right) \\ -\sin\theta_x & -\sin\left(\theta_x - \frac{2\pi}{3}\right) & -\sin\left(\theta_x - \frac{4\pi}{3}\right) \\ \frac{1}{2} & \frac{1}{2} & \frac{1}{2} \end{bmatrix} \begin{bmatrix} f_{as} \\ f_{bs} \\ f_{cs} \end{bmatrix} \quad (12.78)$$

and the inverse transformation is given by the following equation:

$$\begin{bmatrix} f_{as} \\ f_{bs} \\ f_{cs} \end{bmatrix} = T_{as-bs-cs}^{ds^x-qs^x} \begin{bmatrix} f_{ds^x} \\ f_{qs^x} \\ f_{0s^x} \end{bmatrix} = \begin{bmatrix} \cos\theta_x & -\sin\theta_x & 1 \\ \cos\left(\theta_x - \frac{2\pi}{3}\right) & -\sin\left(\theta_x - \frac{2\pi}{3}\right) & 1 \\ \cos\left(\theta_x - \frac{4\pi}{3}\right) & -\sin\left(\theta_x - \frac{4\pi}{3}\right) & 1 \end{bmatrix} \begin{bmatrix} f_{ds} \\ f_{qs} \\ f_{0s} \end{bmatrix} \quad (12.79)$$

where

$f$  = voltage, current, or magnetic flux variable to be transformed

$f_{as}, f_{bs}, f_{cs}$  = variables of the three-phase system with  $a$  –  $b$  –  $c$  axes

$f_{ds^x}$  =  $ds$  component of the stator vector variable  $f$  in the arbitrary reference frame

$f_{qs^x}$  =  $qs$  component of the stator vector variable  $f$  in the arbitrary reference frame

$f_{0s^x}$  = zero sequence component of the stator variable vector  $f$  in the arbitrary reference frame = 0 (for symmetrical supply to the machine)

$\theta_x(t)$  = angle between the axes of the two axes group =  $\theta_x(0) + \int_0^t \omega_x(t) dt$ .

To provide a simple relation for the transformation between the  $a$ – $b$ – $c$  and  $d$ – $q$  reference frames a factor of  $2/3$  in the matrix of the above equation is used so that the  $dq$  variables to be  $2/3$  times the projection of  $abc$  variables on the  $d$ – $q$  axes. The factor of  $2/3$  gives the same space vector amplitude as the amplitude of the phase

variable. If there is symmetry between the variables (i.e.,  $f_{as} + f_{bs} + f_{cs} = 0$ ), then the component  $f_{0s^x} = 0$  and, consequently, Eqs. (12.78) and (12.79) become:

$$\begin{aligned} \begin{bmatrix} f_{ds^x} \\ f_{qs^x} \end{bmatrix} &= T_{ds^x-qs^x}^{as-bs-cs} \begin{bmatrix} f_{as} \\ f_{bs} \\ f_{cs} \end{bmatrix} \\ &= \frac{2}{3} \begin{bmatrix} \cos\theta_x & \cos\left(\theta_x - \frac{2\pi}{3}\right) & \cos\left(\theta_x - \frac{4\pi}{3}\right) \\ -\sin\theta_x & -\sin\left(\theta_x - \frac{2\pi}{3}\right) & -\sin\left(\theta_x - \frac{4\pi}{3}\right) \end{bmatrix} \begin{bmatrix} f_{as} \\ f_{bs} \\ f_{cs} \end{bmatrix} \end{aligned} \quad (12.80)$$

$$\begin{bmatrix} f_{as} \\ f_{bs} \\ f_{cs} \end{bmatrix} = T_{as-bs-cs}^{ds^x-qs^x} \begin{bmatrix} f_{ds^x} \\ f_{qs^x} \end{bmatrix} = \frac{2}{3} \begin{bmatrix} \cos\theta_x & -\sin\theta_x \\ \cos\left(\theta_x - \frac{2\pi}{3}\right) & -\sin\left(\theta_x - \frac{2\pi}{3}\right) \\ \cos\left(\theta_x - \frac{4\pi}{3}\right) & -\sin\left(\theta_x - \frac{4\pi}{3}\right) \end{bmatrix} \begin{bmatrix} f_{ds^x} \\ f_{qs^x} \end{bmatrix} \quad (12.81)$$

The superscript  $x$  of the  $ds^x$ -axis denotes that it is an arbitrary reference component and the  $s$  denotes that the component is referred to the stator.

- 2) Transformation from stationary three-phase reference frame to two-phase stationary orthogonal reference frame ( $a_s$ - $b_s$ - $c_s$  axes to  $ds^s$ - $qs^s$  axes—Clarke transformation)

For this transformation substituting  $\omega_x = 0$  and  $\theta_x = 0^\circ$  into Eqs. (12.80) and (12.81), then the following equations are obtained:

$$\begin{bmatrix} f_{ds^s} \\ f_{qs^s} \\ 0 \end{bmatrix} = T_{ds^s-qs^s}^{as-bs-cs} \begin{bmatrix} f_{as} \\ f_{bs} \\ f_{cs} \end{bmatrix} = \frac{2}{3} \begin{bmatrix} 1 & -\frac{1}{2} & -\frac{1}{2} \\ 0 & \frac{\sqrt{3}}{2} & -\frac{\sqrt{3}}{2} \\ \frac{1}{\sqrt{2}} & \frac{1}{\sqrt{2}} & \frac{1}{\sqrt{2}} \end{bmatrix} \begin{bmatrix} f_{as} \\ f_{bs} \\ f_{cs} \end{bmatrix} \quad (12.82)$$

$$\begin{bmatrix} f_{as} \\ f_{bs} \\ f_{cs} \end{bmatrix} = T_{as-bs-cs}^{ds^s-qs^s} \begin{bmatrix} f_{ds^s} \\ f_{qs^s} \\ f_{cs} \end{bmatrix} = \frac{2}{3} \begin{bmatrix} 1 & 0 \\ -\frac{1}{2} & -\frac{\sqrt{3}}{2} \\ \frac{1}{\sqrt{2}} & -\frac{\sqrt{3}}{2} \end{bmatrix} \begin{bmatrix} f_{ds^s} \\ f_{qs^s} \end{bmatrix} \quad (12.83)$$

where

$f$  = voltage, current, or magnetic flux variable to be transformed

$f_{ds^s}$  = ds component of the stator vector variable  $f$  in the stationary reference frame

$f_{qs^s}$  = qs component of the stator vector variable  $f$  in the stationary reference frame.

The superscript  $s$  of  $ds^s$ -axis denotes that is a stationary frame component. Fig. 12.24 shows the phasor diagram of Clarke transformation where for simplicity reasons the  $a$ -axis is made to coincide with  $ds^s$ -axis.

- 3) Transformation from stationary two-phase orthogonal reference frame to two-phase synchronously rotating reference frame ( $ds^s$ – $qs^s$  axes to  $ds^e$ – $qs^e$  axes—Park transformation)

As it was discussed before, this transformation provides technical advantages in induction motor drive systems because they transforms time variant components into dc components. This transformation, which is shown in Fig. 12.25, is given by the following equation:

$$\begin{bmatrix} f_{ds^e} \\ f_{qs^e} \end{bmatrix} = T_{ds^e-qs^e}^{ds^s-qs^s} \begin{bmatrix} f_{ds^s} \\ f_{qs^s} \end{bmatrix} = \begin{bmatrix} \cos\omega_e t & \sin\omega_e t \\ -\sin\omega_e t & \cos\omega_e t \end{bmatrix} \begin{bmatrix} f_{ds^s} \\ f_{qs^s} \end{bmatrix} \quad (12.84)$$

where

$f$  = voltage, current, or magnetic flux variable to be transformed

$f_{ds^e}$  = ds component of the stator vector variable  $f$  in the synchronous reference frame

$f_{qs^e}$  = qs component of the stator vector variable  $f$  in the synchronous reference frame

$\omega_e$  = angular frequency of the synchronously rotating reference frame.

The superscript  $e$  (i.e., exciter) denotes the synchronously rotating reference frame.

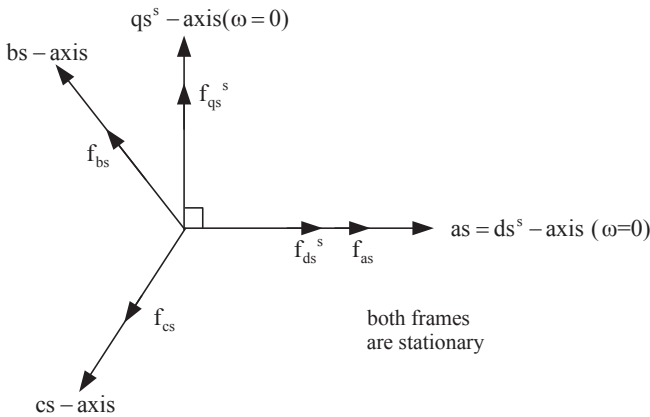


**Figure 12.24** Phasor diagram of the transformation from three-phase stationary reference frame to two-phase stationary orthogonal reference frame ( $a_s$ – $b_s$ – $c_s$  axes to  $ds^s$ – $qs^s$  axes Clarke transformation).



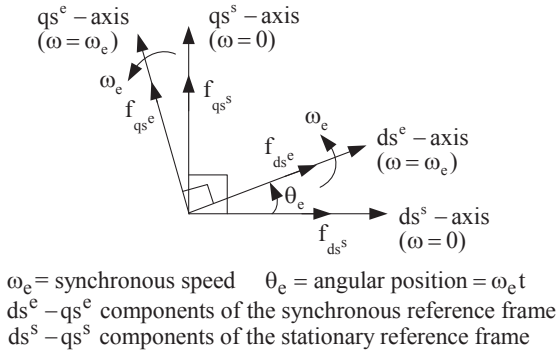


**Figure 12.25** Phasor diagram of the transformation from stationary two-phase reference frame to two-phase synchronously rotating frame ( $ds^s$ - $qs^s$  axes to  $ds^e$ - $qs^e$  axes, Park transformation).

The transformation from the stationary three-phase reference frame to the two-phase synchronously rotating reference frame according to Eq. (12.78) is given by the following equation:

$$\begin{aligned}
 \begin{bmatrix} f_{ds^e} \\ f_{qs^e} \\ f_{0s^e} \end{bmatrix} &= T_{ds^e-qs^e}^{as-bs-cs} \begin{bmatrix} f_a \\ f_b \\ f_c \end{bmatrix} \\
 &= \begin{bmatrix} \cos\omega_e t & \cos(\omega_e t - 120^\circ) & \cos(\omega_e t - 240^\circ) \\ -\sin\omega_e t & -\sin(\omega_e t - 120^\circ) & -\sin(\omega_e t - 240^\circ) \\ \frac{1}{2} & \frac{1}{2} & \frac{1}{2} \end{bmatrix} \begin{bmatrix} f_a \\ f_b \\ f_c \end{bmatrix} \quad (12.85)
 \end{aligned}$$

### Example 12.9

Transform the stator supply three-phase voltages of an induction machine to

- two-phase stationary reference frame and
- synchronously rotating reference frame.

### Solution

Supposing that the stator three-phase voltages are sinusoidal and symmetrical, then the following equations hold:

$$v_{as} = \sqrt{2}\tilde{V}_i \cos\omega t \quad (1)$$

$$v_{bs} = \sqrt{2}\tilde{V}_i \cos(\omega t - 120^\circ) \quad (2)$$

$$v_{cs} = \sqrt{2}\tilde{V}_i \cos(\omega t - 240^\circ) \quad (3)$$

$$v_{as} + v_{bs} + v_{cs} = 0 \quad (4)$$

where

$\omega$  = supply angular frequency.

a) Using Eq. (12.82), the following equations are obtained:

$$\begin{bmatrix} v_{ds^s} \\ v_{qs^s} \end{bmatrix} = \frac{2}{3} \begin{bmatrix} 1 & -\frac{1}{2} & -\frac{1}{2} \\ 0 & \frac{\sqrt{3}}{2} & -\frac{\sqrt{3}}{2} \end{bmatrix} \begin{bmatrix} v_{as} \\ v_{bs} \\ v_{cs} \end{bmatrix} \quad (5)$$

or

$$v_{ds^s} = \frac{2}{3} \left( v_{as} - \frac{1}{2} v_{bs} - \frac{1}{2} v_{cs} \right) \quad (6)$$

$$v_{qs^s} = \frac{2}{3} \left( \frac{\sqrt{3}}{2} v_{bs} - \frac{\sqrt{3}}{2} v_{cs} \right) \quad (7)$$

Substituting  $v_{as} = -(v_{bs} + v_{cs})$  into Eqs. (6) and (7) yields:

$$v_{ds^s} = \frac{2}{3} \left( v_{as} + \frac{1}{2} v_{as} \right) = \frac{2}{3} \left( \frac{3}{2} v_{as} \right) = \sqrt{2}\tilde{V}_i \cos\omega t = \sqrt{2}\tilde{V}_i \angle 0^\circ \quad (8)$$

$$\begin{aligned} v_{qs^s} &= \frac{1}{\sqrt{3}} (v_{bs} - v_{cs}) = \frac{\sqrt{2}\tilde{V}_i}{\sqrt{3}} (\cos(\omega t - 120^\circ) - \cos(\omega t - 240^\circ)) \\ &= \sqrt{\frac{2}{3}}\tilde{V}_i (\sqrt{3} \sin\omega t) = \sqrt{2}\tilde{V}_i \sin\omega t = \sqrt{2}\tilde{V}_i \angle 90^\circ \end{aligned} \quad (9)$$

b) Using Eq. (12.84) the transformation of the supply three-phase voltages to two-phase synchronously rotating reference frame is obtained and is given by the following equation:

$$\begin{bmatrix} v_{ds^e} \\ v_{qs^e} \end{bmatrix} = \begin{bmatrix} \cos\omega_e t & \sin\omega_e t \\ -\sin\omega_e t & \cos\omega_e t \end{bmatrix} \begin{bmatrix} v_{ds^s} \\ v_{qs^s} \end{bmatrix} \quad (10)$$

or

$$v_{ds^e} = v_{ds^s} \cos\omega_e t + v_{qs^s} \sin\omega_e t \quad (11)$$

$$v_{qs^e} = -v_{ds^s} \sin\omega_e t + v_{qs^s} \cos\omega_e t \quad (12)$$

Next, substituting Eqs. (8) and (9) into Eqs. (11) and (12) the synchronously rotating reference frame components are found and are given by:

$$\begin{aligned} v_{ds^e} &= \left( \sqrt{2} \tilde{V}_i \cos\omega_e t \right) (\cos\omega_e t) + \left( \sqrt{2} \tilde{V}_i \sin\omega_e t \right) (\sin\omega_e t) \\ &= \sqrt{2} \tilde{V}_i \left( \frac{1 + \cos 2\omega_e t}{2} \right) + \sqrt{2} \tilde{V}_i \left( \frac{1 - \cos 2\omega_e t}{2} \right) = \sqrt{2} \tilde{V}_i \end{aligned} \quad (13)$$

$$v_{qs^e} = \left( -\sqrt{2} \tilde{V}_i \cos\omega_e t \right) (\sin\omega_e t) + \left( \sqrt{2} \tilde{V}_i \sin\omega_e t \right) (\cos\omega_e t) = 0 \quad (14)$$

Eqs. (13) and (14) indicate that the sinusoidal components of the supply voltages have been transformed to dc components in the synchronously rotating reference frame.

### Example 12.10

The stator currents in an induction motor, which are symmetrical, are given by the following equations:

$$i_{as} = 10 \cos 377t \quad i_{bs} = 10 \cos(377t - 120^\circ) \quad i_{cs} = 10 \cos(377t - 240^\circ)$$

Calculate the above currents (a) in the stationary  $ds^s$ – $qs^s$  reference frame and (b) in the synchronously rotating  $ds^e$ – $qs^e$  reference frame.

### Solution

a) Using Eq. (12.82) the current transformation from the a–b–c axes frame to the stationary frame is given by:

$$\begin{bmatrix} i_{ds^s} \\ i_{qs^s} \end{bmatrix} = \frac{2}{3} \begin{bmatrix} 1 & -\frac{1}{2} & -\frac{1}{2} \\ 0 & \frac{\sqrt{3}}{2} & -\frac{\sqrt{3}}{2} \end{bmatrix} \begin{bmatrix} i_{as} \\ i_{bs} \\ i_{cs} \end{bmatrix} \quad (1)$$

Therefore, using the above equation, the following equations are found:

$$i_{ds^s} = \frac{2}{3} \left( i_{as} - \frac{1}{2} i_{bs} - \frac{1}{2} i_{cs} \right) \quad (2)$$

$$i_{qs^s} = \frac{2}{3} \left( \frac{\sqrt{3}}{2} i_{bs} - \frac{\sqrt{3}}{2} i_{cs} \right) \quad (3)$$

Also, it is known that

$$i_{as} + i_{bs} + i_{cs} = 0 \quad \text{or} \quad i_{as} = -(i_{bs} + i_{cs}) \quad (4)$$

Substituting Eq. (4) into (2) and (3) yields:

$$i_{ds^s} = \frac{2}{3} \left( i_{as} + \frac{1}{2} i_{as} \right) = i_{as} = 10 \cos 377t \quad (5)$$

$$\begin{aligned} i_{qs^s} &= \frac{1}{\sqrt{3}} (i_{bs} - i_{cs}) = \frac{10}{\sqrt{3}} ((\cos(377t - 120^\circ)) - (\cos(377t - 240^\circ))) \\ &= 10 \sin 377t \end{aligned} \quad (6)$$

- b) Using Eq. (12.84), the following transformation from stationary frame to synchronously rotating frame is obtained:

$$\begin{bmatrix} i_{ds^e} \\ i_{qs^e} \end{bmatrix} = \begin{bmatrix} \cos \omega_e t & \sin \omega_e t \\ -\sin \omega_e t & \cos \omega_e t \end{bmatrix} \begin{bmatrix} i_{ds^s} \\ i_{qs^s} \end{bmatrix} \quad (7)$$

or

$$i_{ds^e} = i_{ds^s} \cos \omega_e t + i_{qs^s} \sin \omega_e t \quad (8)$$

$$i_{qs^e} = -i_{ds^s} \sin \omega_e t + i_{qs^s} \cos \omega_e t \quad (9)$$

Substituting Eqs. (5) and (6) into Eqs. (8) and (9) yields:

$$i_{ds^e} = (10 \cos 377t)(\cos \omega_e t) + (10 \sin 377t)(\sin \omega_e t) = 10 \quad (10)$$

$$i_{qs^e} = -(10 \cos 377t)(\sin \omega_e t) + (10 \sin 377t)(\cos \omega_e t) = 0 \quad (11)$$

Eqs. (10) and (11) indicate that the  $ds^e$ – $qs^e$  current components are time invariant components (i.e., dc components).

### 12.4.6 Vector Dynamic Electrical Equivalent Models of an Induction Motor

Depending on the reference frame there are the following vector dynamic electrical equivalent models of an induction motor:

#### 12.4.6.1 Vector Dynamic Electrical Equivalent Model in the Stationary Reference Frame ( $\omega = 0$ )

The three-phase stator and rotor equations can be presented in the stationary reference frame  $a_s$ - $b_s$ - $c_s$  as follows:

$$\vec{v}_s^s = R_s \vec{i}_s^s + \frac{d\vec{\psi}_s^s}{dt} \quad (12.86)$$

$$\vec{v}_r^s = R_r \vec{i}_r^s + \frac{d\vec{\psi}_r^s}{dt} - j\omega_r \vec{\psi}_r^s \quad (12.87)$$

where

$\vec{v}_s^s$  = stator voltage in the stationary reference frame

$\vec{v}_r^s$  = rotor voltage in the stationary reference frame

$\vec{i}_s^s$  = stator current in the stationary reference frame

$\vec{i}_r^s$  = rotor current in the stationary reference frame

$\omega_r$  = electrical rotor speed =  $\omega_m \left( \frac{p}{2} \right)$  rad/s

$\vec{\psi}_s^s$  = stator magnetic flux in the stationary reference frame =  $L_s \vec{i}_s^s + L_m \vec{i}_r^s$

$\vec{\psi}_r^s$  = rotor magnetic flux in the stationary reference frame =  $L_r \vec{i}_r^s + L_m \vec{i}_s^s$

$R_s$  = stator winding resistance

$R_r$  = rotor winding resistance referred to the stator side.

Using the above equations, the vector dynamic electrical equivalent model of an induction motor in the stationary reference plane is developed and is shown in Fig. 12.26.

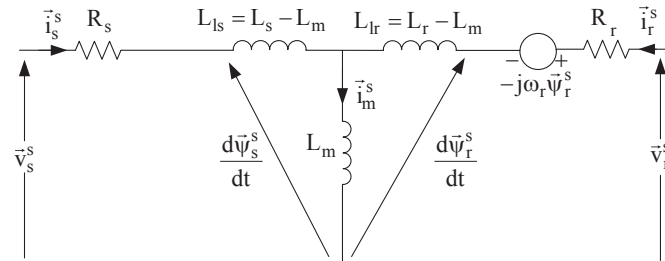


**Figure 12.26** Vector dynamic electrical equivalent model of an induction motor in the stationary reference plane.

### 12.4.6.2 Vector Dynamic Electrical Equivalent Model in the Arbitrary Rotating Reference Frame ( $\omega = \omega_x$ )

If the  $a_s$ – $b_s$ – $c_s$  axes are rotating with an arbitrary angular speed  $\omega_x$  and the rotor is rotating with an angular speed  $\omega_r$ , then the difference  $\omega_x - \omega_r$  is the reference speed between the arbitrary reference plane and the reference plane that is located on the rotor. Therefore, the vector equations in this case using Eqs. (12.86) and (12.87) are the following:

$$\vec{v}_s^x = R_s \vec{i}_s^x + \frac{d\vec{\psi}_s^x}{dt} + j\omega_x \vec{\psi}_s^x \quad (12.88)$$

$$\vec{v}_r^x = R_s \vec{i}_r^x + \frac{d\vec{\psi}_r^x}{dt} + j(\omega_x - \omega_r) \vec{\psi}_r^x \quad (12.89)$$

where

$$\vec{\psi}_s^x = L_s \vec{i}_s^x + L_m \vec{i}_r^x$$

$$\vec{\psi}_r^x = L_r \vec{i}_r^x + L_m \vec{i}_s^x$$

$\omega_x \vec{\psi}_s^x$  = speed voltage due to the rotating reference frame with an arbitrary angular speed  $\omega_x$ .

Using the above equations the vector dynamic electrical equivalent model of an induction motor in the arbitrary reference frame is developed and is shown in Fig. 12.27.

### 12.4.6.3 Vector Dynamic Electrical Equivalent Model in the Synchronous Rotating Reference Frame ( $\omega = \omega_e$ )

If the coordinates  $a_s$ – $b_s$ – $c_s$  are rotating with synchronous speed  $\omega_e$ , then Eqs. (12.88) and (12.89) become:

$$\vec{v}_s^e = R_s \vec{i}_s^e + \frac{d\vec{\psi}_s^e}{dt} + j\omega_e \vec{\psi}_s^e \quad (12.90)$$

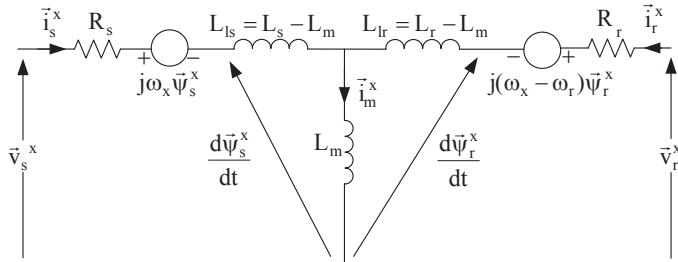


**Figure 12.27** Dynamic electrical equivalent model of an induction motor in the arbitrary rotating reference plane.

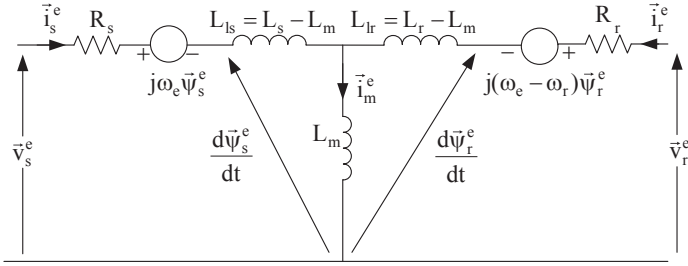


**Figure 12.28** Vector dynamic electrical equivalent model of an induction motor in the synchronous rotating reference frame.

$$\vec{V}_r^e = R_r \vec{i}_r^e + \frac{d\vec{\psi}_r^e}{dt} + j(\omega_e - \omega_r) \vec{\psi}_r^e = R_r \vec{i}_r^e + \frac{d\vec{\psi}_r^e}{dt} + j\omega_{sl} \vec{\psi}_r^e \quad (12.91)$$

Using the above equations the vector dynamic electrical equivalent model of an induction motor in the synchronous rotating reference frame is developed and is shown in Fig. 12.28.

## 12.4.7 Two-Phase Dynamic Electrical Equivalent Models of an Induction Motor

Depending on the reference rotating frame there are two-phase dynamic electrical equivalent models of an induction motor.

### 12.4.7.1 Two-Phase Dynamic Model in the Arbitrary Rotating Reference Frame ( $\omega = \omega_x$ )

Eqs. (12.58) and (12.59) can be written as follows:

$$\vec{V}_{abcs} = R_s \vec{i}_{abcs} + L_s \frac{d\vec{i}_{abcs}}{dt} + L_m \frac{d\vec{i}_{abcr}}{dt} e^{j\theta_r} + j\omega_r L_m \vec{i}_{abcr} e^{j\theta_r} \quad (12.92)$$

$$\vec{V}_{abcr} = R_r \vec{i}_{abcr} + L_r \frac{d\vec{i}_{abcr}}{dt} + L_m \frac{d\vec{i}_{abcs}}{dt} e^{-j\theta_r} - j\omega_r L_m \vec{i}_{abcs} e^{-j\theta_r} \quad (12.93)$$

Using the  $a_s$ - $b_s$ - $c_s$  to  $d_s^x$ - $q_s^x$  transformation, which is given by Eq. (12.80), the following equations are obtained:

$$\vec{V}_{dq_s^x} = R_s \vec{i}_{dq_s^x} + L_s \frac{d\vec{i}_{dq_s^x}}{dt} + j\omega_r (L_s \vec{i}_{dq_s^x} + L_m \vec{i}_{dq_r^x}) \quad (12.94)$$

$$\vec{v}_{dqr^x} = R_r \vec{i}_{dqr^x} + L_r \frac{d \vec{i}_{dqr^x}}{dt} + j(\omega_x - \omega_r) \left( L_r \vec{i}_{dqr^x} + L_m \vec{i}_{dqs^x} \right) \quad (12.95)$$

or in matrix form

$$\begin{bmatrix} v_{qs^x} \\ v_{ds^x} \\ v_{qr^x} \\ v_{dr^x} \end{bmatrix} = \begin{bmatrix} R_s + L_s \frac{d}{dt} & \omega_x L_s & L_m \frac{d}{dt} & \omega_x L_m \\ -\omega_x L_s & R_s + L_s \frac{d}{dt} & -\omega_x L_m & L_m \frac{d}{dt} \\ L_m \frac{d}{dt} & (\omega_x - \omega_r) L_m & R_s + L_r \frac{d}{dt} & (\omega_x - \omega_r) L_r \\ -(\omega_x - \omega_r) L_m & L_m \frac{d}{dt} & -(\omega_x - \omega_r) L_r & R_s + L_r \frac{d}{dt} \end{bmatrix} \begin{bmatrix} i_{qs^x} \\ i_{ds^x} \\ i_{qr^x} \\ i_{dr^x} \end{bmatrix} \quad (12.96)$$

At this point it should be mentioned that for an induction motor with squirrel-cage (short-circuited) rotor  $v_{qr^x} = 0$  and  $v_{dr^x} = 0$ . Moreover, since the rotor electrical speed is  $\omega_r$  then the axes  $ds^x$ – $qs^x$  which are on the rotor are rotating with  $\omega_r - \omega_x$  electrical speed with respect to arbitrary rotating reference frame.

Using Eq. (12.96) one can obtain the dynamic models of an induction motor in the arbitrary reference frame which are shown in Fig. 12.29.

The stator and rotor d–q magnetic flux components of an induction motor in an arbitrary rotating reference frame are given by the following equations:

$$\psi_{ds^x} = L_{ls} i_{ds^x} + L_m (i_{ds^x} + i_{dr^x}) = L_s i_{ds^x} + L_m i_{dr^x} \quad (12.97)$$

$$\psi_{qs^x} = L_{ls} i_{qs^x} + L_m (i_{qs^x} + i_{qr^x}) = L_s i_{qs^x} + L_m i_{qr^x} \quad (12.98)$$

$$\hat{\psi}_{s^x} = \sqrt{\psi_{qs^x}^2 + \psi_{ds^x}^2} \quad (12.99)$$

$$\psi_{dr^x} = L_{lr} i_{dr^x} + L_m (i_{ds^x} + i_{dr^x}) = L_r i_{dr^x} + L_m i_{ds^x} \quad (12.100)$$

$$\psi_{qr^x} = L_{lr} i_{qr^x} + L_m (i_{qs^x} + i_{qr^x}) = L_r i_{qr^x} + L_m i_{qs^x} \quad (12.101)$$

$$\hat{\psi}_{r^x} = \sqrt{\psi_{qr^x}^2 + \psi_{dr^x}^2} \quad (12.102)$$

Also the air-gap d–q magnetic flux components are given by the following equations:

$$\psi_{qm^x} = L_m (i_{qs^x} + i_{qr^x}) \quad (12.103)$$

$$\psi_{dm^x} = L_m (i_{ds^x} + i_{dr^x}) \quad (12.104)$$

$$\hat{\psi}_{m^x} = \sqrt{\psi_{qm^x}^2 + \psi_{dm^x}^2} \quad (12.105)$$



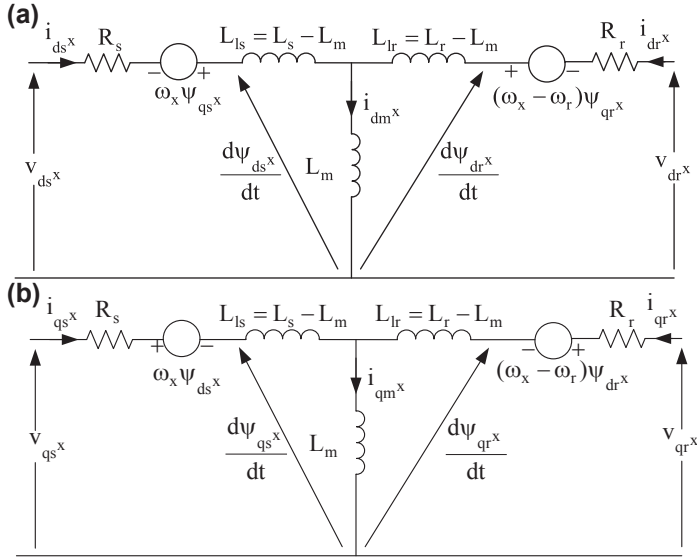


**Figure 12.29** Equivalent circuit models of a three-phase symmetrical induction motor in the arbitrary rotating reference frame. (a) d-axis model and (b) q-axis model.

Knowing that the air-gap power is  $P_g = \omega_m T_e$ , and using Eqs. (12.97)–(12.104), then the following equation for the developed electromagnetic torque of the induction motor can be obtained:

$$\begin{aligned}
 T_e &= \left(\frac{3}{2}\right) \left(\frac{P}{2}\right) (\psi_{dm^x} i_{qr^x} - \psi_{qm^x} i_{dr^x}) \\
 &= \left(\frac{3}{2}\right) \left(\frac{P}{2}\right) (\psi_{ds^x} i_{qs^x} - \psi_{qs^x} i_{ds^x}) \\
 &= \left(\frac{3}{2}\right) \left(\frac{P}{2}\right) \frac{L_m}{L_r} (\psi_{dr^x} i_{qs^x} - \psi_{qr^x} i_{ds^x}) \\
 &= \left(\frac{3}{2}\right) \left(\frac{P}{2}\right) L_m (i_{qs^x} i_{dr^x} - i_{ds^x} i_{qr^x})
 \end{aligned} \tag{12.106}$$

The active input power of the induction motor is given by the following equation:

$$\begin{aligned}
 P_i &= v_{as} i_{as} + v_{bs} i_{bs} + v_{cs} i_{cs} = \vec{v}_{asbscs}^T \vec{i}_{asbscs} \\
 &= \left(\vec{T}^{-1} \vec{v}_{dq0}\right)^T \vec{T}^{-1} \vec{i}_{dq0} = \vec{v}_{dq0}^T \left(\frac{3}{2} \vec{T}^T\right)^T \vec{T}^{-1} \vec{i}_{dq0} \\
 &= \frac{3}{2} \vec{v}_{dq0}^T \vec{i}_{dq0} = \frac{3}{2} ((v_{ds^x} i_{ds^x} + v_{qs^x} i_{qs^x}) + 2v_0 i_0)
 \end{aligned} \tag{12.107}$$

where from Eq. (12.78)

$$\vec{T} = T_{ds^x-qs^x}^{as-bs-cs} = \frac{2}{3} \begin{bmatrix} \cos\theta_x & \cos\left(\theta_x - \frac{2\pi}{3}\right) & \cos\left(\theta_x - \frac{4\pi}{3}\right) \\ -\sin\theta_x & -\sin\left(\theta_x - \frac{2\pi}{3}\right) & -\sin\left(\theta_x - \frac{4\pi}{3}\right) \\ \frac{1}{2} & \frac{1}{2} & \frac{1}{2} \end{bmatrix}$$

$v_{ds^x}, v_{qs^x}$  = stator voltage d-q components in the arbitrary reference frame

$i_{ds^x}, i_{qs^x}$  = stator current d-q components in the arbitrary reference frame.

When the induction machine is symmetrical and there is not zero sequence current then Eq. (12.107) becomes:

$$P_i = \frac{3}{2} (v_{ds^x} i_{ds^x} + v_{qs^x} i_{qs^x}) \quad (12.108)$$

Moreover, the input reactive power of the induction motor is given by the following equation:

$$Q_i = \frac{3}{2} (v_{qs^x} i_{ds^x} - v_{ds^x} i_{qs^x}) \quad (12.109)$$

#### 12.4.7.2 Two-Phase Dynamic Model in the Stationary Reference Frame ( $\omega = 0$ )

Using the transformation  $a_s-b_s-c_s$  to  $ds^s-qs^s$  (Eq. 12.78) Eqs. (12.92) and (12.93) are transformed to the following equation:

$$\begin{bmatrix} v_{qs^s} \\ v_{ds^s} \\ v_{qr^s} \\ v_{dr^s} \end{bmatrix} = \begin{bmatrix} R_s + L \frac{d}{dt_s} & 0 & L_m \frac{d}{dt} & 0 \\ 0 & R_s + L_s \frac{d}{dt} & 0 & L_m \frac{d}{dt} \\ L_m \frac{d}{dt} & -\omega_r L_m & R_s + L_r \frac{d}{dt} & -\omega_r L_r \\ \omega_r L_m & L_m \frac{d}{dt} & \omega_r L_r & R_s + L_r \frac{d}{dt} \end{bmatrix} \begin{bmatrix} i_{qs^s} \\ i_{ds^s} \\ i_{qr^s} \\ i_{dr^s} \end{bmatrix} \quad (12.110)$$

It is known that for an induction motor with squirrel-cage (short-circuited) rotor  $v_{qr^s} = 0$  and  $v_{dr^s} = 0$ . Using Eq. (12.110) the stationary reference frame equivalent

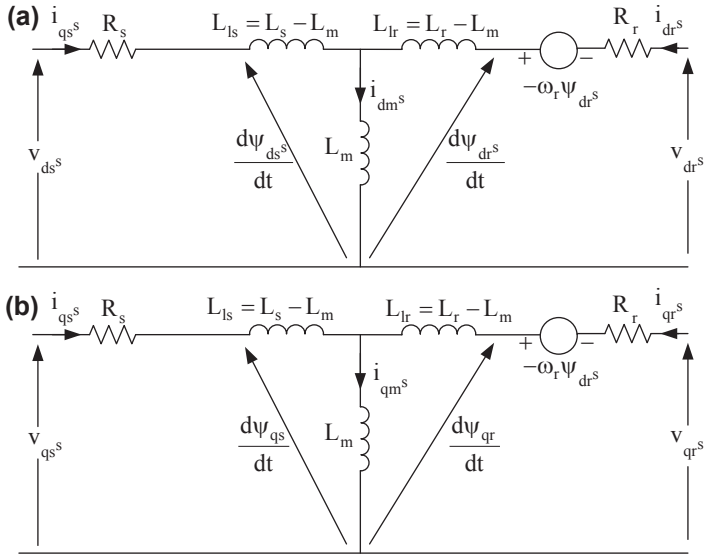


**Figure 12.30** Stationary reference frame equivalent circuit models for a three-phase, symmetrical induction motor. (a) d-axis model and (b) q-axis model.

circuit models for a three-phase symmetrical induction motor are obtained and shown in Fig. 12.30.

### 12.4.7.3 Two-Phase Dynamic Model in the Synchronously Rotating Reference Frame ( $\omega = \omega_e$ )

Transforming Eq. (12.110) from  $ds^s$ – $qs^s$  to  $ds^e$ – $qs^e$  reference frame (Eq. 12.85), the following equation is obtained:

$$\begin{bmatrix} v_{qs^e} \\ v_{ds^e} \\ v_{qr^e} \\ v_{dr^e} \end{bmatrix} = \begin{bmatrix} R_s + L_s \frac{d}{dt} & \omega_e L_s & L_m \frac{d}{dt} & \omega_e L_m \\ -\omega_e L_s & R_s + L_s \frac{d}{dt} & -\omega_e L_m & L_m \frac{d}{dt} \\ L_m \frac{d}{dt} & (\omega_e - \omega_r) L_m & R_s + L_r \frac{d}{dt} & (\omega_e - \omega_r) L_r \\ -(\omega_e - \omega_r) L_m & L_m \frac{d}{dt} & -(\omega_e - \omega_r) L_r & R_s + L_r \frac{d}{dt} \end{bmatrix} \begin{bmatrix} i_{qs^e} \\ i_{ds^e} \\ i_{qr^e} \\ i_{dr^e} \end{bmatrix} \quad (12.111)$$

or

$$\begin{bmatrix} v_{qs^e} \\ v_{ds^e} \\ v_{qr^e} \\ v_{dr^e} \end{bmatrix} = \begin{bmatrix} R_s + SL_s & \omega_e L_s & SL_m & \omega_e L_m \\ -\omega_e L_s & R_s + SL_s & -\omega_e L_m & SL_m \\ SL_m & (\omega_e - \omega_r)L_m & R_r + SL_r & (\omega_e - \omega_r)L_r \\ -(\omega_e - \omega_r)L_m & SL_m & -(\omega_e - \omega_r)L_r & R_r + SL_r \end{bmatrix} \begin{bmatrix} i_{qs^e} \\ i_{ds^e} \\ i_{qr^e} \\ i_{dr^e} \end{bmatrix} \quad (12.112)$$

where  $S$  is the Laplace operator.

It is known that for an induction motor with squirrel-cage (short-circuited) rotor the components,  $v_{qr^e} = 0$  and  $v_{dr^e} = 0$ . Using Eq. (12.111), the synchronously rotating reference frame equivalent circuit models for a three-phase, symmetrical induction motor can be obtained and are shown in Fig. 12.31.

Using Eqs. (12.106)–(12.110), the following equations are obtained for the synchronous rotating reference frame:

$$\begin{aligned} \psi_{ds^e} &= d\text{-component of the stator flux linkage in the synchronous} \\ &\text{rotating reference frame} \\ &= L_{ls}i_{ds^e} + L_m(i_{ds^e} + i_{dr^e}) = L_s i_{ds^e} + L_m i_{dr^e} \end{aligned} \quad (12.113)$$

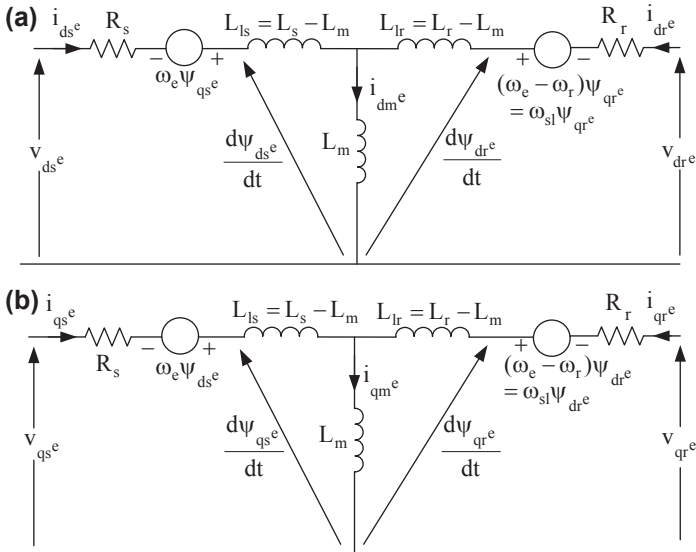


**Figure 12.31** Synchronously rotating reference frame equivalent circuit models for a three-phase, symmetrical induction motor. (a) d-axis model and (b) q-axis model.

$$\begin{aligned}\psi_{qs^e} &= q\text{-component of the stator flux linkage in the synchronous} \\ &\text{rotating reference frame}\end{aligned}\quad (12.114)$$

$$= L_{ls}i_{qs^e} + L_m(i_{qs^e} + i_{qr^e}) = L_s i_{qs^e} + L_m i_{qr^e}$$

$$\begin{aligned}\hat{\psi}_{s^e} &= \text{amplitude of the stator flux linkage in the synchronous} \\ &\text{rotating reference frame}\end{aligned}\quad (12.115)$$

$$= \sqrt{\psi_{qs^e}^2 + \psi_{ds^e}^2}$$

$$\begin{aligned}\psi_{dr^e} &= d\text{-component of the rotor flux linkage in the synchronous} \\ &\text{rotating reference frame}\end{aligned}\quad (12.116)$$

$$= L_{lr}i_{dr^e} + L_m(i_{ds^e} + i_{dr^e}) = L_r i_{dr^e} + L_m i_{ds^e}$$

$$\begin{aligned}\psi_{qr^e} &= q\text{-component of the rotor flux linkage in the synchronous} \\ &\text{rotating reference frame}\end{aligned}\quad (12.117)$$

$$= L_{lr}i_{qr^e} + L_m(i_{qs^e} + i_{qr^e}) = L_r i_{qr^e} + L_m i_{qs^e}$$

$$\begin{aligned}\hat{\psi}_{r^e} &= \text{amplitude of the rotor flux linkage in the synchronous} \\ &\text{rotating reference frame}\end{aligned}\quad (12.118)$$

$$= \sqrt{\psi_{qr^e}^2 + \psi_{dr^e}^2}$$

As mentioned previously an induction motor can exhibit the torque characteristic of a dc motor (Eq. 12.4  $T_e = K_t i_a$ ) if it is controlled in the synchronous rotating reference frame ( $ds^e$ – $qs^e$ ) where in steady-state the time variant variables of the motor are presented as dc quantities. Using Eq. (12.111), the electromagnetic torque of the induction motor as a function of the  $ds^e$ – $qs^e$  components is given by the following equation:

$$\begin{aligned}T_e &= \left(\frac{3}{2}\right) \left(\frac{P}{2}\right) (\psi_{dm^e} i_{qr^e} - \psi_{qm^e} i_{dr^e}) \\ &= \left(\frac{3}{2}\right) \left(\frac{P}{2}\right) (\psi_{ds^e} i_{qs^e} - \psi_{qs^e} i_{ds^e}) \\ &= \left(\frac{3}{2}\right) \left(\frac{P}{2}\right) \frac{L_m}{L_r} (\psi_{dr^e} i_{qs^e} - \psi_{qr^e} i_{ds^e}) \\ &= \left(\frac{3}{2}\right) \left(\frac{P}{2}\right) L_m (i_{qs^e} i_{dr^e} - i_{ds^e} i_{qr^e})\end{aligned}\quad (12.119)$$

Eqs. (12.113)–(12.119) indicate that to successfully control an induction motor an appropriate control technique should be applied to achieve independent control of the magnetic flux and the electromagnetic torque. Today most of the control techniques are oriented towards this method.

### Example 12.11

A three-phase induction motor with short circuited Y-connected rotor has the following parameters:

2 hp, line-to-line rms voltage 311 V, 50 Hz, four poles,  $R_s = 0.277 \Omega$ ,  $R_r = 0.14 \Omega$ ,  $L_m = 0.054$  H,  $L_s = 0.055$  H,  $L_r = 0.057$  H,  $\frac{N_s}{N_r} =$  windings turns ratio = 4, symmetrical ac supply.

Calculate the voltages and currents of the motor when the rotor is stationary. Use the induction motor model referred to the stator.

### Solution

The input phase voltages of the induction motor are given by:

$$v_{as} = \frac{311\sqrt{2}}{\sqrt{3}} \sin \omega t = 253.93 \sin \omega t \quad (1)$$

$$v_{bs} = \frac{311\sqrt{2}}{\sqrt{3}} \sin \left( \omega t - \frac{2\pi}{3} \right) = 253.93 \sin \left( \omega t - \frac{2\pi}{3} \right) \quad (2)$$

$$v_{cs} = \frac{311\sqrt{2}}{\sqrt{3}} \sin \left( \omega t - \frac{4\pi}{3} \right) = 253.93 \sin \left( \omega t - \frac{4\pi}{3} \right) \quad (3)$$

where  $\omega =$  ac supply angular frequency  $= 2\pi f = 2\pi(50) = 314.16 \frac{\text{rad}}{\text{s}}$ .

Knowing that the ac supply is symmetrical and using Eq. (12.76), then the  $ds^s$ – $qs^s$  axes voltage components of the stationary reference frame are given by:

$$\begin{bmatrix} v_{qs^s} \\ v_{ds^s} \end{bmatrix} = \frac{2}{3} \begin{bmatrix} 1 & -\frac{1}{2} & -\frac{1}{2} \\ 0 & \frac{\sqrt{3}}{2} & \frac{\sqrt{3}}{2} \\ 0.5 & 0.5 & 0.5 \end{bmatrix} \begin{bmatrix} v_{as} \\ v_{bs} \\ v_{cs} \end{bmatrix} \quad (4)$$

$$v_{qs^s} = \frac{2}{3} \left( v_{as} - \frac{1}{2} (v_{bs} + v_{cs}) \right) \quad (5)$$

$$v_{ds^s} = \frac{2}{3} \left( -\frac{\sqrt{3}}{2} v_{bs} + \frac{\sqrt{3}}{2} v_{cs} \right) = \frac{1}{\sqrt{3}} (v_{cs} - v_{bs}) \quad (6)$$

For symmetrical ac voltage supply, the following equation holds:

$$v_{as} + v_{bs} + v_{cs} = 0 \quad \text{or} \quad v_{bs} + v_{cs} = -v_{as} \quad (7)$$

Substituting (7) into (5) and (6) yields:

$$v_{qs^s} = \frac{2}{3} \left( v_{as} + \frac{1}{2} v_{as} \right) = \frac{2}{3} \left( \frac{3}{2} v_{as} \right) = 253.93 \sin \omega t = 253.93 \angle 0^\circ \quad (8)$$

$$v_{ds^s} = \frac{1}{\sqrt{3}} (v_{cs} - v_{bs}) = 253.93 \sin \omega t = 253.93 \angle 90^\circ \quad (9)$$

Since the rotor of the motor is stationary  $\frac{d\theta_r}{dt} = 0$ , the voltages  $v_{qr}$  and  $v_{dr}$  have zero value and, therefore, using the parameters of the motor and Eq. (12.112) the equations of the induction motor are given by:

$$\begin{bmatrix} v_{qs^s} \\ v_{ds^s} \\ 0 \\ 0 \end{bmatrix} = \begin{bmatrix} 0.277 + j314.16 & 0 & j16.96 & 0 \\ 0 & 0.277 + j314.16 & 0 & j16.96 \\ j16.96 & 0 & 0.277 + j314.16 & 0 \\ 0 & j16.96 & 0 & 0.277 + j314.16 \end{bmatrix} \begin{bmatrix} i_{qs^s} \\ i_{ds^s} \\ i_{qr^s} \\ i_{dr^s} \end{bmatrix} \quad (10)$$

or

$$\left. \begin{aligned} v_{qs^s} &= i_{qs^s}(0.277 + j314.16) + j16.96 i_{qr^s} = 253.93 \angle 0^\circ \\ v_{ds^s} &= i_{ds^s}(0.277 + j314.16) + j16.96 i_{dr^s} = 253.93 \angle 90^\circ \\ 0 &= j16.96 i_{qs^s} + i_{qr^s}(0.277 + j314.16) \\ 0 &= j16.96 i_{ds^s} + i_{dr^s}(0.277 + j314.16) \end{aligned} \right\} \quad (11)$$

Solving the system of Eq. (11) the current components  $i_{qs^s}$ ,  $i_{ds^s}$ ,  $i_{qr^s}$ , and  $i_{dr^s}$  can be found.

### 12.4.8 Power Electronics Topologies Used in AC Motor Drive Systems (Asynchronous and Synchronous)

To control an asynchronous or synchronous electric motor a power converter is applied between the power source and the motor. Through this power converter the rms

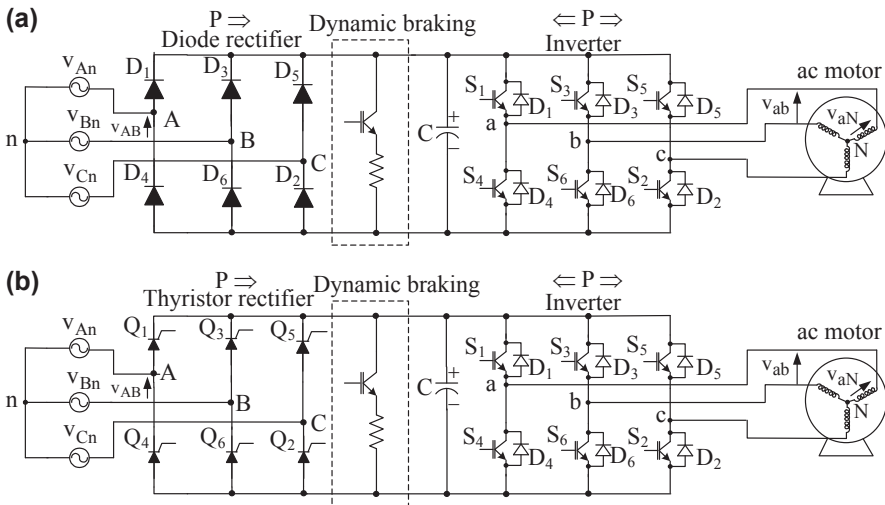


**Figure 12.32** Unidirectional ac motor drive systems with low input power factor. (a) With diode rectifier stage; (b) with thyristor rectifier stage.

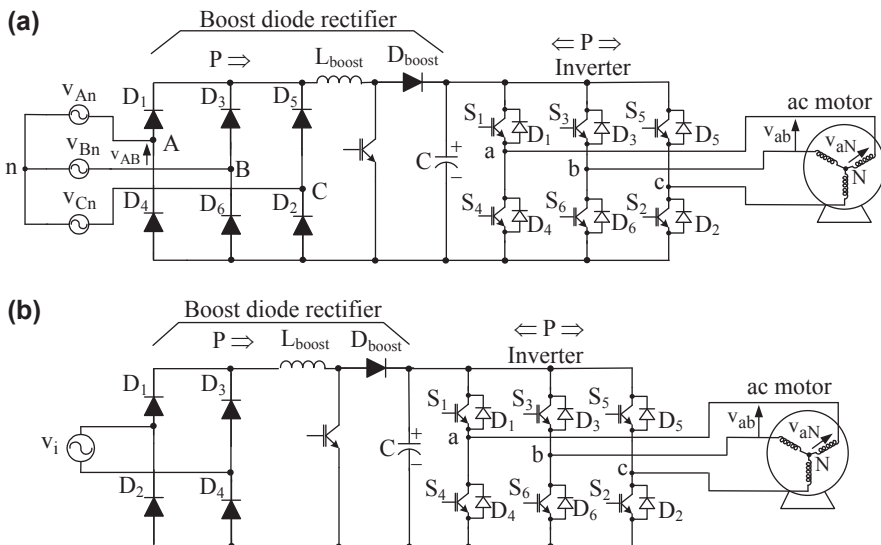
voltage and frequency applied to the electric motor is controlled and, consequently, the control of the electric motor is achieved. This converter topology is an inverter, capable of controlling its output rms voltage and frequency at the same time through the PWM reference signal. At this point it should be mentioned that the inverter acts also as a soft starter because it can apply current control at motor starting. Fig. 12.32 presents two ac motor drive systems that use unidirectional rectifiers and a two-level three-phase inverter. Both motor drive systems exhibit the following disadvantages:

- High input current harmonic distortion which consequently increases the need of a large input filter.
- Although the inverter stage exhibits bidirectional power flow, the rectifier stage is unidirectional and, consequently, power flow from the motor to the input ac source (regenerative operation or regenerative braking) is not possible.

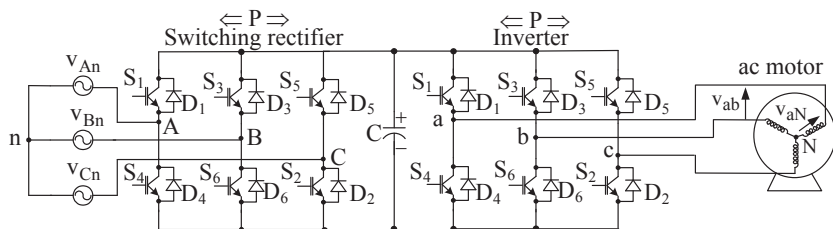
Fig. 12.33 presents two ac motor drive systems that use a unidirectional rectifier, a boost converter, and a two-level three-phase inverter. By inserting the boost converter input current with low harmonic content is achieved, thus reducing the size and the cost of the input filter. With the insertion of the boost converter almost unity input factor can be achieved.

Fig. 12.34 presents an ac motor drive system that uses bidirectional PWM rectifier and a two-level three-phase inverter allowing power bidirectionality. When the ac machine operates as a generator both topologies allow power to flow towards the ac source. Moreover, input current with low harmonic content and in phase with the input ac voltage is achieved (i.e., unity power factor). When the ac machine operates as a generator the power is transferred to the ac side through the inverter that operates as





**Figure 12.33 Unidirectional ac motor drive systems with high input power factor.** (a) With three-phase boost diode rectifier stage; (b) with single-phase boost diode rectifier stage.



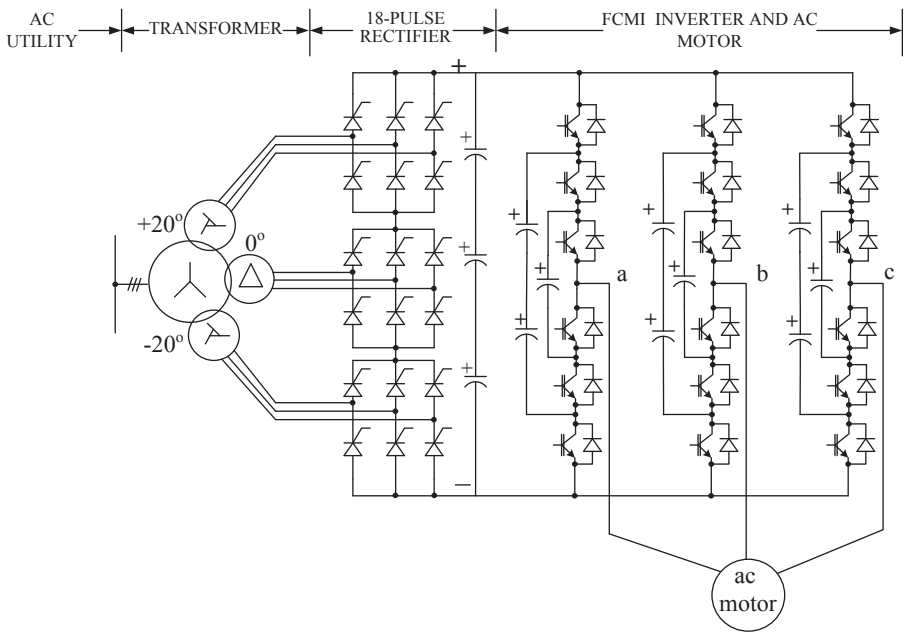
**Figure 12.34 Bidirectional ac motor drive system with unity power factor pulse width modulation switching rectifier (four-quadrant drive).**

a rectifier and through the rectifier that operates as an inverter. This mode of operation is called regenerative braking.

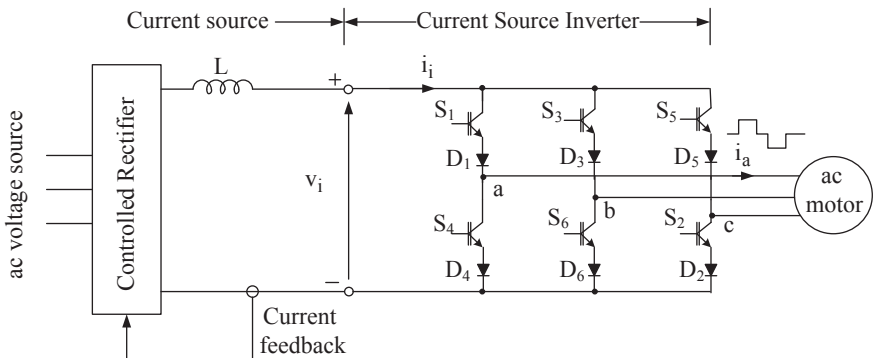
Fig. 12.35 presents an ac motor drive system that uses an 18-pulse rectifier and a multilevel inverter for high power applications.

Fig. 12.36 presents an ac motor drive system that uses a current source inverter. The current source is generated by a three-phase controlled rectifier through an inductor and a current control technique. Since the current at the input and output of the inverter is constant the inverter exhibits high reliability and for this reason this system is used for applications above 6 MW.

Fig. 12.37 presents a motor drive system that includes the control circuit and feedback signals. In this system, the input voltages and currents together with the speed are



**Figure 12.35** Unidirectional high power ac motor drive system with 18-pulse rectifier and a multilevel inverter.



**Figure 12.36** Current source ac motor drive system.

chosen as the feedback of the system. Next, the analog feedback signals are converted to digital signals and are fed to the microprocessor. The microprocessor having all the necessary feedback and reference signals generates, according to a specific control technique, the gating signals of the inverter stage.

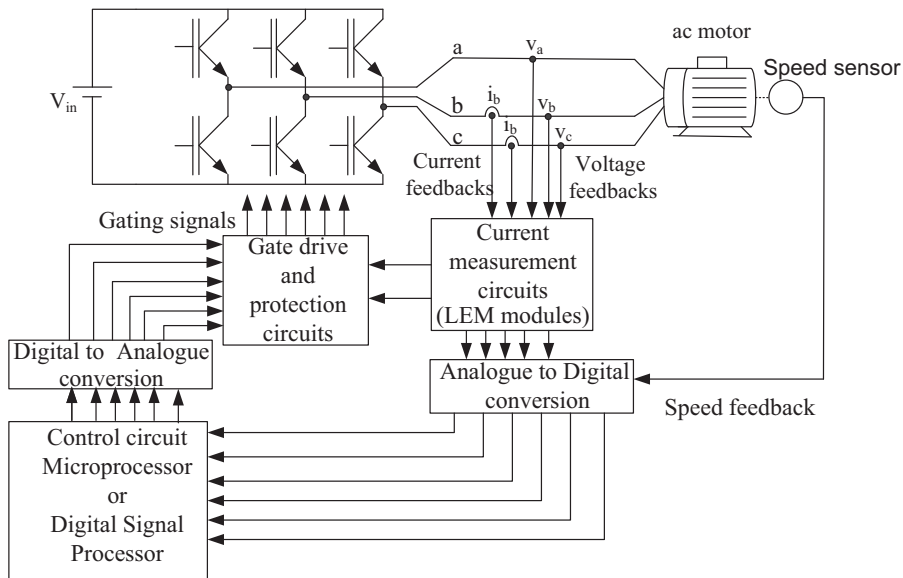


Figure 12.37 A motor drive system that includes the control circuit.

### 12.4.9 Induction Motor Drive Control Techniques

The control techniques of an induction motor can be divided into three major categories:

#### 1) Scalar control techniques

Scalar control relates only to the magnitude control of a variable and the command and feedback signals are dc quantities, which are proportional to the respective variables. Scalar control can be achieved through the following methods:

- By varying the rms value of the stator voltage and keeping the frequency constant. Simple control method but reduces the capability of the generated electromagnetic torque.
- By varying the frequency of the stator voltage and keeping the rms value constant. Simple control method but reduces the capability of the generated electromagnetic torque.
- By varying the rms value and frequency of the stator voltage at the same time so that the ratio  $\tilde{V}_s/f_s$  to be constant. It is a very simple method that maximizes the electromagnetic torque capability of the induction motor.

The most popular in industry is the  $\tilde{V}_s/f_s$  constant control technique.

Since the induction motor has a nonlinear structure a coupling effect exists in the motor, between the magnetic flux and the electromagnetic torque and, consequently, the scalar control techniques provide poor torque response. The main disadvantages of the scalar control technique with ratio  $\tilde{V}_s/f_s$  constant are the following:

- Field orientation is not used
- Motor status is ignored
- Torque is not controlled
- Delaying modulator is used

## 2) Direct torque and flux control (DTC or DTFC) technique with space vector modulation and voltage source inverter

In contrast with the scalar control technique, direct torque and flux control (DTC) can control independently the stator magnetic flux and the electromagnetic torque of the induction motor. The basic principle of DTC with space vector modulation (SVM) is the direct selection of a space vector and respective control signals, to control instantaneously the electromagnetic torque,  $T_e$ , and stator flux magnitude  $|\vec{\psi}_s|$ . The selection of the space vector is made such that to restrict the stator flux and electromagnetic torque errors within the respective flux and torque hysteresis bands, to obtain fast torque response, low inverter switching frequency and low harmonic content. The DTC technique requires only knowledge of the stator resistance and, consequently, reduces the sensitivity associated with the parameters variation and feedback speed is not needed. In the DTC as inputs are considered the desired torque and flux values. The stator magnetic flux is measured by placing Hall sensors in the gap of the motor or by placing inductor sensors in the stator or by using the stator windings as sensors. The DTC, which uses algorithms based on hysteresis control, has the disadvantage of variable switching frequency of the inverter. The DTC presents the following disadvantages:

- Difficulty to control torque and flux at very low speed
- High current and torque ripple
- Variable switching frequency
- High noise level at low speed
- Lack of DC control

## 3) Rotor field-oriented control (FOC) techniques

Field-oriented control (FOC) control technique provides decoupling between the torque and magnetic flux of the motor and, consequently, fast torque response can be obtained. FOC is applicable to both induction and synchronous motor drives. Unlike the scalar control the FOC technique, which uses equations and models of the induction motor dynamic state, has the ability to control the amplitude, the frequency, and the position of the space vectors of the voltages, currents, and magnetic flux. This method achieves the decoupling between the torque and magnetic flux control. Using FOC an ac motor is controlled as a dc separately excited motor. Although the FOC techniques can control separately the torque and the magnetic flux of the induction motor, they are heavily dependent from the parameters and the speed of the motor which results to the reduction of the control robustness. FOC is divided to the following two main types:

### i) Direct field-oriented control (DFOC)

When DFOC is used the rotor flux vector (amplitude and position) is calculated directly from the measured quantities of the motor.

### ii) Indirect field-oriented control (IFOC)

When IFOC is used the rotor flux (amplitude and position) is calculated indirectly from existing speed and slip estimations using the field control equations (current model).

The terminology sensorless, which is used in some motor drive systems, signifies that no position/speed feedback devices are used.

## 4) Combinations of the above control techniques with intelligent control techniques

Advanced control based on artificial intelligence technique is called intelligent control. The high power, high speed, and low cost modern processors such as DSP, FPGA, and ASIC IC's along with power technique switches such as IGBT made the intelligent control to be used widely in electric drives. The intelligent control includes the following techniques:

- a) Artificial neural network (ANN)
- b) Fuzzy logic set (FLS)
- c) Fuzzy-neural network (FNN)

- d) Genetic algorithm based system (GAB)
- e) Genetic Algorithm Assisted system (GAA)
- f) Adaptive control
- g) Sliding mode control
- h) Predictive mode control

The intelligent control techniques provide the following advantages to a motor drive system:

- Fast adaptation
- High degree of tolerance
- Smooth operation
- Reduce the effect of nonlinearity
- Learning ability
- Inherent approximation capability

#### 12.4.9.1 *Scalar Control by Varying the rms Value or Frequency of the Stator Voltage*

Eq. (12.51) indicates that by varying the stator voltage  $\tilde{V}_s$ , the speed and torque control of an induction motor can be achieved. However, reducing the stator voltage reduces simultaneously with the speed and the torque of the motor, which in many applications is undesirable. For example, if an electric vehicle is running uphill the speed may be low but there is a need for maximum torque which cannot be provided by the particular control technique. Fig. 12.38 presents the block diagram of such motor drive system and the respective torque—speed characteristics. As shown in Fig. 12.38(b) when the value of the stator voltage is reduced the torque capabilities of the induction motor are also reduced.

Examining Eq. (12.51) indicates that by varying the frequency of the stator voltage,  $\omega_s$ , the control of the induction motor speed is achieved. However, in this case as before the torque capabilities of the motor are reduced in low speed operation. In all motor drive applications at any speed the motor must provide maximum torque. Fig. 12.39 presents the block diagram of such motor drive system and the respective torque—speed characteristics.

#### 12.4.9.2 *Scalar Control by Keeping the Ratio $\tilde{V}_s/f_s$ Constant*

When the speed of the induction motor is adjusted to values less than the nominal, the variation of the stator voltage is followed by the corresponding variation of the stator voltage frequency such that the ratio  $\tilde{V}_s/f_s$  to be kept constant. Keeping  $\tilde{V}_s/f_s$  constant the magnetic flux of the air gap is kept approximately constant and, consequently, the electromagnetic torque capability of the induction motor at any instant is maximized. Because of its simplicity the open loop  $\tilde{V}_s/f_s$  constant control technique is the most widely used.

The behavior of an asynchronous motor, when the rotor is stationary (i.e.,  $\omega_r = 0$ ), is similar to that of a transformer and, consequently, an air gap is inserted in the magnetic circuit. In this case the induced voltages in the rotor have the same frequency as

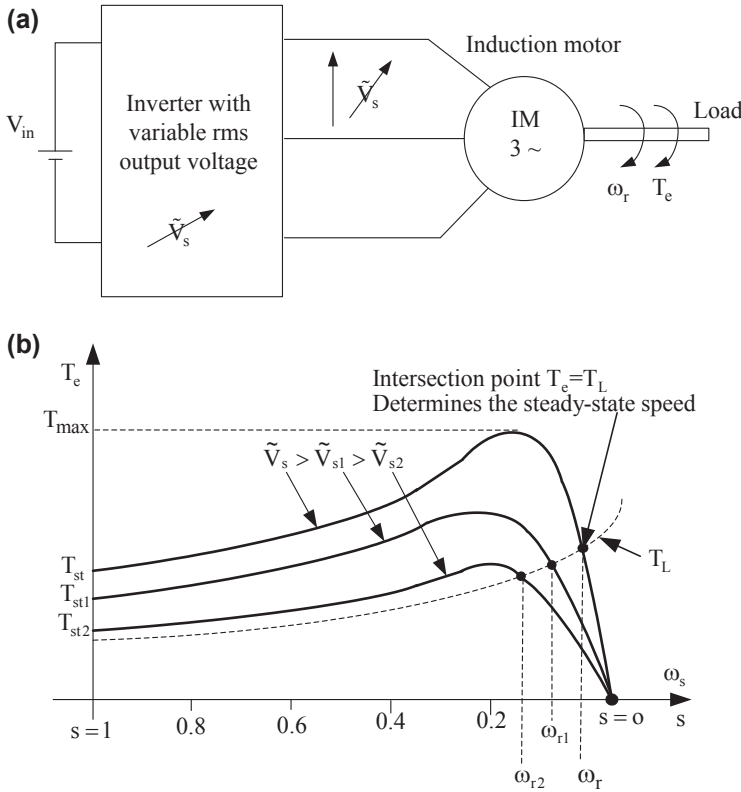


**Figure 12.38** Scalar control by varying the root mean square value of the stator voltage.

(a) Power circuit; (b) torque–speed characteristics.

the supply voltage. Therefore, the stator and rotor per-phase induced (counter) EMF are respectively given by:

$$\tilde{V}_s = \text{stator induced voltage} = 4.44K_s f_s N_s \psi_{mp} \quad (12.120)$$

$$\tilde{V}_m = \text{rotor induced voltage} = 4.44K_r f_r N_r \psi_{mp} \quad (12.121)$$

where

$K_s, K_r$  = stator and rotor windings construction factors, respectively

$N_s, N_r$  = stator and rotor windings number of turns, respectively

$\psi_{mp}$  = magnetic flux per pole

$f_s$  = stator electrical frequency

$f_r$  = rotor electrical frequency.

Also, using Fig. 12.19, the following equation is obtained:

$$\vec{V}_s = (R_s + jX_s) \vec{i}_s + \vec{V}_m \quad (12.122)$$

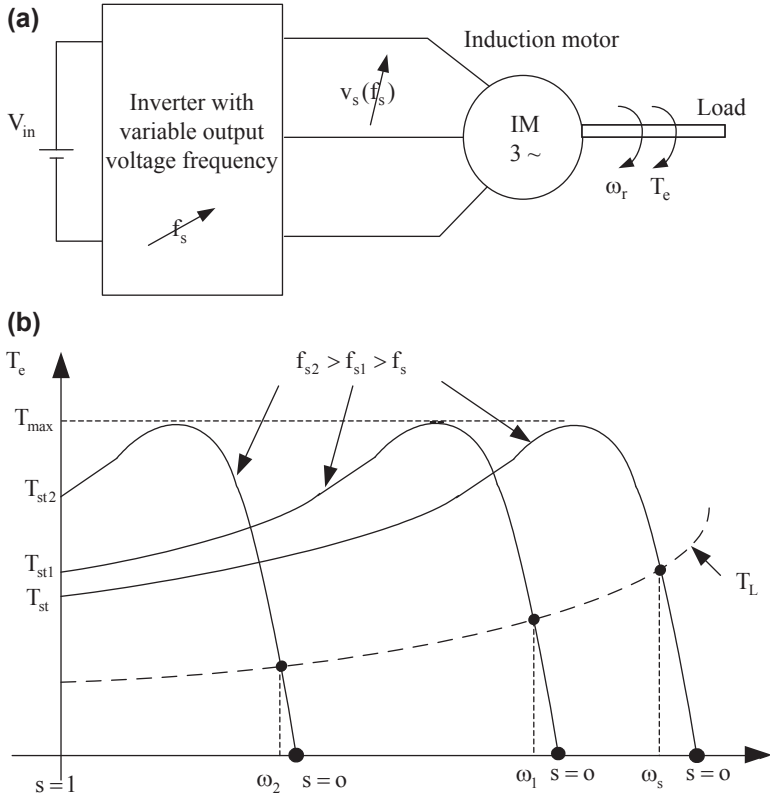


**Figure 12.39** Scalar control by varying the value of the stator frequency. (a) Power circuit; (b) torque–speed characteristics.

Under normal motor operation conditions, the stator-induced voltage is much smaller than the induced rotor voltage and, consequently, from Eq. (12.122), the following expression is obtained:

$$|\vec{i}_s(R_s + jX_s)| \ll |\vec{V}_m| \rightarrow \tilde{V}_s \approx \tilde{V}_m = 4.44K_s f_s N_s \psi_{mp} \quad (12.123)$$

or

$$\frac{\tilde{V}_s}{f_s} \approx 4.44K_s N_s \psi_{mp} \quad (12.124)$$

Eq. (12.124) indicates that to keep maximum possible flux  $\psi_{mp}$ , in the air gap for any stator frequency voltage a corresponding stator frequency should be chosen. Since the speed of the motor depends directly on the stator-induced voltage, then to obtain variable speed with maximum air-gap magnetic flux the frequency of the stator voltage

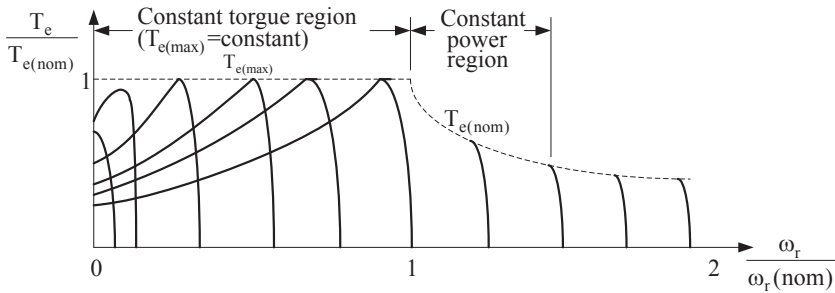


**Figure 12.40** Torque—speed characteristic of an induction motor when the ratio  $\tilde{V}_s/f_s$  is constant.

should be chosen such that to maintain the ratio  $\tilde{V}_s/f_s$  constant and equal to their rated values. Fig. 12.40 presents the torque—speed characteristic of an induction motor when the ratio  $\tilde{V}_s/f_s$  is constant. As can be seen from Fig. 12.40 in a wide range of speeds the torque of the motor is the rated. However, at low speeds (practically below 10 Hz) the torque of the motor is smaller. This is because at low speeds the voltage drop across the stator's resistance becomes significant and the approximation that was applied to Eq. (12.123) is not valid anymore. The torque reduction is due to the reduction of the air-gap magnetic flux. To maintain constant magnetic flux (and consequently maximum torque) during low-speed operation, the voltage drop of the stator resistance should be taken into consideration and the stator voltage should be increased. Fig. 12.41 presents the stator voltage—frequency characteristics when the ratio  $\tilde{V}_s/f_s$  is constant. There are two types of characteristics: one with boost voltage that takes care of low-speed operation and one without. Usually the boost characteristic is based on the following equation:

$$V_s = V_0 + k\omega_s \quad (12.125)$$

where  $V_0$  and  $k$  are chosen depending on the required boost at low frequencies, and the slope that are needed for the characteristic.

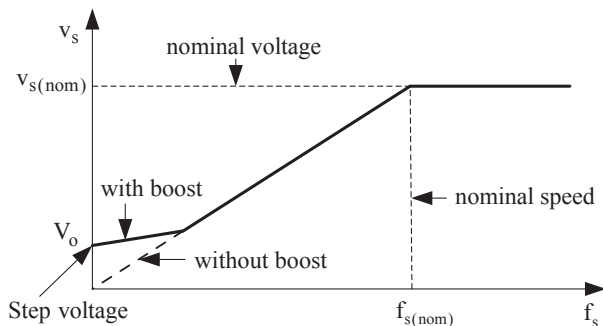


**Figure 12.41** Voltage—frequency characteristics when the ratio  $\tilde{V}_s/f_s$  is constant.



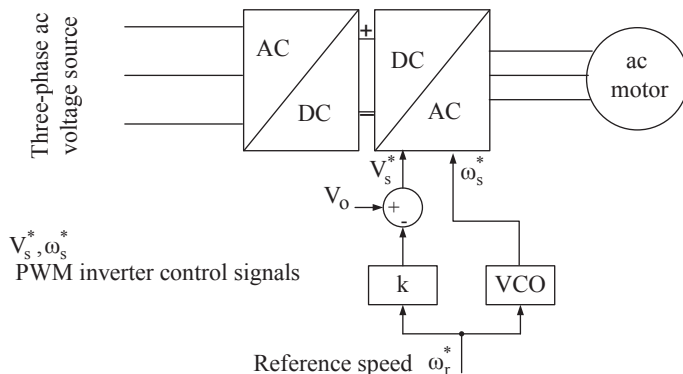


**Figure 12.42** Block diagram of an open loop control system and ratio  $\tilde{V}_s/f_s$  constant.

According to the above discussions operating the motor with constant magnetic flux nominal torque can be achieved at any operating speed. In practice, since we should adapt to the nominal specifications of a motor, for frequencies greater than the nominal, the stator voltage remains constant and equal to its nominal value. This region of operation is called constant power region. The motor drive systems that implement such control technique are divided to open and closed loop systems. The open loop systems are very simple to implement but cannot give precise operation accuracy of the system because the controlled variables of the system are not monitored. Fig. 12.42 presents the block diagram of an open loop system. The closed loop motor drive systems are more complicated to be implemented but exhibit higher operation accuracy because they continuously monitor their controlled variables (speed, rotor current, stator voltage, etc.). Figs. 12.43 and 12.44 present two different closed loop

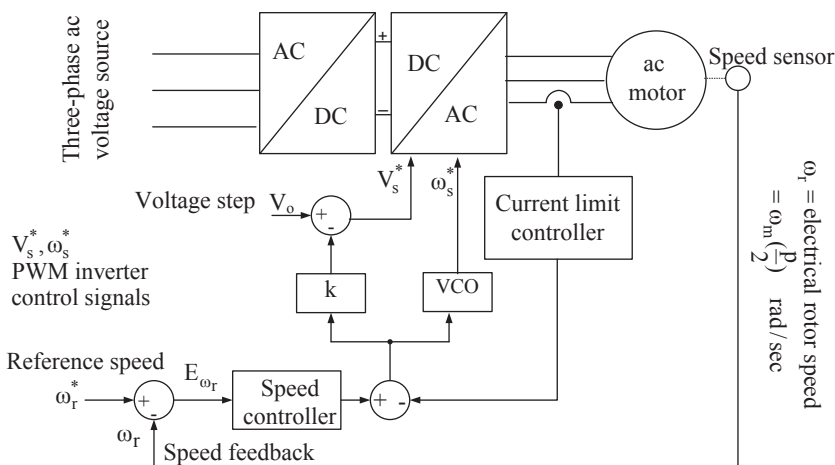


**Figure 12.43** Block diagram of a closed loop control system with current limit control and ratio  $\tilde{V}_s/f_s$  constant.



**Example 12.12**

A two pole induction motor designed for operation from a three-phase 415 V (rms) 50 Hz supply has the following parameters at rated frequency:

$X_s = 0.75 \Omega$ ;  $R_s$  is assumed to be negligible;  $X'_r = 0.7 \Omega$ ;  $R'_r = 0.07 \Omega$ ; and  $L_m$  is assumed to be large.

The motor is to be operated at variable speed from a three-phase inverter which operates in open loop with constant voltage to frequency ratio ( $\tilde{V}_s/f_s = \text{constant}$ ).

Perform the following:

- Calculate the motor torque and current when operating at a slip of 0.2 and with a supply frequency half of the rated value.
- If the supply frequency is rapidly increased to the rated value, calculate the values of motor torque and current immediately after the step change in frequency.
- Comment on the behavior of the motor in question (b), and how can be improved.

**Solution**

- a) The parameters of the motor, when operating at half frequency will be:

$$X_s = \frac{0.75}{2} = 0.375 \Omega \quad X'_r = 0.35 \Omega \quad R'_r = 0.07 \Omega$$

The motor is operating through an inverter with constant ratio  $\frac{\tilde{V}_s}{f_s} = \frac{415}{50} = 4.79$ .

Since the supply frequency is half of the rated value the inverter to keep the same  $\tilde{V}_s/f_s$  the value of  $\tilde{V}_s$  has to be reduced to half,  $\tilde{V}_s = 415/2 = 207.5\text{V}$ .

Therefore, the following results are obtained:

$$n_{e(f/2)} = \text{rotational synchronous speed} = \frac{120f}{P} = \frac{120(25)}{2} = 1500 \text{ rpm}$$

$$\omega_{e(f/2)} = \text{synchronous frequency} = \frac{4\pi f}{P} = \frac{2}{P} \omega = \frac{4\pi(25)}{2} = 157.08 \text{ rad/s}$$

where  $f$  = electrical frequency of the stator voltage

$$n_m = \text{motor speed} = (1 - s)n_e = (1 - 0.2) \times 1500 = 1200 \text{ rpm}$$

$$\begin{aligned}
 T_e = \text{developed torque} &= \frac{P_m}{\omega_m} = \frac{(1-s)P_g}{(1-s)\omega_e} \\
 &= \frac{3\tilde{I}_s^2 R'_r}{s\omega_e} = \frac{3}{\omega_e} \frac{\frac{\tilde{V}_{s(\text{phase-rated})}^2}{2}}{\left(R_s + \frac{R'_r}{s}\right)^2 + (X_{ls} + X'_{lr})^2} \frac{R'_r}{s} \\
 &= \frac{3}{157.08} \frac{\left(\frac{207.5}{\sqrt{3}}\right)^2}{\left(\left(0 + \frac{0.07}{0.2}\right)^2 + (0.375 + 0.35)^2\right)} \frac{0.07}{0.2} \\
 &= \frac{3013.94}{20.36} = 148 \text{ Nm}
 \end{aligned}$$

The stator rms current is given by:

$$\begin{aligned}
 \tilde{I}_s &= \frac{\frac{\tilde{V}_{s(\text{phase-rated})}}{2}}{\sqrt{\left(R_s + \frac{R'_r}{s}\right)^2 + (X_{ls} + X'_{lr})^2}} \\
 &= \frac{\frac{207.5}{\sqrt{3}}}{\sqrt{\left(0 + \frac{0.07}{0.2}\right)^2 + (0.375 + 0.35)^2}} = \frac{119.8}{0.81} = 147.9 \text{ A}
 \end{aligned}$$

- b)** If the supply frequency  $f$  is increased from 25 Hz to rated value of 50 Hz, then the following results are obtained:

$$n_e = \frac{120f}{P} = \frac{120(50)}{2} = 3000 \text{ rpm}$$

$$\omega_e = \text{synchronous frequency} = \frac{4\pi f}{P} = \frac{2}{P} \omega = \frac{4\pi \times (50)}{2} = 314.16 \text{ rad/s}$$

Since the motor speed at this instant remains at the same value of 1200 rpm the slip will be

$$s = \text{slip} = \frac{n_e - n_m}{n_e} = \frac{3000 - 1200}{3000} = 0.6$$

In this case the torque and the armature current are given by:

$$T_e = \frac{3}{314.16} \frac{\left(\frac{415}{\sqrt{3}}\right)^2}{\left(\left(0 + \frac{0.07}{0.6}\right)^2 + (0.75 + 0.7)^2\right)} \frac{0.07}{0.6} = \frac{12055.75}{398.41} = 30.26 \text{ Nm}$$

$$\begin{aligned} \tilde{I}_s &= \frac{\tilde{V}_{s(\text{phase-rated})}}{\sqrt{\left(R_s + \frac{R_r}{s}\right)^2 + (X_{ls} + X'_{lr})^2}} = \frac{\frac{415}{\sqrt{3}}}{\sqrt{\left(0 + \frac{0.07}{0.6}\right)^2 + (0.75 + 0.7)^2}} \\ &= \frac{239.6}{1.45} = 165.24 \text{ A} \end{aligned}$$

- c) The previous results indicate that the torque is suddenly changed from 148 to 30.26 Nm and the stator current from 147.9 to 165.24 A. To avoid such abrupt change the variations in voltage and frequency of the inverter has to be gradually changed from 207.5 V, 20 Hz to 415 V, 50 Hz with a ratio  $\frac{V}{f} = 4.79$ .

### 12.4.9.3 Direct Torque Control (DTC) With Space Vector Modulation (SVM-PWM)

Fig. 12.46 presents the block diagram of the direct torque control with voltage space vector modulation (DTC-SVM) technique. The required values of the stator magnetic flux  $|\psi_s^*|$  and the electromagnetic torque  $T_e^*$  are compared with the respective estimated values. As shown in Fig. 12.46 the main key of the control circuit is the use of two hysteresis controllers. The stator flux hysteresis controller that imposes the time duration of the active voltage vectors ( $V_1$ – $V_6$ ) moving the stator flux along the reference trajectory and the electromagnetic torque hysteresis controller that determines the time duration of the zero voltage vectors ( $V_0$ ,  $V_7$ ) which keep the motor torque in the predefined hysteresis tolerance band. The resulted flux and torque errors  $E_\psi$  and  $E_{T_e}$  are going through the hysteresis controllers. The stator flux hysteresis controller depending on the error value creates at its output the following two voltage levels:

$$H_\psi = 1 \quad \text{If } E_\psi > +HB_\psi, \text{ then flux is increased} \quad (12.126)$$

$$H_\psi = -1 \quad \text{If } E_\psi < -HB_\psi, \text{ then flux is decreased} \quad (12.127)$$

where  $2HB_\psi$  = hysteresis bandwidth of the stator flux controller.

The maximum value of the stator flux is limited by the hysteresis band of the flux controller. The vector of the stator flux is moving within a circular path created by the boundaries of the hysteresis band. The output of the torque controller depending on the error value has the following three voltage levels:

$$H_{T_e} = 1 \quad \text{if } E_{T_e} > +HB_{T_e} \Rightarrow \text{torque is increased} \quad (12.128)$$

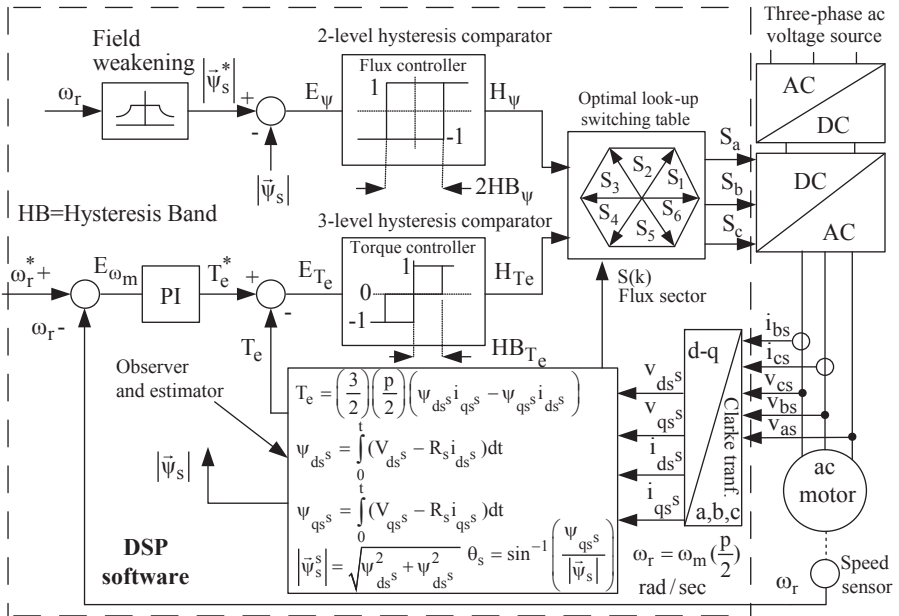


**Figure 12.46** Block diagram of direct torque control with voltage space vector modulation.

$$H_{T_e} = -1 \quad \text{if } E_{T_e} < -HB_{T_e} \Rightarrow \text{torque is decreased} \quad (12.129)$$

$$H_{T_e} = 0 \quad \text{if } -HB_{T_e} < E_{T_e} < +HB_{T_e} \Rightarrow \text{torque is kept constant} \quad (12.130)$$

The torque ripple is only affected by the width of the torque hysteresis band and is almost independent of the width of the stator flux hysteresis band. Torque ripple changes proportional with change in the torque hysteresis band. If the torque hysteresis band decreases, switching frequency increases and, consequently, the inverter switching losses increase proportionally. To reduce the ripples at the output of a motor drive system, intelligent controllers such as fuzzy logic, predictive control, neural network, and others can be applied.

The feedback values of the stator flux and electromagnetic torque of the motor are calculated from the motor terminal voltages and currents that are obtained using special sensors. These calculations are performed by the estimator unit of the control circuit. The observer also calculates the sector in which the system operates. As shown in Fig. 12.46, voltage and current measurements are taken from the motor stator and are transformed to two-phase stationary reference frame coordinates  $ds^s$ – $qs^s$ .

The voltage vector selection system takes as inputs the values  $H_\psi$ ,  $H_{T_e}$ , and the flux sector. Using these values, the voltage vector selection unit selects the proper voltage vector and the respective switching states to be applied to the inverter semiconductor switches.

The induction motor equations, which are used in the estimator unit, for the estimation of the stator magnetic flux  $\psi_s$ , and the amplitude of the electromagnetic torque,

$T_e$ , in the stationary reference frame according to Eqs. (12.86) and (12.119) are given by:

$$\vec{\psi}_s = \text{stator flux} = \int (\vec{v}_s^s - R_s \vec{i}_s^s) dt \quad \text{or} \quad \begin{bmatrix} \psi_{ds^s} \\ \psi_{qs^s} \end{bmatrix} = \begin{bmatrix} \int (v_{ds^s} - R_s i_{ds^s}) dt \\ \int (v_{qs^s} - R_s i_{qs^s}) dt \end{bmatrix} \quad (12.131)$$

$$T_e = \text{electromagnetic torque} = \left(\frac{3}{2}\right) \left(\frac{P}{2}\right) (\psi_{ds^s} i_{qs^s} - \psi_{qs^s} i_{ds^s}) \quad (12.132)$$

The amplitude and the position of the magnetic flux in the stationary reference frame are given by:

$$|\vec{\psi}_s| = \text{amplitude of } \vec{\psi}_s = \sqrt{\psi_{ds^s}^2 + \psi_{qs^s}^2} \quad (12.133)$$

$$\theta_s = \text{position of } \vec{\psi}_s = \tan^{-1} \left( \frac{\psi_{qs^s}}{\psi_{ds^s}} \right) = \sin^{-1} \left( \frac{\psi_{qs^s}}{|\vec{\psi}_s|} \right) = \cos^{-1} \left( \frac{\psi_{ds^s}}{|\vec{\psi}_s|} \right) \quad (12.134)$$

Eq. (12.131) indicates that to estimate the values of Eqs. (12.133) and (12.134) the stator resistance,  $R_s$ , must be known.

The inverter voltage vectors (six active and two zero) and a typical stator flux vector,  $\vec{\psi}_s$ , are shown in Fig. 12.47. Moreover, ignoring the stator winding resistance,  $R_s$ , from Eqs. (12.86) and (12.131), the following equations are obtained:

$$\vec{V}_s = \frac{d}{dt} (\vec{\psi}_s) \quad (12.135)$$

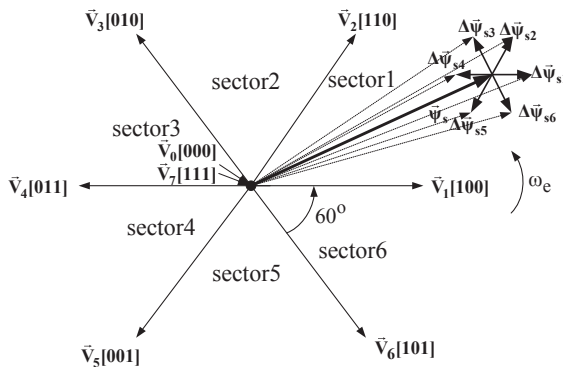


**Figure 12.47** Inverter output voltage space vectors and corresponding stator flux variations in a time interval  $\Delta t$ .

or

$$d\vec{\psi}_s = \vec{V}_s dt \quad (12.136)$$

Therefore, the variation of the stator flux space vector due to the application of the stator voltage vector,  $\vec{V}_s$ , during a time interval  $\Delta t$  is given approximately by:

$$\Delta\vec{\psi}_s = \vec{V}_s \Delta t \quad (12.137)$$

Eq. (12.137) indicates that the stator flux,  $\vec{\psi}_s$ , can be changed incrementally by applying a particular stator voltage  $\vec{V}_s$  for a time increment  $\Delta t$ . The change of stator flux,  $\Delta\vec{\psi}_s$ , has the same direction of  $\vec{V}_s$ . Fig. 12.47 shows the flux increments corresponding to each of the six inverter voltage vectors. The amplitude of  $\Delta\vec{\psi}_s$  is dependent on the stator voltage vector,  $\vec{V}_s$ , and the duration  $\Delta t$  for which this vector is applied. It is then possible to drive  $\vec{\psi}_s$  along any prefix track curve. As shown in Fig. 12.47, flux vector  $\vec{\psi}_s$  is increased when the increment  $\Delta\vec{\psi}_{s1}$  or  $\Delta\vec{\psi}_{s2}$  is added to  $\vec{\psi}_s$ . When the increment  $\Delta\vec{\psi}_{s1}$  or  $\Delta\vec{\psi}_{s2}$  is added to  $\vec{\psi}_s$ , then  $\vec{\psi}_s$  is decreased. Therefore, selecting the appropriate increments the stator flux can be forced to be within a specific hysteresis band. Fig. 12.48 shows the trajectory of stator flux vector within a hysteresis band.

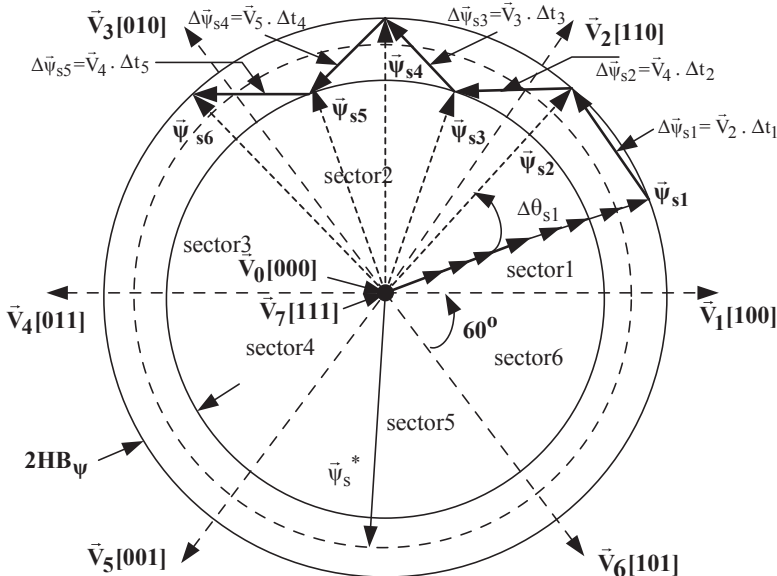


Figure 12.48 Trajectory of stator flux vector control within a hysteresis band.



**Table 12.6 Direct torque and flux control look-up table optimum inverter output voltage vector selection according to the status of  $H_\psi$  and  $H_{T_e}$**

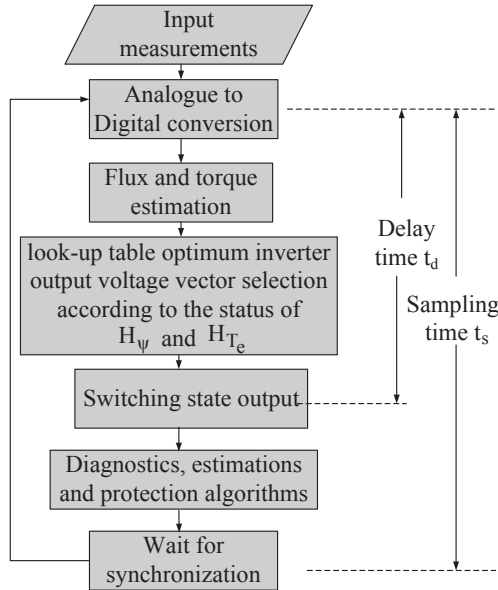
Flux error status $H_\psi$	Torque error status $H_{T_e}$	Sector 1	Sector 2	Sector 3	Sector 4	Sector 5	Sector 6
1 Increase	1	$V_2$	$V_3$	$V_4$	$V_5$	$V_6$	$V_1$
	0	$V_0$	$V_7$	$V_0$	$V_7$	$V_0$	$V_7$
	-1	$V_6$	$V_1$	$V_2$	$V_3$	$V_4$	$V_5$
-1 Decrease	1	$V_3$	$V_4$	$V_5$	$V_6$	$V_1$	$V_2$
	0	$V_7$	$V_0$	$V_7$	$V_0$	$V_7$	$V_0$
	-1	$V_5$	$V_6$	$V_1$	$V_2$	$V_3$	$V_4$

Table 12.6 presents the DTC optimum switching vectors (voltages and gating signals) look-up table in all sectors that provide the inverter with the appropriate switching states depending on the outputs of the two hysteresis controllers (i.e.,  $H_\psi$  and  $H_{T_e}$ ). Moreover, Table 12.7 presents the effect of the inverter voltage vectors on the values of the stator flux and the electromagnetic torque.

The control circuit of the DTC is implemented using DSPs. The DSP-based controller reads the flux and torque references, the dc inverter input voltage, and two of the motor line currents at the beginning of each sampling period. Next, the controller executes analog to digital conversions, performs all necessary computations, and outputs the optimum switching state that will drive the switching semiconductor devices. Fig. 12.49 presents the flowchart of the DTC algorithm.

**Table 12.7 Effect of the output voltage space vectors to stator flux and electromagnetic torque**

Output voltage space vectors	$V_1$	$V_2$	$V_3$	$V_4$	$V_5$	$V_6$	$V_0$ or $V_7$
Stator flux, $\Psi_s$	↑	↑	↓	↓	↓	↑	0
Electromagnetic torque $T_e$	↓	↑	↑	↑	↓	↓	↓



**Figure 12.49** Flowchart of direct torque and flux control algorithm.

#### 12.4.9.4 Field-Oriented Control (FOC)

As mentioned before, the FOC technique transforms the dynamics of an induction motor to become similar to dc motors. The FOC is usually applied to squirrel-cage induction motors. The ac electric drive systems that use FOC technique are characterized by their high performance and high precision in controlling the speed and flux both on static and dynamic conditions in the four quadrants of the torque—speed characteristics even at low speeds. The response in the absence of coupling, is very rapid and without oscillatory behavior, which characterizes the performance and accuracy of systems using this technique as a very optimal control (the vector control is theoretically optimal).

The FOC implies the transformation of coordinates from the stationary reference stator frame to the synchronously rotating frame. This transformation makes possible the decoupling of the stator current in two orthogonal components  $i_{qs^e}$  and  $i_{ds^e}$ . The decoupling is achieved in the synchronous rotating reference frame when the rotor flux vector,  $\vec{\psi}_r$ , is aligned with  $d^e$ -axis of the synchronously rotating reference frame. The component  $i_{qs^e}$  controls the electromagnetic torque of the induction motor and the component  $i_{ds^e}$  the magnetic flux independently. Fig. 12.50 shows the phasor diagram that describes the FOC technique.

Using the vector diagram of rotor FOC technique, shown in Fig. 12.50, the following useful equations can be obtained:

$$\psi_{dr^s} = |\vec{\psi}_r| \cos \theta_e \quad (12.138)$$

$$\psi_{qr^s} = |\vec{\psi}_r| \sin \theta_e \quad (12.139)$$



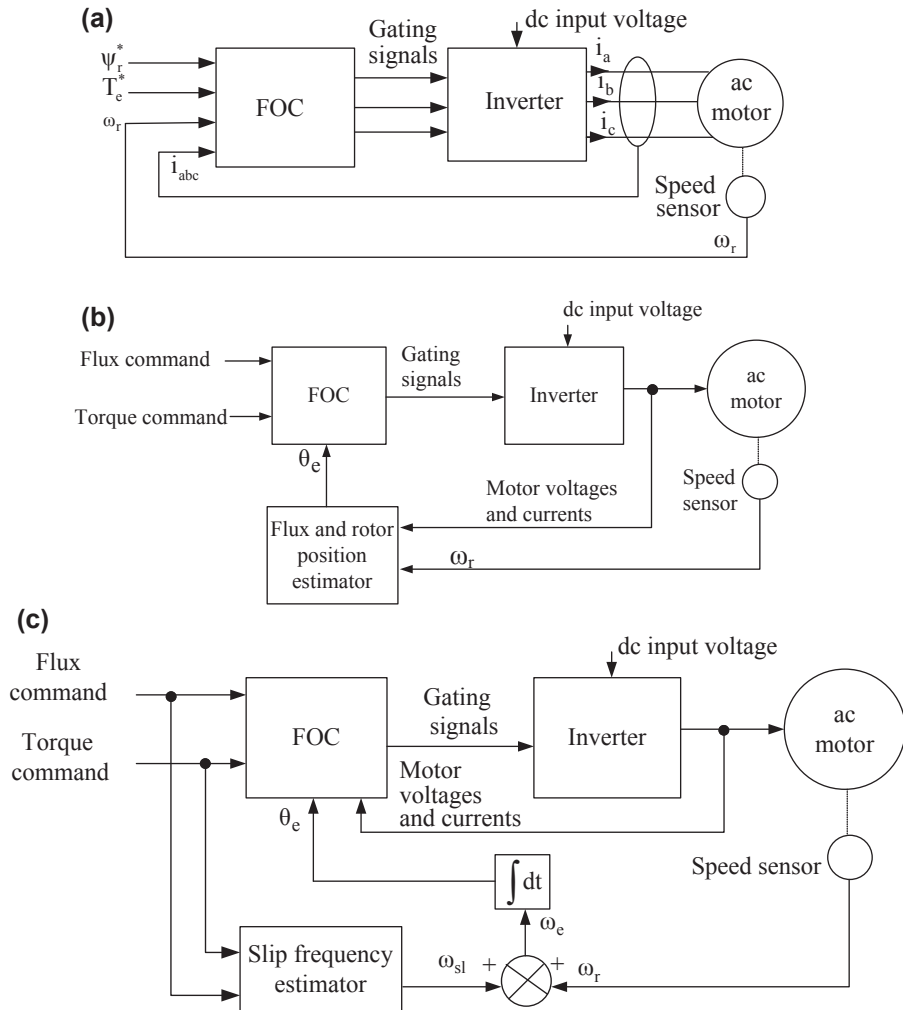


**Figure 12.51 Rotor field-oriented control (FOC) simplified block diagrams.** (a) FOC; (b) direct FOC; (c) indirect FOC.

- 3) Transform the two-quadrature stationary components into two-quadrature components in the synchronous rotating frame (Park transformation):

$$i_{ds^e} = i_{ds^s} \cos \theta_e + i_{qs^s} \sin \theta_e \quad \text{and} \quad i_{qs^e} = -i_{ds^s} \sin \theta_e + i_{qs^s} \cos \theta_e$$

- 4) Estimate the rotor magnetic flux  $|\vec{\psi}_r|$  and its orientation angle  $\theta_e$ .
- 5) Using the orientation angle  $\theta_e$  calculated in step 4 the stator current component in the synchronously rotating frame  $i_{ds^e}$  is aligned with the rotor flux vector  $\vec{\psi}_r$ . This step provides decoupling between the torque and flux control.

- 6) The current error signals are used in controllers to generate the reference currents or voltages depending on the modulation technique used.
- 7) a) If current hysteresis PWM control is used,  $i_{ds}^*$  and  $i_{qs}^*$  are converted through inverse Park and Clarke transformations to a set of three-phase currents to produce  $i_a^*$ ,  $i_b^*$  and  $i_c^*$ . Next,  $i_a^*$ ,  $i_b^*$  and  $i_c^*$  and  $i_a$ ,  $i_b$ ,  $i_c$  are compared using hysteresis comparator to generate the inverter gating signals (see Chapter 6).
- b) If space vector PWM is used, then the current error signals are used in the controllers to generate the required voltage references  $v_{qs}^*$  and  $v_{ds}^*$  (see Chapter 6).

Using Eq. (12.115) the rotor voltage components of a squirrel-cage induction motor in the two-phase synchronously rotating reference frame (i.e.,  $\omega = \omega_e$ ) are given by:

$$v_{qr^e} = 0 = L_m \frac{di_{qs^e}}{dt} + (\omega_e - \omega_r) L_m i_{ds^e} + (R_r + L_r) \frac{di_{qr^e}}{dt} + (\omega_e - \omega_r) L_m i_{dr^e} \quad (12.143)$$

$$v_{dr^e} = 0 = L_m \frac{di_{ds^e}}{dt} + (\omega_e - \omega_r) L_m i_{qs^e} + (R_r + L_r) \frac{di_{dr^e}}{dt} + (\omega_e - \omega_r) L_m i_{qr^e} \quad (12.144)$$

Substituting  $i_{ds^e}$  and  $i_{qs^e}$ , which are given by Eqs. (12.116) and (12.117), into Eqs. (12.143) and (12.144), the following equations are obtained for the squirrel-cage induction motor:

$$\frac{d\psi_{qr^e}}{dt} + R_r i_{qr^e} + (\omega_e - \omega_r) \psi_{dr^e} = 0 \quad (12.145)$$

$$\frac{d\psi_{dr^e}}{dt} + R_r i_{dr^e} + (\omega_e - \omega_r) \psi_{qr^e} = 0 \quad (12.146)$$

Solving Eq. (12.145) with respect to  $i_{qr^e}$  and Eq. (12.146) with respect to  $i_{dr^e}$ , the following equations are obtained:

$$\begin{aligned} i_{qr^e} &= \text{rotor current q - component in the synchronously rotating frame} \\ &= \frac{1}{L_r} \psi_{qr^e} - \frac{L_m}{L_r} i_{qs^e} \end{aligned} \quad (12.147)$$

$$\begin{aligned} i_{dr^e} &= \text{rotor current d - component in the synchronously rotating frame} \\ &= \frac{1}{L_r} \psi_{dr^e} - \frac{L_m}{L_r} i_{ds^e} \end{aligned} \quad (12.148)$$

Substituting the rotor current components given by Eqs. (12.147) and (12.148), into (12.145) and (12.146), the following equations are obtained:

$$\frac{d\psi_{qr^e}}{dt} + \frac{R_r}{L_r} \psi_{qr^e} - \frac{L_m}{L_r} R_r i_{qs^e} + (\omega_e - \omega_r) \psi_{dr^e} = 0 \quad (12.149)$$

$$\frac{d\psi_{dr^e}}{dt} + \frac{R_r}{L_r} \psi_{dr^e} - \frac{L_m}{L_r} R_r i_{ds^e} - (\omega_e - \omega_r) \psi_{qr^e} = 0 \quad (12.150)$$

Next, aligning the rotor flux vector  $\vec{\psi}_r$  so that to coincide with  $d^e$ -axis, then according to Fig. 12.50, the following equations hold:

$$\psi_{qr^e} = 0 \quad (12.151)$$

$$\frac{d\psi_{qr^e}}{dt} = 0 \quad (12.152)$$

$$\psi_{dr^e} = |\vec{\psi}_r| \quad (12.153)$$

Substituting Eqs. (12.151)–(12.153) into Eqs. (12.149) and (12.150), the following equations are obtained for the squirrel-cage induction motor:

$$\left(\frac{L_r}{R_r}\right) \frac{d}{dt} |\vec{\psi}_r| + |\vec{\psi}_r| = L_m i_{ds^e} \quad (12.154)$$

$$\omega_e - \omega_r = \omega_{slip} = \frac{L_m}{|\vec{\psi}_r|} \frac{R_r}{L_r} i_{qs^e} \quad (12.155)$$

If the amplitude of the rotor flux vector is kept constant (i.e.,  $|\vec{\psi}_r| = C$  and  $\frac{d}{dt} |\vec{\psi}_r| = 0$ ), then from Eqs. (12.154) and (12.119), the following equations are obtained:

$$|\vec{\psi}_r| = L_m i_{ds^e} \quad (12.156)$$

$$T_e = \left(\frac{3}{2}\right) \left(\frac{P}{2}\right) \frac{L_m}{L_r} |\vec{\psi}_r| i_{qs^e} = K i_{qs^e} \quad (12.157)$$

where  $K = \left(\frac{3}{2}\right) \left(\frac{P}{2}\right) \frac{L_m}{L_r} |\vec{\psi}_r|$ .

Eqs. (12.156) and (12.157) indicate that by using the FOC technique control, the decoupling between the rotor flux and electromagnetic torque for the squirrel-cage induction motor is achieved. By controlling the current component  $i_{ds^e}$  the amplitude of the rotor flux is controlled and by controlling the current component  $i_{qs^e}$  the electromagnetic torque of the motor is controlled independently. Therefore, using FOC an induction motor is controlled in the same manner as a dc motor. This is true because the current component  $i_{ds^e}$  represents the field current,  $i_f$ , of the dc motor and  $i_{qs^e}$  represents stator current  $i_a$ . The current components  $i_{ds^e}$  and  $i_{qs^e}$  are perpendicular to each other and are called flux current and torque current, respectively. Eq. (12.156)

indicates that the rotor flux is controlled by the current component  $i_{ds^e}$  with a delay time due to the rotor time constant which is given by:

$$\tau_r = \text{rotor time constant} = \frac{L_r}{R_r} \quad (12.158)$$

The rotor position phasors  $\cos\theta_r$  and  $\sin\theta_r$  are found from an angle decoder and are added to respective slip phasors to calculate the position of the synchronously rotating phasors  $\cos\theta_e$  and  $\sin\theta_e$  given by:

$$\cos \theta_e^* = \cos(\theta_r + \theta_{sl}^*) = \cos \theta_r \cos \theta_{sl}^* - \sin \theta_r \sin \theta_{sl}^* \quad (12.159)$$

$$\sin\theta_e^* = \sin(\theta_r + \theta_{sl}^*) = \sin\theta_r \cos\theta_{sl}^* + \cos\theta_r \sin\theta_{sl}^* \quad (12.160)$$

Therefore, with FOC the rotor flux is aligned with the  $d^e$ -axis of the synchronously rotating reference frame and that results to the decoupling of the torque and flux control that allows controlling an ac motor with the same way as a dc motor. Fig. 12.52 presents the decoupling control of an induction motor.

Fig. 12.53 presents the block diagram of DFOC that uses hysteresis band control, and Fig. 12.54 presents the block diagram of IFOC that uses hysteresis band current control.

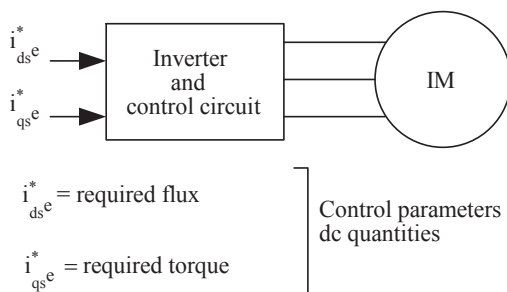


**Figure 12.52** Parameters for flux and torque control of an induction motor.

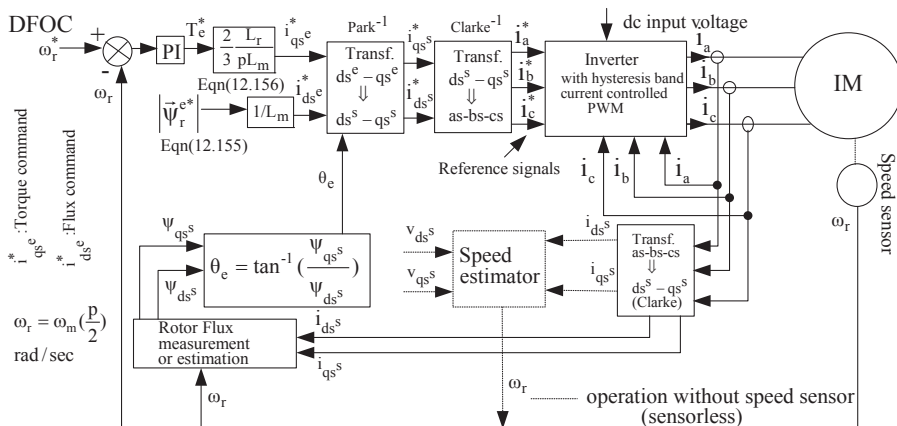


**Figure 12.53** Block diagram of direct field-oriented control that uses hysteresis band current control pulse width modulation.

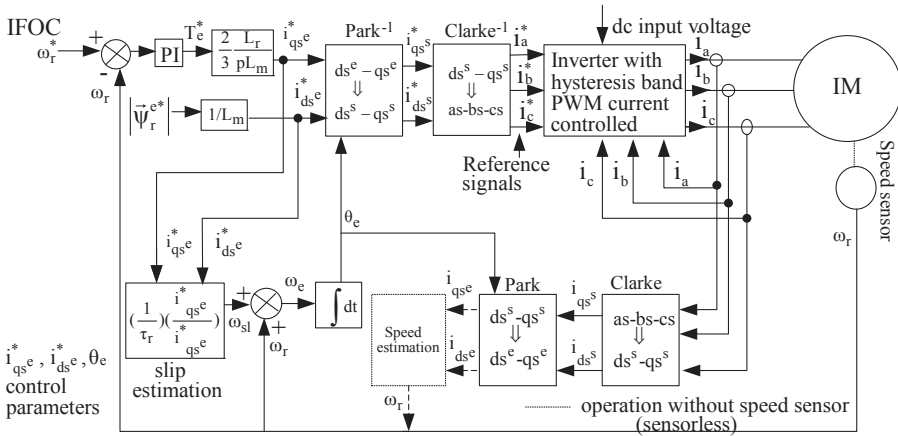


**Figure 12.54** Block diagram of rotor indirect field-oriented control that uses hysteresis band current control pulse width modulation.

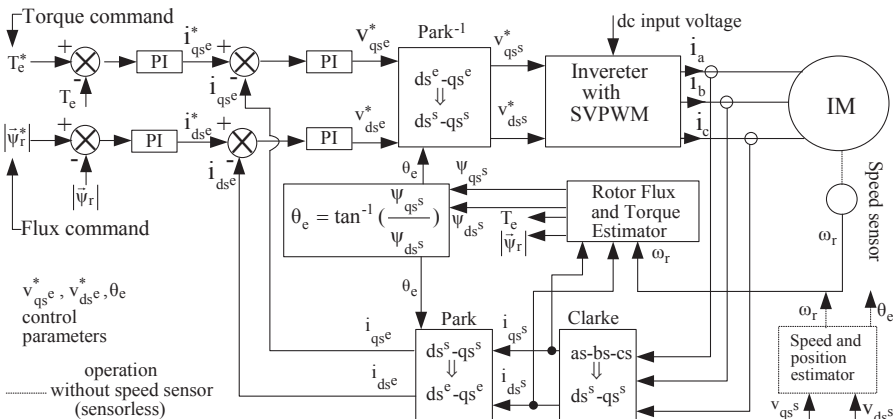


**Figure 12.55** Block diagram of rotor indirect field-oriented control that uses space vector pulse width modulation control.

As shown in Figs. 12.53 and 12.54 the motor drive systems can operate with speed sensor (sensored) or without (sensorless). The term sensorless indicates the lack of speed and/or position sensor and a speed estimator is used. This feature decreases the cost and the size of the motor drive system. Finally, Fig. 12.55 presents the block diagram of rotor IFOC that uses space vector PWM control.

## 12.5 Synchronous Motor Drive Systems

### 12.5.1 Permanent Magnet (PM) Synchronous Motors

PM synchronous motors are constantly gaining popularity among the scientific community, especially in the fields of electric traction and power generation. This occurs



mainly due to their inherent advantages of high power density, high efficiency, and reliability. Their performance and efficiency have rendered them the dominant choice in many applications. Permanent magnet motor (PMM) is related to the classical synchronous motor with the difference that the dc winding is replaced by PMs that produce steady magnetic flux. This way the copper losses in the rotor are eliminated, since there is no field winding and, consequently, the overall motor efficiency is increased. Additionally, the high efficiency values incur significant reduction in the motor size and weight (high power density) and lower moment of inertia. On the other hand, however, the control systems are very complicated due to the permanent nature of the excitation that can cause rotor demagnetization phenomena.

### 12.5.1.1 PM Motor Rotor Configurations

PMMs can be classified, based on the rotor configuration that occurs, into the following:

1) Surface-mounted PM motors with sinusoidal flux

In this type of PMM, the stator comprises a sinusoidal three-phase winding, which produces an air-gap flux rotating with the synchronous speed. The PMs are placed on the rotor surface using epoxy glue. The rotor magnetic circuit is either made of compact or laminated steel. In the case of variable speed operation, the motor can include a squirrel-cage or a damping winding, which of course incurs additional ohmic losses. If the machine operates as a generator, rotated by an external source, then the stator windings produce symmetrical sinusoidal three-phase voltages. Since the magnets magnetic permeability is very close to that of the air ( $\mu_r \approx 1$ ) and the magnets are placed on the rotor surface, the machine active air-gap length is very big and it exhibits practically no saliency. This contributes to the limitation of the armature reaction phenomenon due to the low values of magnetizing inductance.

2) Interior PM motors with sinusoidal flux

Contrary to surface-mounted PMMs, in an interior PMM the magnets are placed inside the rotor body. Several different geometric configurations of rotor structures with interior magnets have been tested and reported in recent bibliography, mainly regarding the magnet shape and orientation. The stator comprises a conventional three-phase sinusoidal winding. The main characteristics of interior PMMs are the following:

- The motor structure is very compact and mechanically robust, allowing higher operating speed values
- The motor active length is small, which incurs higher armature reaction
- The motor active length is higher along the d axis than along the q axis, therefore the motor exhibits high saliency

3) Surface-mounted PM motors with trapezoidal flux

A synchronous PMM with trapezoidal flux is a motor that exhibits no saliency, like a sinusoidal flux surface-mounted PMM, but comprises a stator with concentrated windings instead of sinusoidal distributed windings. To increase the sinusoidality of the produced magnetic field distribution in trapezoidal flux motors the use of fractional slot windings is a common practice. As the motor rotates, the magnetic flux that is associated with a specific phase winding varies linearly with time, except for the instant that the gap between the magnets aligns with the phase axis. If the motor is rotated by an external mechanical source, which means that operates as a generator, the phase voltages will exhibit symmetrical trapezoidal waveforms. For this reason, the use of an electronic converter is necessary, to

produce six step current waveforms in the motor terminals, to be able to produce mean electromagnetic torque. Since the use of the converter is mandatory, this type of motors is utilized as electronic motors. Through the use of an inverter and an absolute position sensor that is placed on the motor shaft, trapezoidal flux motors can be controlled and operated as brushless dc motors. Trapezoidal flux motors have more similar performance characteristics to the dc motors than the sinusoidal flux motors. They are simple, less expensive and have higher torque density values than sinusoidal motors. They are typically used in low-power drive systems, as servomotors and in domestic applications where the phenomena associated with brushed dc motors have to be avoided.

### 12.5.1.2 Mathematical Model of PM Motors

For the analysis and the control of the synchronous PMM two models have been reported. The abc coordinates model and the dynamic d–q model. The first is preferred for the analysis of problems involving harmonic components, and the second is used for the transient analysis of the motor operation. The majority of the control strategies of PMMs are based on the dynamic d–q model. Fig. 12.56 shows the equivalent circuit of a synchronous PMM according to the abc coordinates model.

The voltage equations of synchronous PMM are:

$$\begin{bmatrix} v_a \\ v_b \\ v_c \end{bmatrix} = \begin{bmatrix} R_a & 0 & 0 \\ 0 & R_b & 0 \\ 0 & 0 & R_c \end{bmatrix} \begin{bmatrix} i_a \\ i_b \\ i_c \end{bmatrix} + \frac{d}{dt} \begin{bmatrix} \psi_a \\ \psi_b \\ \psi_c \end{bmatrix} \quad (12.161)$$

where  $R_a$  is the resistance of the phase a,  $i_a$  is the current of the phase a, and  $\psi_a$  is the magnetic flux of the phase a.

The magnetic flux equations can be derived as:

$$\begin{bmatrix} \psi_a \\ \psi_b \\ \psi_c \end{bmatrix} = \begin{bmatrix} L_{aa}(\theta_e) & M_{ab}(\theta_e) & M_{ac}(\theta_e) \\ M_{ab}(\theta_e) & L_{bb}(\theta_e) & M_{bc}(\theta_e) \\ M_{ac}(\theta_e) & M_{bc}(\theta_e) & L_{cc}(\theta_e) \end{bmatrix} \begin{bmatrix} i_a \\ i_b \\ i_c \end{bmatrix} + \begin{bmatrix} \psi_{ma}(\theta_e) \\ \psi_{mb}(\theta_e) \\ \psi_{mc}(\theta_e) \end{bmatrix} \quad (12.162)$$

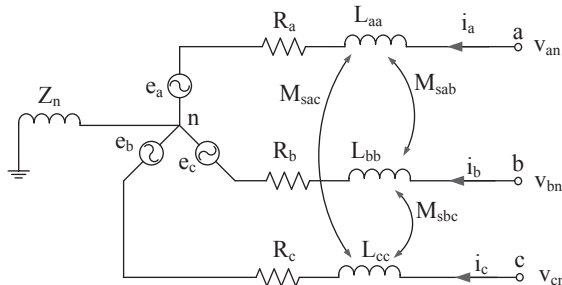


**Figure 12.56** Equivalent circuit of a synchronous permanent magnet motor according to the abc coordinates model.

where  $L_{aa}$  is the self-inductance of the a-phase winding,  $M_{ab}$  is the mutual inductance between the windings of the a and b phases, and  $\psi_{ma}$  is the remanence flux due to the PMs in the phase a.

Due the magnetic saturation and the mechanical construction of the synchronous PMM, the self and mutual inductances are functions of the electrical angle of the rotor  $\theta_r$ , which is equal to the synchronous angle  $\theta_e$ . The electrical angle of the rotor is practically the direction of rotor magnetic flux (north pole of the rotor magnets). At zero angle, the flux direction aligns with phase a. The relation between the mechanical and the electric rotor angle is given:

$$\theta_e = \theta_r = \frac{P\theta_m}{2} \quad \text{where } P \text{ is the number of poles } \omega_e = \frac{P\omega_m}{2} \quad (12.163)$$

In the general case, the inductances of a synchronous PMM consist of a constant component and a sum of odd harmonics associated with the variation of the electrical rotor angle. As far as the control of ac motors, according to modern bibliography, the following assumptions are made:

- The stator windings are considered sinusoidally distributed and the effect of the specific geometry of the stator teeth is neglected. The magnetomotive force produced by the stator is considered sinusoidal.
- The radial distribution of the magnetic flux density produced by the PMs is considered sinusoidal.
- The magnetic flux associated with the stator armature reaction only involves the fundamental component.
- The magnetic saturation is neglected.

Considering the above mentioned assumptions, the variations of the inductances contain only a sinusoidal component, and since the inductance of each phase is maximum when the magnetic flux is aligned with the phase, can be concluded (see Eq. 12.164 for  $\theta_e = 0$ ) that the values of the inductances are functions of the angle  $2\theta_e$ . If also a sinusoidal distribution of the saliency is considered, the mutual and self inductances of the windings can be written as follows:

$$\begin{bmatrix} L_{aa}(\theta_e) \\ L_{bb}(\theta_e) \\ L_{cc}(\theta_e) \end{bmatrix} = L_0 + L_2 \begin{bmatrix} \cos(2\theta_e) \\ \cos(2\theta_e - 2\pi/3) \\ \cos(2\theta_e + 2\pi/3) \end{bmatrix} \quad (12.164)$$

and

$$\begin{bmatrix} M_{ab}(\theta_e) \\ M_{ac}(\theta_e) \\ M_{bc}(\theta_e) \end{bmatrix} = M_0 + M_2 \begin{bmatrix} \cos(2\theta_e + 2\pi/3) \\ \cos(2\theta_e - 2\pi/3) \\ \cos(2\theta_e) \end{bmatrix} \quad (12.165)$$

where  $L_0$  and  $M_0$  are the mean components of the self and mutual inductances, respectively,  $L_2$  and  $M_2$  are the respective amplitudes of the sinusoidal components.

Finally, the flux produced by the PMs is a function of the rotor electrical angle and can be written as:

$$\begin{bmatrix} \psi_{ma}(\theta_e) \\ \psi_{mb}(\theta_e) \\ \psi_{mc}(\theta_e) \end{bmatrix} = \psi_m \begin{bmatrix} \cos(\theta_e) \\ \cos(\theta_e - 2\pi/3) \\ \cos(\theta_e + 2\pi/3) \end{bmatrix} \quad (12.166)$$

Under no load operation, the equations for the induced EMF by the PM excitation are obtained:

$$\begin{bmatrix} e_a \\ e_b \\ e_c \end{bmatrix} = \begin{bmatrix} V_a^{i=0} \\ V_b^{i=0} \\ V_c^{i=0} \end{bmatrix} = \frac{d}{dt} \begin{bmatrix} \psi_{ma} \\ \psi_{mb} \\ \psi_{mc} \end{bmatrix} = \psi_m \cdot \frac{d\theta}{dt} \cdot \frac{d}{d\theta} \begin{bmatrix} \cos(\theta_e) \\ \cos(\theta_e - 2\pi/3) \\ \cos(\theta_e + 2\pi/3) \end{bmatrix}$$

or

$$\begin{bmatrix} e_a \\ e_b \\ e_c \end{bmatrix} = -\psi_m \omega_m \begin{bmatrix} \sin(\theta_e) \\ \sin(\theta_e - 2\pi/3) \\ \sin(\theta_e + 2\pi/3) \end{bmatrix} \quad (12.167)$$

where  $\omega_m$  is the mechanical synchronous rotating speed.

From Eqs. (12.166) to (12.167) the final voltage equations can be derived:

$$\begin{bmatrix} v_a \\ v_b \\ v_c \end{bmatrix} = \begin{bmatrix} R_a & 0 & 0 \\ 0 & R_b & 0 \\ 0 & 0 & R_c \end{bmatrix} \begin{bmatrix} i_a \\ i_b \\ i_c \end{bmatrix} + \begin{bmatrix} L_{aa} & M_{ab} & M_{ac} \\ M_{ab} & L_{bb} & M_{bc} \\ M_{ac} & M_{bc} & L_{cc} \end{bmatrix} \frac{d}{dt} \begin{bmatrix} i_a \\ i_b \\ i_c \end{bmatrix} + \begin{bmatrix} e_a \\ e_b \\ e_c \end{bmatrix} \quad (12.168)$$

The produced electromagnetic torque is given:

$$T_e = \frac{e_a i_a + e_b i_b + e_c i_c}{\omega_m} \quad (12.169)$$

### 12.5.1.2.1 Dynamic d–q Model of Permanent Magnet Motors

The per-phase equivalent circuit developed in the previous paragraph becomes very complicated when associated with a rotating system where the phase inductances of the stator and the respective mutual inductances are functions of the rotor electrical angle. Therefore, for the analysis of a VSD system a model that does not include the time-varying inductances, which occur due to the relevant movement between the electrical circuits, has to be developed. For the analysis of ac systems the approach

of three-phase components through the use of complex phasors has been adopted. These phasors are called space vectors and will be explained later.

Any three-phase variable  $x$  can be represented by a complex phasor (space vector) through the Clarke transformation. Variable  $x$ , that can be either the magnetic flux or the phase current or the phase voltage, is multiplied by the matrix  $K$  of the transformation to be transformed into a space vector  $x_\alpha + j x_\beta$ :

$$\begin{bmatrix} x_\alpha \\ x_\beta \\ x_0 \end{bmatrix} = \frac{2}{3} \begin{bmatrix} \cos(\theta) & \cos(\theta - 2\pi/3) & \cos(\theta + 2\pi/3) \\ \sin(\theta) & \sin(\theta - 2\pi/3) & \sin(\theta + 2\pi/3) \\ 1/2 & 1/2 & 1/2 \end{bmatrix} \begin{bmatrix} x_a \\ x_b \\ x_c \end{bmatrix} \quad (12.170)$$

For the inverse transformation, the inverse matrix is utilized:

$$\begin{bmatrix} x_a \\ x_b \\ x_c \end{bmatrix} = \frac{2}{3} \begin{bmatrix} \cos(\theta) & \sin(\theta) & 1 \\ \cos(\theta - 2\pi/3) & \sin(\theta - 2\pi/3) & 1 \\ \cos(\theta + 2\pi/3) & \sin(\theta + 2\pi/3) & 1 \end{bmatrix} \cdot \begin{bmatrix} x_\alpha \\ x_\beta \\ x_0 \end{bmatrix} \quad (12.171)$$

In Eq. (12.171) the angle  $\theta$  represents the angle between the real axis of the complex plane and the direction of phase a. This angle can be chosen at will. The coefficient  $2/3$  in the equation of the transformation refers to the use of the simple coordinate transformation where the length of the space vector  $x_\alpha + j x_\beta$  is equal to the peak value of the three-phase variable  $x$ . Finally, the zero-order component  $x_0$  has nonzero values only in case of faults (i.e., phase asymmetries). For the rest of the analysis, the zero-order component will be neglected. For the control of synchronous PMMs the typical choices for the value of the angle of the reference frame is 0 and the rotor electrical angle  $\theta_e$ . If the angle is zero the transformation is associated with the stator reference frame, where the real axis is aligned with phase a. Since the angle value is maintained at 0, the reference frame is called stationary reference frame and the transformation is known as Clarke transformation. If the reference frame angle is chosen to be  $\theta_e$ , then the real axis of the complex plane is rotated synchronously to the motor rotor. In that case, the synchronous (rotor) reference frame is considered. Bibliographically, Park transformation refers to the transformation to the rotating reference frame, while Clarke transformation refers to the stationary reference frame (Fig. 12.57).

Through the use of the Park transformation, the mathematical model of the synchronous PMM is significantly simplified. In the rotating d-q reference frame, the voltage equations are:

$$v_{ds} = R_s i_{ds} + \frac{d\psi_{ds}}{dt} - \omega_e \psi_{qs} \quad (12.172)$$

$$v_{qs} = R_s i_{qs} + \frac{d\psi_{qs}}{dt} + \omega_e \psi_{ds} \quad (12.173)$$

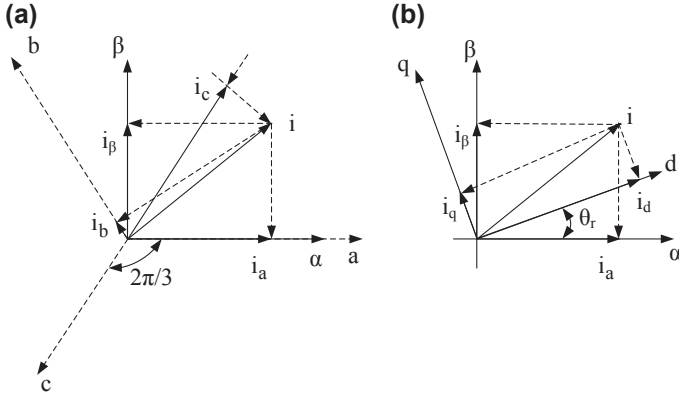


**Figure 12.57** Current vector transformations for permanent magnet motor. (a) From the abc coordinates reference frame to the stationary reference frame  $\alpha$ – $\beta$  (Clarke transformation); (b) from the stationary reference frame to the synchronously rotating frame d–q (Park transformation).

The d-axis and q-axis flux components are obtained, for the rotating reference frame:

$$\psi_{ds} = \text{direct flux linkage referred to the stator} = \psi_m + L_{ds}i_{ds} \quad (12.174)$$

$\psi_m$  = flux linkage induced by permanent magnet

$$\psi_{qs} = \text{quadrature flux linkage referred to the stator} = L_{qs}i_{qs} \quad (12.175)$$

where

$$L_{ds} = \text{d-axis inductance component} = L_0 - M_0 + L_2/2 + M_2 \quad (12.176)$$

$$L_{qs} = \text{q-axis inductance component} = L_0 - M_0 - L_2/2 - M_2 \quad (12.177)$$

$\omega_e$  = electrical speed of the synchronously rotating reference frame

$R_s$  = stator resistance

$L_0$  = average component of the self inductance

$M_0$  = average component of the mutual inductance

$L_2$  = amplitude of the sinusoidal component of the self inductance

$M_2$  = amplitude of the sinusoidal component of the mutual inductance

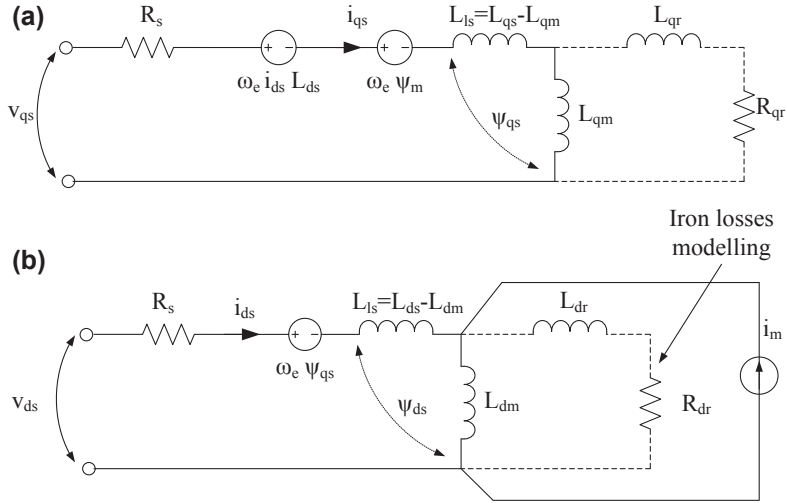


**Figure 12.58** Equivalent circuits of a synchronous permanent magnet motor for the synchronously rotating reference frame. (a) q model and (b) d model.  $\psi_m = L_m i_m$

Substituting Eqs. (12.174) and (12.175) into (12.172) and (12.173) the voltage equations can be rewritten:

$$v_{ds} = R_s i_{ds} + L_{ds} \frac{di_{ds}}{dt} - \omega_e L_{qs} i_{qs} \quad (12.178)$$

$$v_{qs} = R_s i_{qs} + L_{qs} \frac{di_{qs}}{dt} + \omega_e (\psi_m + L_{ds} i_{ds}) \quad (12.179)$$

The electromagnetic torque in the rotating reference frame is also obtained:

$$T_e = \frac{3}{2} \frac{P}{2} (\psi_{ds} i_{qs} - \psi_{qs} i_{ds}) \quad (12.180)$$

The equivalent circuits of the q- and d-axis for the synchronously rotating reference frame of the PMM is shown in Fig. 12.58.

It is worth mentioning that the d-q analysis model is valid for both surface-mounted and interior PMM with sinusoidal flux, but not for trapezoidal flux motors. The difference between the surface-mounted and interior PMMs lies in the different saliency values that incur different values for the d-axis and q-axis inductances for the interior PMM.

### 12.5.1.3 PM Motor Control Techniques

The general block diagram of the control strategy of a high-efficiency PMM is shown in Fig. 12.59. The core of the system consists of the internal flux control loop, the internal

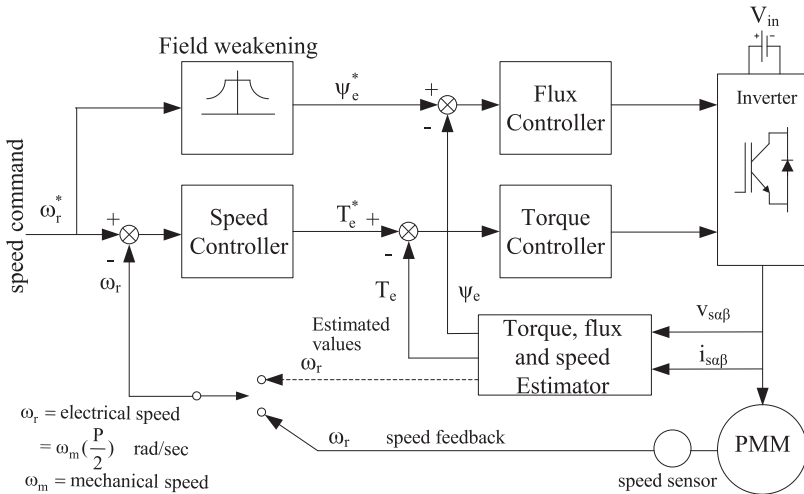


**Figure 12.59** Block diagram of the flux controller of a permanent magnet motor comprising internal flux and torque control loops.

torque control loop, and the estimator, which can be implemented with various different ways. The external speed control loop is practically the same for every control technique and produces flux and torque commands using the appropriate controllers. The speed feedback signal can be acquired through a mechanical movement sensor (i.e., encoder or resolver) or can be estimated providing the capability for sensorless control.

#### 12.5.1.3.1 Scalar V/f Open Loop Control

Scalar control only alters the amplitude of the control variables and neglects the coupling of the motor's equations. Therefore, both the voltage of the motor and the frequency of its phase currents simultaneously affect and control both the magnetic flux and the electromagnetic torque of the motor. As a result, the coupled nature of the motor's equations prevents the achievement of high performance levels. However, drive systems with scalar controllers are currently very popular in low power applications with relatively low construction cost. Fig. 12.60 shows the block diagram of the scalar V/f speed control methodology, which is the most popular open loop control methodology with independent frequency control.

Scalar control is based on the demand for constant stator magnetic flux, to maximize the produced electromagnetic torque. To maintain a constant flux value, the ratio of the motor voltage to the motor frequency should remain constant ( $V/f = \text{const}$ ). For this reason, the phase voltage—amplitude command  $V_s^*$  is produced by the frequency control command through the gain factor  $G$ . For low-speed operation, the voltage drop along the stator winding is significant and, consequently, the produced magnetic flux is limited. To avoid this phenomenon and to maintain the value of the magnetic flux near the nominal for low-speed operation, a boost voltage  $V_0$  is added to the reference amplitude of the phase voltage. The impact of the boost voltage is negligible in higher frequencies.



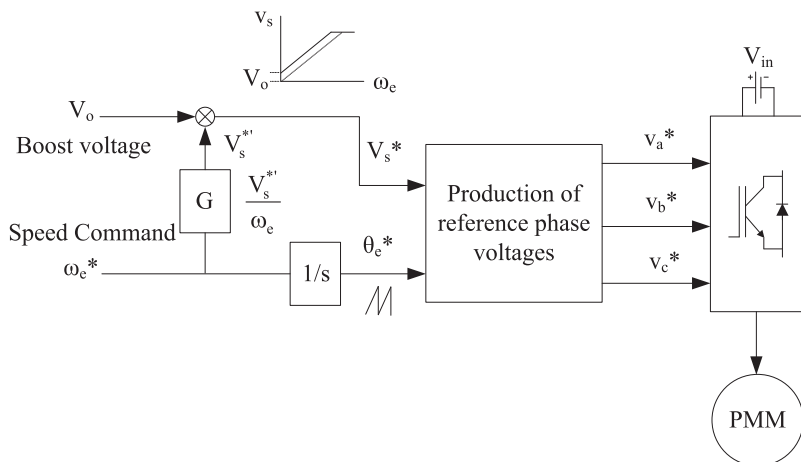


**Figure 12.60** Block diagram of the V/f open loop control with a three-phase voltage-fed inverter.

Finally, the reference speed signal  $\omega_e^*$  is integrated, producing the reference angle signal  $\theta_e^*$  and the respective reference phase voltages  $V_a^*$ ,  $V_b^*$ , and  $V_c^*$  are produced as:

$$\begin{cases} v_a^* = \sqrt{2}V_s \sin\theta_e \\ v_b^* = \sqrt{2}V_s \sin\left(\theta_e - \frac{2\pi}{3}\right) \\ v_c^* = \sqrt{2}V_s \sin\left(\theta_e + \frac{2\pi}{3}\right) \end{cases} \quad (12.181)$$

It should be noted, that the PWM controller is integrated in the inverter block. In Fig. 12.61 the operation regions of the control system are shown. Both motor and generator operation mode are considered. Considering zero initial load torque  $T_L$  on the motor axis, the motor can easily start rotating and go from operating point 0 to operating point A, slowly increasing its frequency. At this point, the load torque starts to gradually increase. In steady-state operation, where  $T_L = T_e$ , the operating point will move vertically along AB in the first quadrant. The electromagnetic torque is given by:

$$T_e = 3 \frac{P}{2} \frac{\psi_s \psi_m}{L_s} \sin\delta = 3 \frac{P}{2} \psi_s i_s \cos\varphi \quad (12.182)$$

where

$i_s$  = stator current

$P$  = the number of poles

$\delta$  = torque angle between rotor magnetic flux and total magnetic flux

$\varphi$  = phase displacement between stator voltage and current

$\psi_s$  = stator magnetic flux

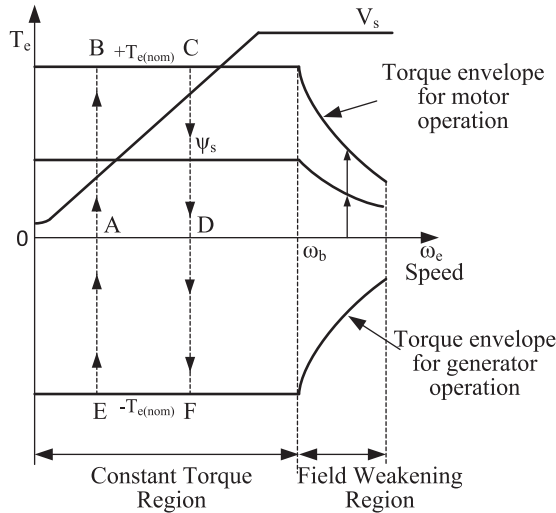


**Figure 12.61** Operational characteristics of the constant V/f scalar control.

$\psi_m$  = permanent magnet (rotor) induced flux  
 $L_s$  = stator inductance.

Therefore, for a constant value of the stator magnetic flux  $\psi_s$ , the power angle and the stator current will gradually increase until the production of the nominal value of electromagnetic torque at point B. At that point, either the power angle has reached its boundary value ( $\pi/2$ ) or the stator current has reached its nominal value. Usually, the operation of the system reaches the current limit of the inverter before the stability limit of the motor  $\delta = \pi/2$ . The operating point can change from B to C by gradually increasing the frequency command. Finally, the system can return to operating point D by gradually reducing the load torque.

At nominal speed ( $\omega_b$ ), the voltage will saturate. Beyond that point, the motor enters the flux weakening operating region. That way, the maximum available torque is reduced due to the reduced stator magnetic flux  $\psi_s$ , as shown in Fig. 12.61. Any rapid change in the signal  $\omega_e^*$  can lead to system instability due to loss of synchronization. For variable speed operation, the speed of the motor should follow the frequency command without losing synchronization. The rate of change of the signal  $\omega_e^*$  or the maximum acceleration/deceleration capability is dictated by the following equation:

$$\frac{2J}{P} \frac{d\omega_e}{dt} = T_e - T_L \quad (12.183)$$

where  $J$  is the moment of inertia,  $\omega_e = \frac{P\omega_r}{2}$  is the synchronous rotational speed,  $P$  is the number of poles, and  $\omega_m$  is the mechanical speed in rad/s. Consequently, the maximum acceleration and deceleration capability are respectively given by:

$$\frac{d\omega_e^*}{dt} = + \frac{P}{2J} (T_{e(nom)} - T_L) \quad (12.184)$$

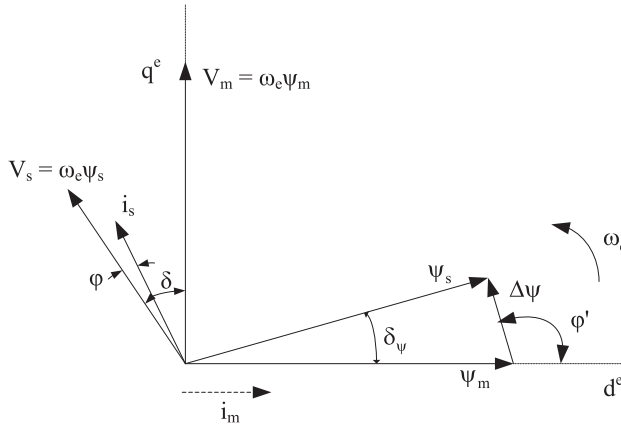


**Figure 12.62** Vector diagram of the permanent magnet motor (motor operation).

$$\frac{d\omega_e^*}{dt} = -\frac{P}{2J} (T_{e(nom)} - T_L) \quad (12.185)$$

where the nominal electromagnetic torque  $T_{e(nom)}$  and the load torque  $T_L$  contribute to the deceleration of the motor.

At point A, if the speed command is a ramp function with high slew rate, the produced electromagnetic torque will jump to point B and the motor will accelerate along the segment BC until the speed reaches a steady state at point D. Similarly, the operating point sequence for deceleration is D-E-F-A. The electric energy that is gained during deceleration can be consumed in a dynamic brake or can be induced back to power source (i.e., in case it is composed of batteries). The rotation of the motor towards the opposite direction can be achieved through the inversion of the sequence of two phases of the inverter. In Fig. 12.62 the vector diagram of the PMM is given. The stator resistance is considered negligible and the magnetic flux of the rotor excitation  $\psi_f$  is chosen as the reference vector. The vector of the constant equivalent excitation current  $I_f$  for a PMM is also shown.

### 12.5.1.3.2 Linear Torque Control Methods

Over the last 40 years, various closed loop torque control techniques has been developed. However, not all have been successfully introduced to industrial applications. In this section the most popular and widely used control strategies along with some new and promising ones will be introduced. The control strategies can be classified into two main categories: linear and nonlinear. Linear torque controllers operate combined with PWM techniques. They initially calculate the mean required voltage vector in a period. The vector is composed through a PWM technique, which in most cases is the SVM technique. Contrary to nonlinear control techniques, linear torque control (TC) methodologies employ linear PI (proportional-integral) controllers. The sampling frequency ranges from 2 to 5 kHz, while for nonlinear controller it reaches a value of 40 kHz. In the following paragraphs most important linear control techniques will

be analyzed, namely, the FOC, DTC-SVM, and the direct torque control with flux space vector modulation (DTC-FVM).

12.5.1.3.3 Field-Oriented Control (FOC)

FOC was proposed during the 1970s from Hasse and Blaschke and is based on the analogy of the ac motor with the dc motor, where the current commutation is achieved mechanically. In the dc motor the magnetic flux is separately controlled by the excitation current, while the torque is controlled by the armature current. Therefore, the two currents are electrically and magnetically decoupled. On the contrary, in AC motors, the armature current of the stator affects both the magnetic field and the produced torque. The decoupling of flux and torque can be achieved using the analysis of the instantaneous current into two components: the field current and the current associated with the development of torque, in a rotor reference rotating frame, as shown in Fig. 12.63. This technique enables the control of the motor in a way very similar to the control of a dc motor with independent excitation and can be implemented through current control with linear PI controller and a PWM inverter using an SVM technique. The core of this control system consists of the reference frame transformation blocks, that render the calculation of the d-axis and q-axis currents ( $i_{sd}$  and  $i_{sq}$ ) and the

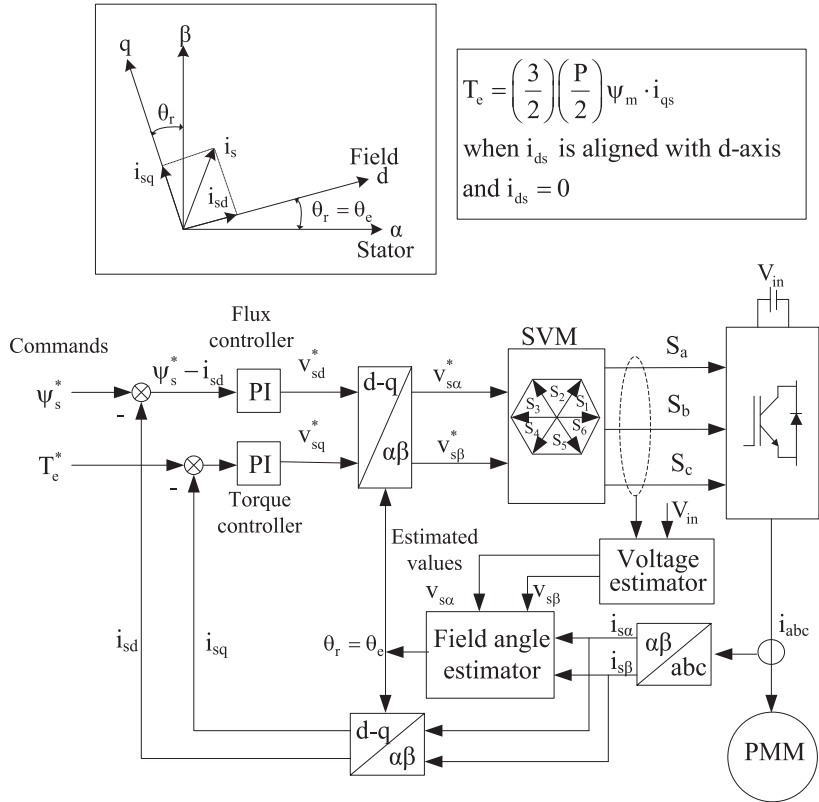


Figure 12.63 Block diagram of the FOC technique.

reference voltage vectors ( $v_{sz}^*$  and  $v_{sb}^*$ ) feasible, through the  $\alpha\beta/dq$  and  $dq/\alpha\beta$  transformation, respectively. Therefore, this control scheme allows for indirect control of the developed torque and magnetic field through current vectors aligned with the rotor magnetic field.

#### 12.5.1.3.4 Direct Torque Control With Space Vector Modulation (DTC-SVM)

Direct torque control can be considered a simplified version of the FOC oriented to the stator field and without any current control loops. Its operation is based on the equation of the developed electromagnetic torque of the motor. According to it, the developed torque is proportional to the amplitude of the PM flux vector, the amplitude of the stator flux vector, and the angle between them. Therefore, the maintenance of the amplitude of the stator flux vector at a constant value, allows for precise control of the electromagnetic torque through the variation of the angle of the two flux vectors. By neglecting the variation of the stator resistance, the variation of the stator flux is proportional to the applied voltage. Consequently, the developed torque can be controlled by rapidly changing the flux direction through the control of the applied voltage.

The block diagram of the DTC-SVM scheme with closed loop torque and flux control is shown in Fig. 12.64. The output signals of the PI controllers are the reference

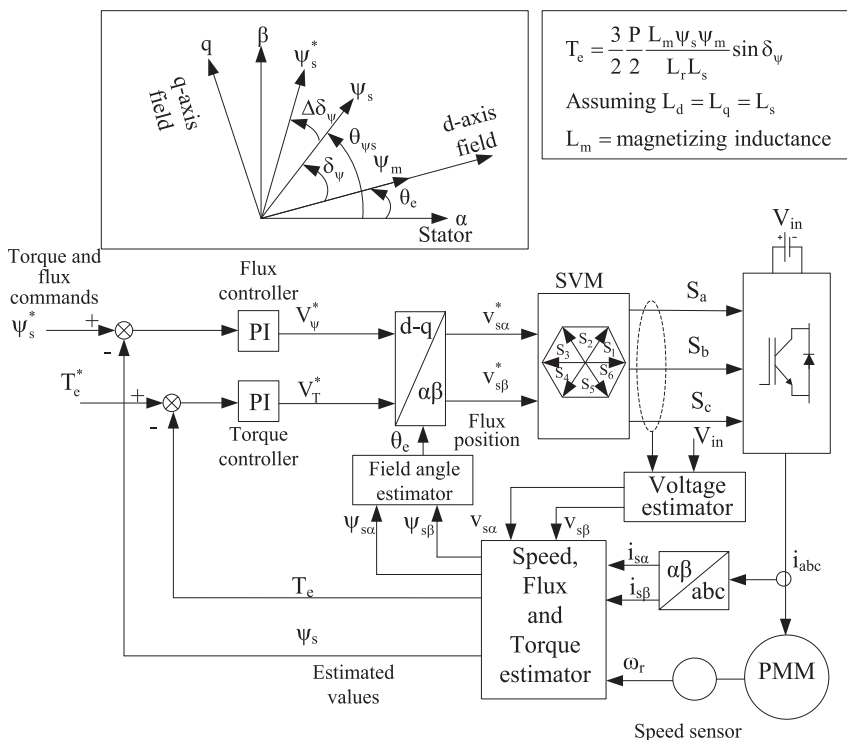


**Figure 12.64** Block diagram of the DTC-SVM technique.

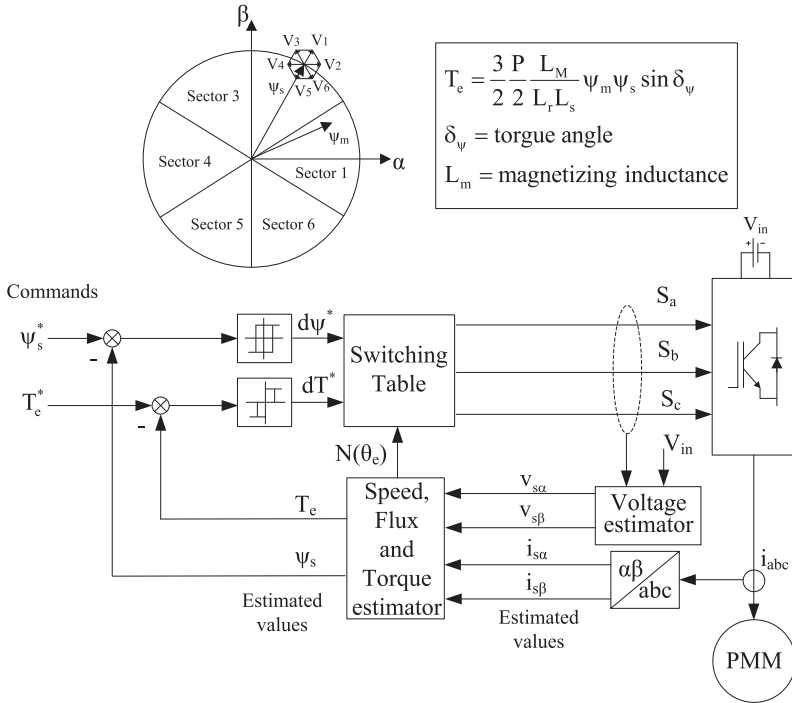


**Figure 12.65** Block diagram of the ST-DTC-SVM technique.

stator voltage signals  $v_\psi^*$  and  $v_T^*$ , oriented towards the stator magnetic field (dq). These dc command signals are transformed into stationary coordinates ( $\alpha\beta$ ) and the command signals  $v_{s\alpha}^*$  and  $v_{s\beta}^*$  are applied into the SVM block. It should be noted, that the specific control scheme is very similar to the classic switching table DTC (ST-DTC) scheme, which is shown in Fig. 12.65, where the switching table has been replaced by an SVM block and the flux and torque hysteresis controllers have been replaced by PI controllers. In the DTC-SVM scheme, the torque and flux are directly controlled through closed loop and, consequently, a precise torque and field estimation is mandatory.

This specific control technique, unlike the ST-DTC operates with a constant switching frequency. This feature improves the performance of the overall system, as it reduces the flux and torque fluctuations and offers improved low-speed operation.

#### 12.5.1.3.5 Direct Torque Control With Flux Vector Modulation (DTC-FVM)

To further simplify the DTC technique, a flux vector modulation (FVM) technique can be utilized, as shown in Fig. 12.66. For the control of the electromagnetic torque, a PI controller is used, whose output produces an increase in the power angle  $\Delta\delta_\psi$  (as shown in the vector diagram of Fig. 12.66). Considering that the amplitude of the rotor flux vector remains practically constant, the electromagnetic torque can be controlled

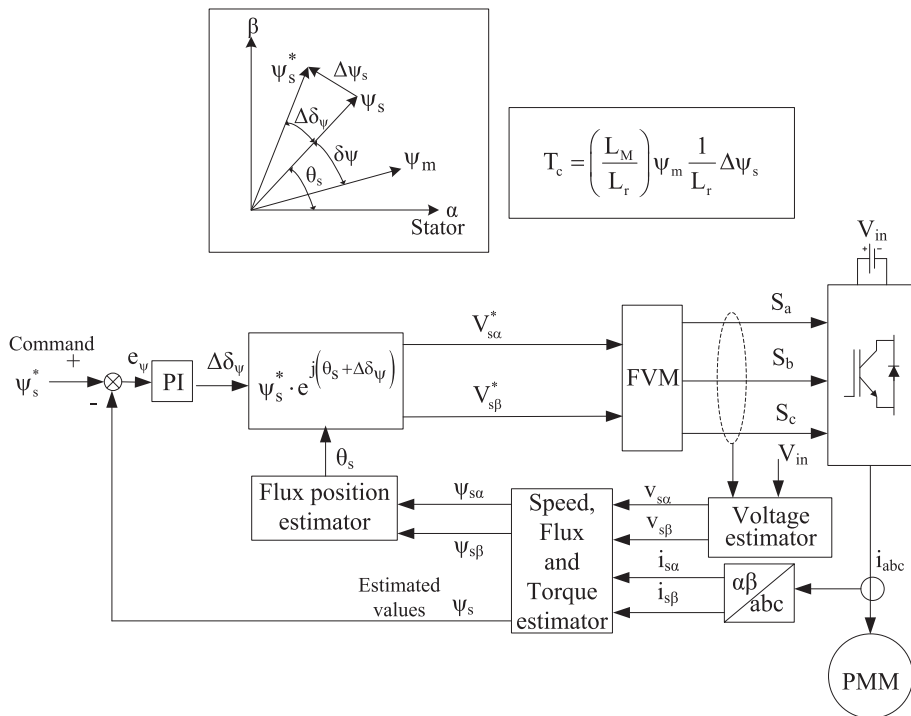


**Figure 12.66** Block diagram of the DTC-FVM technique.

by changing the power angle  $\delta\psi$ , which corresponds to an increase to the stator flux vector  $\Delta\psi_s$ . The command for the angle of the stator flux vector is calculated as the sum of the estimated position of the field  $\theta_s$  and the change in the power angle  $\Delta\delta\psi$ . Its value is compared to the estimated flux and the error signal  $\Delta\psi_s$  is used to directly dictate the switching state of the voltage fed inverter (FVM block). The PI controller of Fig. 12.64 can be omitted, due to the internal stator flux control loop that is used to calculate the change in the flux vector  $\Delta\psi_s$ .

#### 12.5.1.3.6 Nonlinear Torque Control Techniques

Nonlinear controllers adapt the bang–bang control type that is suitable to the switching nature of the operation of the semiconductor switches of the power inverter. In comparison to the FOC, nonlinear DTC controllers exhibit the following characteristics:

- Simple structure
- Absence of current control loops
- Indirect current control
- No need for independent voltage PWM
- No need for framework transformations

- No need for speed sensor
- Necessity for accurate estimation of stator flux and torque

In the following section, the most widely used nonlinear control techniques will be analyzed, namely the switching table DTC, the direct self control (DSC) and the online-optimized model-predictive DTC.

#### 12.5.1.3.7 Switching Table Direct Torque Control (ST-DTC)

The block diagram of the ST-DTC technique is shown in Fig. 12.65. The commands of the stator flux  $\psi_s^*$  and the motor torque  $T_e^*$  are the signals that are compared to the estimated values  $\psi_s$  and  $T_e$ , respectively. The error signals that are produced by the hysteresis controllers,  $d_\psi$  and  $d_T$ , as well as the position sector signal  $N(\theta_s)$  of the stator flux vector that is obtained through the calculation of its angular position  $\theta_s = \tan^{-1} \left( \frac{\psi_{sb}}{\psi_{sa}} \right)$  are used to select the suitable voltage vector from the switching table.

The latter controls the switching state of the power converter using the signals  $S_a$ ,  $S_b$ , and  $S_c$ . The ST-DTC technique has the following operating features:

- Sinusoidal flux and stator current waveforms. The harmonic content is dictated by the tolerance of the respective hysteresis band.
- Excellent dynamic behavior (depending on the voltage level).
- The flux and torque hysteresis bands dictate the switching frequency of the inverter, which varies with the synchronous speed and the load variations.

Over the last decades several modifications of the ST-DTC technique have been proposed to improve the motor transient behavior at start-up, the overload operation, the low speed operation, and the acoustic noise.

#### 12.5.1.3.8 Direct Self Control (DSC)

The block diagram of the DSC technique is shown in Fig. 12.67. Based on the stator flux command signal  $\psi_s^*$  and the components  $\psi_{sa}$ ,  $\psi_{sb}$ , and  $\psi_{sc}$ , the flux controllers produce the output signals  $d_a$ ,  $d_b$ , and  $d_c$  that correspond to active voltage states (V1–V6). The torque hysteresis controller produces the signal  $d_T$  that determines the zero voltage states. The flux controller dictates the duration of the active voltage states that implement the defined stator flux orbit. The torque controller dictates the duration of the zero voltage states that maintain the produced torque within the hysteresis band. The DSC technique, as shown in Fig. 12.67, has the following operating features:

- Non-sinusoidal flux and stator current waveforms.
- The locus of the stator flux vector path is an octagon.
- The inverter capability is fully exploited and, consequently, no voltage surplus is required.
- The switching frequency is smaller than the respective of the ST-DTC technique.
- Excellent transient behavior regarding the torque for both constant flux and field weakening operation.



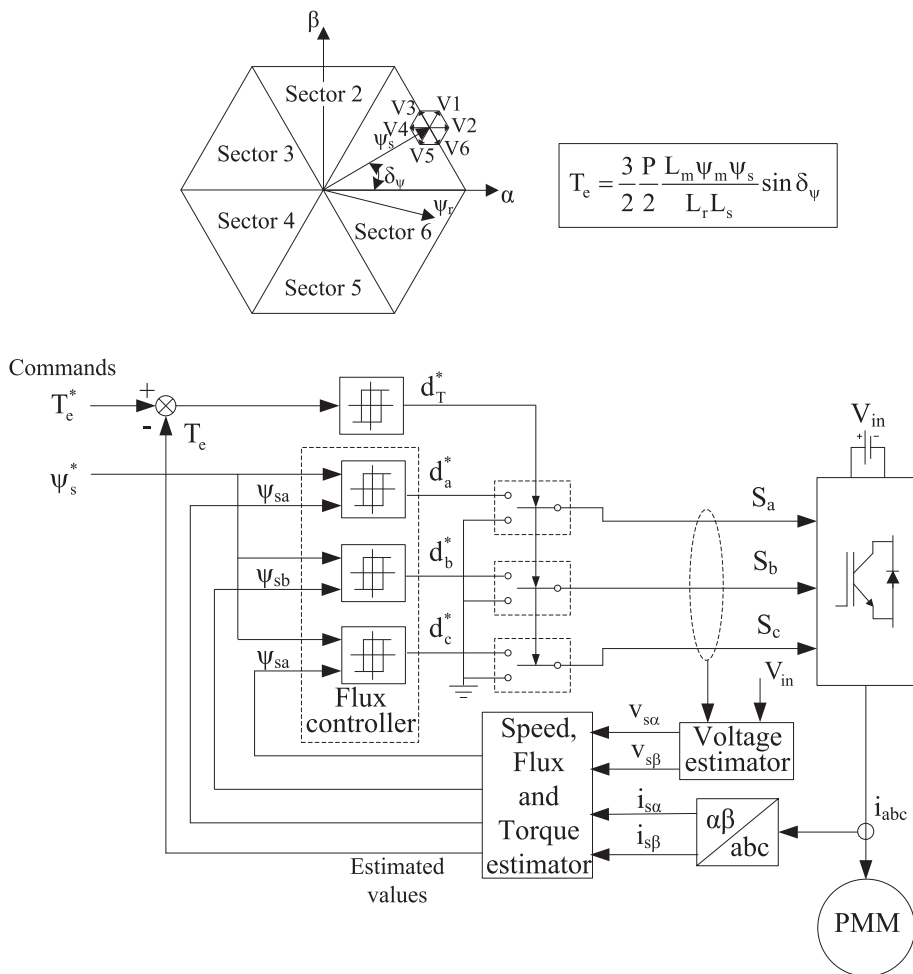


**Figure 12.67** Block diagram of the DSC technique.

### 12.5.1.3.9 Online-Optimized Model Predictive Direct Torque Control

The basic principle of predictive control is the utilization of a particular model of the system to be controlled to predict the future behavior of the control variables. This information is used by the controller to calculate the optimum action that will minimize a prescribed cost function. A simplified block diagram of the model-predictive DTC technique is shown in Fig. 12.68. This type of control is called finite control set model predictive control (FCS-MPC), as there are seven available switching states for a two-level voltage source inverter. Contrary to a conventional continuous MPC control operates without a PWM block because the switching state is calculated and optimized online through the minimization of the cost function. In most cases, the cost function is

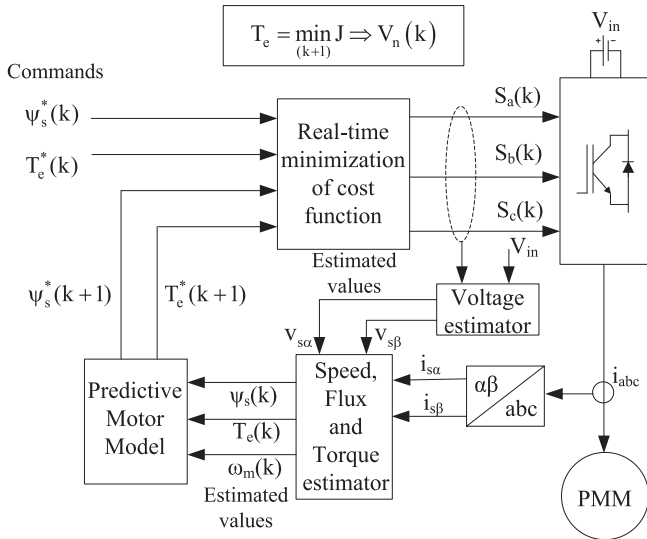


**Figure 12.68** Block diagram of the online-optimized model-predictive direct torque and flux control scheme.

defined as the weighted sum of the torque and flux errors. However, other objectives could be considered, i.e., the reduction of harmonic content, the dc voltage stabilization, etc., that improve the performance of the drive system.

The most important advantages of the MPC technique are:

- Ease of implementation.
- Consideration of nonlinearity of the motor model.
- Ease of implementation.
- Adaptability to the demands of the system.

However the implementation of the MPC demands:

- Increased computation power compared to other DTC methods.
- The accuracy of the model strongly affects the performance of the drive system and the quality of the control.

### 12.5.2 Switched Reluctance Motor (SRM) Drive Systems

RM is defined as the electric motor in which torque is produced from the natural tendency of the moving part (rotor) to rotate towards the position that maximizes the magnetic induction of the excited winding. This definition includes both switched and synchronous RMs. Synchronous RMs comprise a cylindrical rotor with lamination sheets of appropriate configuration, so that it exhibits different magnetic reluctance to each direction, and are generally fed by symmetrical sinusoidal voltages. Switched reluctance motors (SRMs) comprise both a stator and a rotor with salient poles and the name switched derives from the need for switched current feeding to consecutive windings, to achieve continuous rotation. Both of the aforementioned types of electric

motors are synchronous and the aforementioned distinction only aims to define the saliency type, i.e., artificial or inherent. For the needs of the analysis undertaken, only SRMs will be investigated and from now on will be referred to as SRM.

### 12.5.2.1 Description of SRM Structure

The structure of a variable RM is quite simple. In particular, it consists of a stator with salient poles made of magnetic lamination sheets and a rotor with salient poles, which is, in most cases, also made from conventional magnetic lamination sheets. However, in high performance applications, the lamination sheets are thinner than those normally used in conventional AC motors, and are made from advanced materials like silicon steel sheets, to reduce eddy current losses. The reason is that in an SRM drive system the switching frequency is higher than that of a conventional ac motor drive system of the same dimensions and with the same reference speed. The rotor does not comprise either windings or PMs. The number of stator and rotor poles is inherently different ( $N_s \neq N_r$ ), for example, some possible combinations are  $N_s = 6$  and  $N_r = 4$ ,  $N_s = 8$  and  $N_r = 6$ ,  $N_s = 12$  and  $N_r = 10$ , etc. Such a choice, guarantees that the rotor will never be in a position of zero electromagnetic torque, considering all potential stator winding alternative excitations. The higher the number of stator and rotor poles, the smaller the incurring torque pulsations. By choosing a combination where the number of stator poles is higher than the respective rotor poles by two (one additional pole pair in the stator), a high mean torque value and a low switching frequency in the converter that drives the motor are achieved. It is also possible to select the number of poles so that instead of imposing  $N_s - N_r = 2$ , that difference could be negative, so that  $N_s - N_r = -2$ , i.e.,  $N_s = 6$  and  $N_s = 8$ . For the same number of stator poles ( $N_s$ ), the most important advantage that the higher number of rotor poles ( $N_r$ ) offers is the smaller step angle and possibly, reduced torque ripple. Such a configuration has the disadvantage of smaller stator pole pitch, resulting in a smaller value of the inductances ratio. The inductances ratio is the ratio of the inductance in aligned position of the stator winding that corresponds to the respective pole to inductance in the not aligned position, and it will be thoroughly analyzed in a following paragraph. In any case, an odd number of stator poles should be avoided, as it alters the balance of the force that act in the motor. It should be noted, that there are viable configurations exhibiting dual teeth on every stator pole, i.e., a motor with six stator poles with two teeth in every pole and a rotor with 10 poles. This can lead to an increase in mean torque per ampere, but consequently will increase magnetization losses. Therefore, such configurations are used in low-speed applications.

The windings of the stator of an SRM are concentrated windings (which are cheaper than the respective distributed). Stator windings of inverse poles (teeth) are connected in series to form a stator phase. Consequently, this way it can be derived that a motor with six stator poles and four rotor poles is actually a three-phase motor (generalized three-phase motor). A motor with  $N_s = 12$ ,  $N_r = 8$  is also a three-phase motor, but with four stator poles connected in series in every phase. A three-phase motor has the ability to develop electromagnetic torque during starting either towards the positive or the negative rotational direction. If  $N_s = 2$  and  $N_r = 2$ , then it is a single-phase

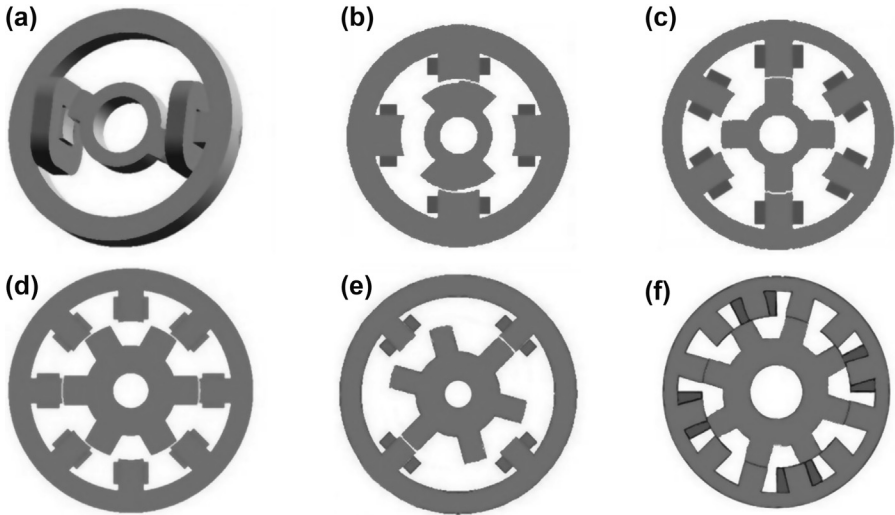


**Figure 12.69** Various types of switched reluctance motor (SRM). (a) One-phase bipolar SRM; (b) two-phase 4/2\*SRM; (c) three-phase 6/4\*SRM; (d) four-phase 8/6\*SRM; (e) two-phase 4/6\*SRM; (f) three-phase 12/8\*SRM.

motor, but this motor can only be rotated from any given rotor position provided that specific starting options are utilized (i.e., stepped air-gap). If  $N_s = 4$  and  $N_r = 2$ , then it's the generalized two-phase motor, which can also be started from any given rotor position only provided that specific starting options are utilized (i.e., stepped air-gap). If  $N_s = 8$  and  $N_r = 6$ , then the motor is a four-phase motor, it can be started from any given rotor position and produces smoother electromagnetic torque than the respective three-phase one. Some of the aforementioned configurations are shown in Fig. 12.69.

### 12.5.2.2 Principles of SRM Operation

The foundation stone of the operation of the SRM is the variable inductance of the windings with the position of the rotor. The rotor moves spontaneously towards positions of increased inductance of the respective winding that is fed, decreasing this way its total mechanical energy (potential that becomes kinetic). The movement of the rotor is actually a repetitive movement between two extreme positions. The first one is the unaligned position, where the magnetic induction (or magnetic flux density) of the winding that is fed is minimum and is a point of unstable equilibrium. The second is called aligned position, and it's the position of maximum magnetic induction for the winding that is fed and is a point of stable equilibrium. The continuous movement is guaranteed through the synchronized excitement of consecutive windings.

To clarify the abovementioned, the simplest case, i.e., the single-phase 2/2 SRM will be analyzed. The motor under analysis is shown in Fig. 12.70. In this figure, the two extreme positions of the rotor are depicted; the aligned position (a) and the unaligned position (b). Additionally, the main characteristics that describe the operation

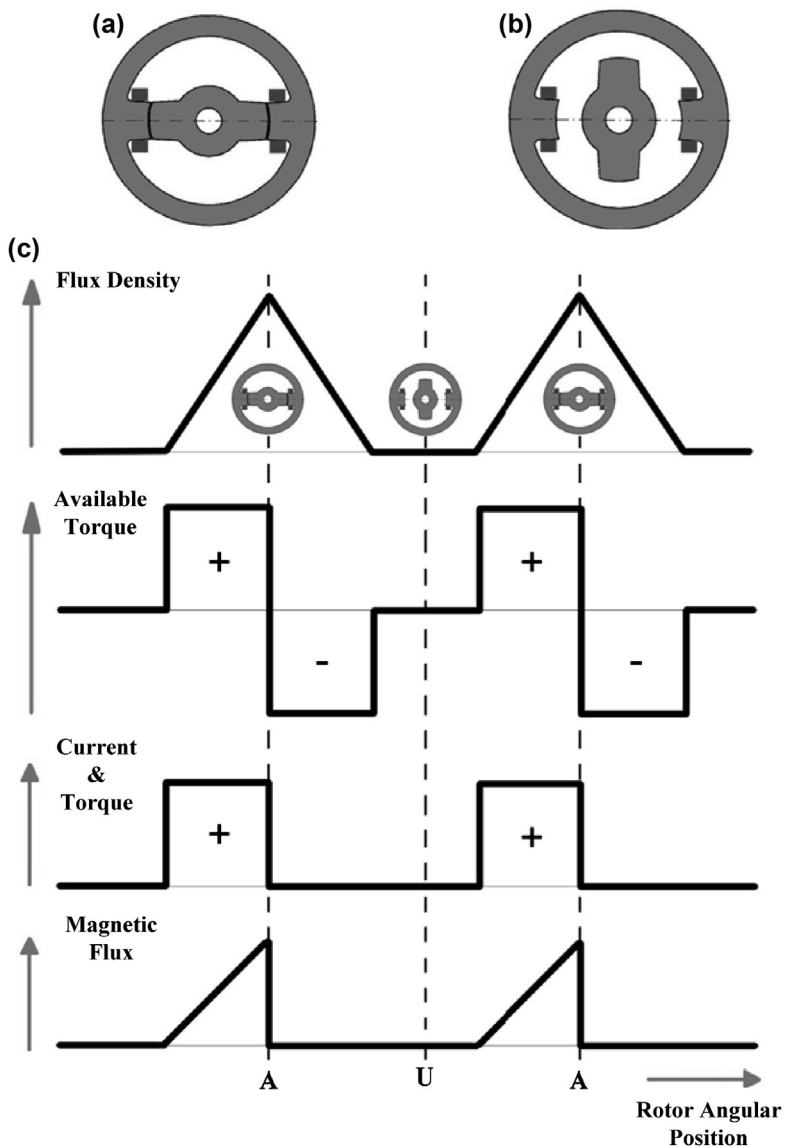


**Figure 12.70** Description of the 2/2 switched reluctance motor (SRM). (a) Aligned rotor position; (b) unaligned rotor position; (c) waveforms related to the ideal operation of a single-phase 2/2 SRM.

of the SRM are shown. It should be noted, that for the aforementioned characteristics the ideal case of linear operation has been considered. Thus, the nonlinear phenomena of magnetic saturation and magnetic flux leakage around the pole edges have been ignored, and it has been considered that the magnetic flux travels through the air

gap in radial paths. We can see that in the aligned position the magnetic flux density of the stator winding takes its maximum value, while in the unaligned position it reaches its minimum value. In practice, when there is no overlap between the poles of the stator and the rotor, the magnetic induction reaches a very small minimum value which is not zero. As soon as the overlapping starts and while moving towards the alignment position, the induction values increase, and in fact in a linear manner. If we consider the fact that during the aforementioned rotor movement the stator windings are constantly excited, then the motor develops the electromagnetic torque that is shown in the second waveform. This can be considered as the possible electromagnetic torque that the motor is capable of producing. We can see that the produced torque takes both positive and negative values, while exhibiting a zero mean value. Apparently, such a torque waveform is far from desired. Consequently, we come to the realization that the stator windings should not be constantly excited, but they should be excited with switched currents depending on the position of the rotor, as shown in the third waveform. The waveform depicts simultaneously the ideal positive current and the consequent ideal positive electromagnetic torque of the motor. However such a tetragonal pulse is not practically feasible. This is mainly due to the fact that the value of the magnetic induction at the start of the pulse is not exactly zero, to achieve rapid current increase, and the fact that the available negative voltage should be infinite to achieve a rapid current interruption. Such an ideal current waveform, in conjunction with the ideal induction waveform, leads to a triangular waveform of the magnetic flux. The ideal torque waveform resembles in shape with the respective current waveform. The torque production cycle, associated with a certain current pulse is called a stroke. Apparently, to produce constant mean torque more than one phases are required, and the mean torque will be produced from the superposition of the respective strokes. Under normal operating conditions, there is a stroke per rotor pole arc for every phase and for each phase current flows only for a fraction of the rotor pole pitch.

Based on the aforementioned analysis, considering a linear magnetic circuit and neglecting the mutual inductances between the windings (which have zero values) the mathematical description of the phase voltages can be derived:

$$v = Ri + \frac{d\psi}{dt} = Ri + \frac{d\psi}{d\theta} \frac{d\theta}{dt} = Ri + \omega_m \frac{d(Li)}{d\theta} = Ri + L \frac{di}{dt} + \omega_m i \frac{dL}{d\theta} \quad (12.186)$$

where  $v$  and  $i$  are the instantaneous values of the voltage and the current of the winding,  $R$  is the winding resistance,  $\psi$  is the instantaneous value of the magnetic flux,  $\omega_m$  is the mechanical rotational speed,  $\theta$  is the angular position of the rotor, and  $L$  is the inductance of the stator winding. The last term of the equation is called back-EMF of the motor and is given by:

$$e = \omega_m i \frac{dL}{d\theta} \quad (12.187)$$

From the above analysis, the equivalent per-phase circuit of the SRM is derived, which is described by [Eqs. \(12.186\) and \(12.187\)](#). It consists of a resistance connected in series with a variable inductance and a variable back-EMF, as shown in [Fig. 12.71](#).

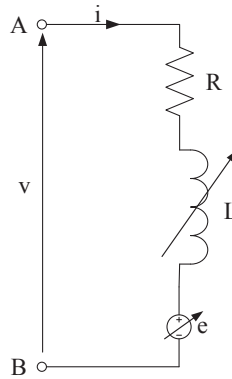


**Figure 12.71** Per-phase equivalent circuit of a switched reluctance motor neglecting mutual inductances.

Therefore, utilizing the visualization of Fig. 12.71, we can distinguish the three voltage terms of Eq. (12.186) in the voltage drop along the winding resistance  $R$ , the back-EMF on the variable inductance  $L$ , and the velocity back-EMF  $e$ , respectively. At this point it should be noted, that the electric equivalent of an SRM is particularly simple as it consists of independent electric circuits, one for each phase, due to the negligible nature of the respective stator mutual inductances. The independence of the electric circuits is a very important characteristic of the SRMs because it facilitates the precise current control and increases the motor's reliability and fault tolerance, as a potential fault in a single phase does not involve the other phases that continue their normal operation. This feature is especially important in applications that require increased reliability or applications where maintenance is difficult.

To fully understand the operation of the SRM, the mathematical description of the torque production mechanism is essential, additionally to the electric equivalent circuit. This procedure will lead to the extraction of the full mathematical model of the SRM. Contrary to the electric equivalent circuit, the description of the aforementioned mechanism is particularly difficult, because of the complex nonlinear electromagnetic phenomena related to it. Initially, a simplified linear approach shall be made, which will produce results adequately close to the real motor behavior.

From Eq. (12.186), the per-phase instantaneous electric power of an SRM is derived:

$$v_i = Ri^2 + Li \frac{di}{dt} + \omega_m i^2 \frac{dL}{d\theta} \quad (12.188)$$

Considering a linear magnetic circuit and neglecting hysteresis and eddy currents, the instantaneous stored magnetic power of the magnetic circuit is given by equation:

$$\frac{d}{dt} \left( \frac{1}{2} Li^2 \right) = \frac{1}{2} \left( 2Li \frac{di}{dt} + i^2 \frac{dL}{dt} \right) = Li \frac{di}{dt} + \frac{1}{2} i^2 \omega_m \frac{dL}{d\theta} \quad (12.189)$$

According to the law of conservation of energy, electric power finally changing to mechanical is derived from the circuit input power, if the ohmic thermal losses on the resistance  $R$  and the instantaneous power stored in the magnetic circuit are subtracted:

$$p = \omega_m T_e = Ri^2 + Li \frac{di}{dt} + \omega_m i^2 \frac{dL}{d\theta} - Ri^2 - Li \frac{di}{dt} - \frac{1}{2} i^2 \omega_m \frac{dL}{d\theta} = \frac{1}{2} i^2 \omega_m \frac{dL}{d\theta} \quad (12.190)$$

where  $T_e$  is the instantaneous electromagnetic torque of each phase of the SRM.

Consequently, by solving Eq. (12.190) we obtain:

$$T_e = \frac{1}{2} i^2 \frac{dL}{d\theta} \quad (12.191)$$

where  $dL/d\theta$  is the slope of the magnetic flux density waveform, shown in Fig. 12.70(c). It should be mentioned that for the analysis undertaken, linear magnetic circuit and ideal operational characteristics of the motor are considered, as shown in Fig. 12.70(c). From Eq. (12.191) fundamental conclusions regarding the nature and the operation of the SRM can be deduced. First, it can be concluded that the sign of the produced electromagnetic torque does not depend on the sign of the phase current, because it is proportional to the square of the current value, as shown from Eq. (12.191). That means that unidirectional currents are necessary for the operation of such a motor, something that significantly simplifies the driving converter configuration. Second, it can be concluded that the sign of the produced electromagnetic torque only depends on the sign of the term  $dL/d\theta$ , namely the slope of the magnetic flux density waveform. If we take a closer look at the ideal waveform of flux density, shown in Fig. 12.70(c), it becomes apparent that the slope is initially positive and then becomes negative. Consequently, the electromagnetic torque, shown in Fig. 12.70(c), changes sign exactly at the point that the magnetic flux density slope changes. This practically means that if a positive electromagnetic torque is desired, the winding should be excited only during the time when the magnetic flux density is increasing and the excitation should stop as soon as its values starts decreasing, as shown in Fig. 12.70(c). For the aforementioned analysis a nonrealistic consideration of linearity of the magnetic circuit is employed.

### 12.5.2.3 Power Electronics Converter for SRM Drive Systems

Various different power electronic converters have been proposed for SRM drive systems that meet the aforementioned requirements. The simplest and most often used converter for that purpose is the single-phase asymmetrical voltage source inverter, which is shown in Fig. 12.72. The converter is fed by a dc voltage source  $V_{dc}$  and comprises two semiconductor switches ( $S_1$  and  $S_2$ ) and two diodes ( $D_1$  and  $D_2$ ).

The load of the converter is the stator winding of a phase of the SRM. Therefore, a number of converters equal to the number of the phases of the SRM are required. It is possible to reduce the number of the semiconductor switches through the merging of



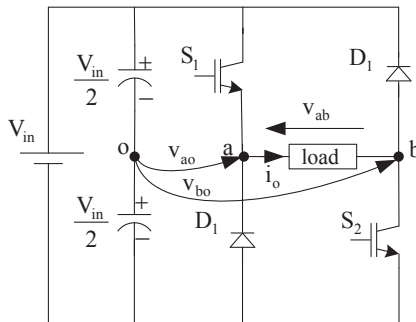


**Figure 12.72 Single-phase asymmetrical voltage source inverter.**

specific legs of the converters. However, this could result in decreased reliability due to the fact that it cancels the modularity of the converter, as if one phase has a fault the others are unable to normally operate. Therefore, a single-phase asymmetrical inverter per-phase is used in most applications, as shown in Fig. 12.72. Additionally, in practice, as will be revealed by the following analysis, only a single semiconductor switch per-phase is actually necessary. Consequently, the second switch can be replaced by a diode. The drawback of this option is the inability to achieve equal use of all the switches and even distribution of their respective losses. This is a major disadvantage that is usually evaluated as of higher significance than the extra cost of a semiconductor switch compared to that of a diode. The overall converter for a three-phase SRM drive comprises the same number of switches with a typical three-phase inverter, while rendering its potential reduction feasible. However, the establishment of the three-phase inverters as standard driving systems and their wide production renders them more economical than a respective SRM converter.

In the following paragraph, the operation of the single-phase asymmetrical voltage source inverter will be analyzed in detail and its mathematical model will be extracted. In Fig. 12.73, all possible switching states of the converter are shown.

From the above analysis, it becomes apparent that such a converter is able to drive an SRM, as it allows the production of both positive and negative voltage and unidirectional currents. The mathematical model of the converter, which fully describes its operational states, is shown below. The various switching states shown in Fig. 12.73, can be analytically described using the following equation:

$$v_{ab} = \frac{V_{in}}{2} (v_a + v_b)$$

$$= \begin{cases} V_{in}, & S_1 = \text{on}, S_2 = \text{on} \Rightarrow \text{Positive voltage, Fig.12.73(a)} \\ 0, & S_1 = \text{on}, S_2 = \text{off} \Rightarrow \text{Freewheeling 1, Fig.12.73(b)} \\ 0, & S_1 = \text{off}, S_2 = \text{on} \Rightarrow \text{Freewheeling 2, Fig.12.73(c)} \\ -V_{in}, & S_1 = \text{off}, S_2 = \text{off} \Rightarrow \text{Negative voltage, Fig.12.73(d)} \end{cases} \quad (12.192)$$

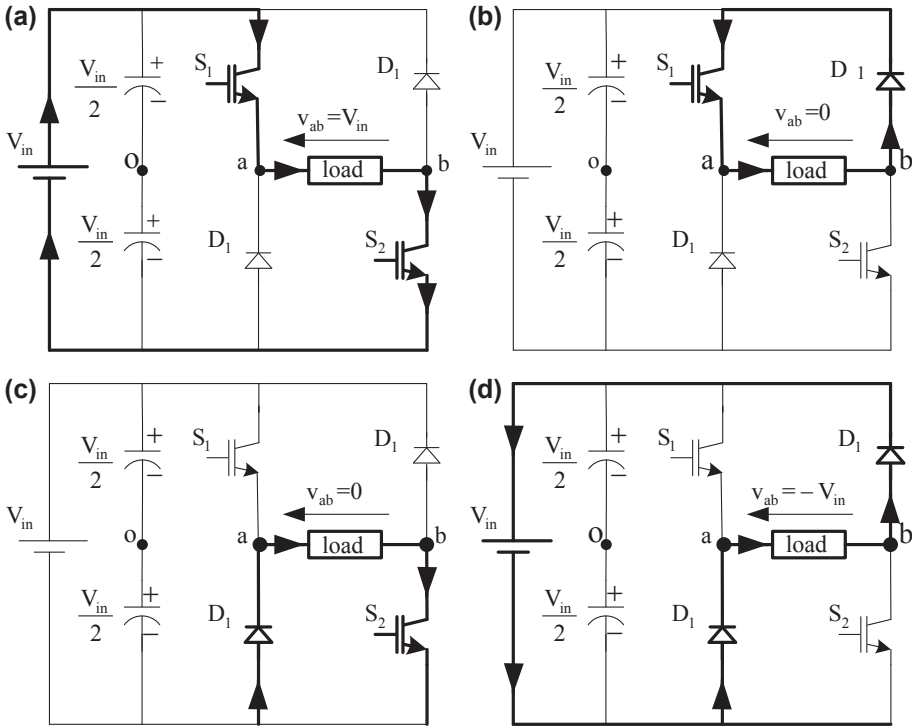


**Figure 12.73** Possible switching states and the respective output voltages of the converter.

(a) Both switches ( $S_1$  and  $S_2$ ) are conducting and positive voltage is applied to the load; (b) one switch ( $S_1$ ) and a diode ( $D_2$ ) are conducting, short-circuiting the load (freewheeling); (c) one switch ( $S_2$ ) and a diode ( $D_1$ ) are conducting, short-circuiting the load (freewheeling); (d) none of the switches is conducting and negative voltage is applied to the load through the diodes ( $D_1$  and  $D_2$ ).

where the variables  $v_a$  and  $v_b$  are defined by the switching state of the semiconductor switches  $S_1$  and  $S_2$  as follows:

$$v_a = \begin{cases} 1, & \text{if } S_1 = \text{on} \\ -1, & \text{if } S_1 = \text{off} \end{cases} \quad (12.193)$$

$$v_b = \begin{cases} 1, & \text{if } S_2 = \text{on} \\ -1, & \text{if } S_2 = \text{off} \end{cases} \quad (12.194)$$

Eq. (12.192) combined with Eqs. (12.193) and (12.194) comprise the simplified mathematical model of the single-phase asymmetrical voltage source inverter that is used to drive an SRM.

**Table 12.8 Comparison between different motor drive systems**

<b>Motor drive system</b>	<b>Advantages</b>	<b>Disadvantages</b>
DC motor drive systems	Accuracy Control simplicity Fast torque control Good dynamic speed response Direct torque control	Motor with low reliability The motor needs periodic maintenance High cost motor Needs a feedback translator
AC motor drive systems with frequency control	Low cost For simple applications they do not need translator Robustness Simple maintenance Simple simulation	Field-oriented control techniques are not used The state of the motor is ignored Torque is not adjustable There are delays caused by the modulator Mostly used in open loop motor drive systems The load is affecting the torque level
AC motor drive systems with vector control	Good torque response Accurate speed adjustment Maximum torque can be achieved at zero value speed General performance of the order of dc motor drive systems Is used in closed loop systems	Feedback is needed Moderate cost There are delays caused by the pulse width modulator Indirect torque adjustment
AC motor drive systems with direct field-oriented control	Fast torque response Good torque setting at low frequencies Linear torque response Accurate speed increase without the use of translators Maximum torque at zero speed	High cost Need for high computational capability digital signal processors Complicated motor model

## 12.6 Conclusions

In this chapter some of the most well-known motor drive systems were presented. From the above discussions it was clear that there are different possibilities to design a motor drive system from which an electrical engineer should know so that to choose every time the proper one for a particular application. The design procedure starts with the examination of the load and then the type and power of the motor is selected, depending on the design application and economic factors. Based on the type of motor the proper power converter topology is selected together with the appropriate control technique and observation system. Finally, after the design procedure the implementation of the motor drive system follows, which must operate according to the initial specifications. Table 12.8 presents the advantages and disadvantages of the motor drive systems discussed in this chapter.

## Bibliography and Publications

- [1] B.K. Bose, *Modern Power Electronics and AC Drives*, Prentice Hall PTR, 2002.
- [2] P. Vas, *Sensorless Vector and Direct Torque Control* (Monographs in Electrical and Electronic Engineering), Oxford University Press, 2003.
- [3] P.C. Krause, *Analysis of Electric Machinery*, McGraw-Hill, 1987.
- [4] M.G. Say, *Alternating Current Machines*, Longman Scientific and Technical, fifth ed., 1983.
- [5] M.H. Rashid, *Power Electronics Handbook*, Academic Press, 2001.
- [6] P.A. Laplante, *Real-Time Systems Design and Analysis*, IEEE Press-Wiley, 2004.
- [7] J. Chiasson, *Modeling and High Performance Control of Electric Machines*, IEEE Press-Wiley, 2005.
- [8] J.A. Santisteban, R.M. Stephan, Vector control methods for induction machines: an Overview, *IEEE Transactions on Education* 44 (2) (May 2001).
- [9] A. Makouf, M.E.H. Benbouzid, D. Diallo, N.E. Bouguechal, Induction motor robust control: an  $H_\infty$  control approach with field orientation and input-output linearizing, in: *IECON'01*, 2001.
- [10] Z. Béres, P. Vranka, Sensorless IFOC with current regulators in current reference frame, *IEEE Transactions on Industry Applications* 37 (4) (July/August 2001).
- [11] F.F.M. El-Sousy, Design and Implementation of 2DOF I-PD Controller for Indirect Field Orientation Control of Induction Machine Drive System, *IEEE*, Pusan, Korea, 2001.
- [12] Y.-S. Lai, Machine modeling and Universal controller for vector-controlled induction motor drives, *IEEE Transactions on Energy Conversion* 18 (1) (March 2003).
- [13] M. Jayne, I. Ludtke, L. Yiqiang, T. Arias, Evaluation of vector and direct torque controlled strategies for cage rotor induction motor drives, in: *Power Electronics and Motion Control Conference PIEMC*, vol. 1, 2000.  $\sigma\epsilon\lambda$ . 452–457.
- [14] P. Marino, M. D'Incecco, N. Visciano, A comparison of direct torque control methodologies for induction motor, in: *IEEE Porto Power Tech Conference*, Portugal, 2001.
- [15] M. Rodič, K. Jezernik, Continuous Approach to the Direct Torque and Flux Control of Induction Motor, *AMC*, Maribor, Slovenia, 2002.

- [16] N. Rumzi, N. Idris, A.H.M. Yatim, Direct torque control of induction machines with constant switching frequency and reduced torque ripple, *IEEE Transactions on Industrial Electronics* 51 (4) (August 2004).
- [17] K. Ohyama, G.M. Asher, M. Sumner, Comparative analysis of Experimental performance and stability of sensorless induction motor drives, *IEEE Transactions on Industrial Electronics* 53 (1) (February 2006).
- [18] X. Del Toro, M.G. Jayne, P.A. Witting, J. Pou, A. Arias, J.L. Romeral, *New Direct Torque Control Scheme for Induction Motors*, EPE, Dresden, 2005, ISBN 90-75815-08-5.
- [19] I. Manolas, A.G. Kladas, S.N. Manias, Finite-element-based estimator for high-performance switched reluctance machine drives, *IEEE Transactions on Magnetics* 45 (3) (2009) 1266–1269.
- [20] A. Kaletsanos, F. Xepapas, S.N. Manias, Sliding-mode observer for speed-sensor less induction motor drives, *IEE Proceedings on Control Theory and Applications* 150 (6) (November 2003) 611–617.
- [21] A. Vamvacari, A. Kandianis, A.G. Kladas, S.N. Manias, Analysis of supply voltage distortion effects on induction motor operation, *IEEE Transactions on Energy Conversion* 16 (3) (September 2001) 209–213.